

General Disclaimer

One or more of the Following Statements may affect this Document

- This document has been reproduced from the best copy furnished by the organizational source. It is being released in the interest of making available as much information as possible.
- This document may contain data, which exceeds the sheet parameters. It was furnished in this condition by the organizational source and is the best copy available.
- This document may contain tone-on-tone or color graphs, charts and/or pictures, which have been reproduced in black and white.
- This document is paginated as submitted by the original source.
- Portions of this document are not fully legible due to the historical nature of some of the material. However, it is the best reproduction available from the original submission.

9950-798

ASTRO

(NASA-CR-173765) EXCESS SCIENCE ACCOMMODATION CAPABILITIES AND EXCESS PERFORMANCE CAPABILITIES ASSESSMENT FOR MARS GEOSCIENCE AND CLIMATOLOGY ORBITER: EXTENDED STUDY Final Report (RCA Government G3/12 17782 N84-28882 Unclass

Excess Science Accommodation Capabilities and Excess Performance Capabilities Assessment for Mars Geoscience and Climatology Orbiter

Extended Study - Final Report

Prepared for
Jet Propulsion Laboratory
California Institute of Technology
Sponsored by the National Aeronautics and Space Administration under Contract NAS7-918

Prepared by
RCA Government Systems Division
Astro-Electronics
Princeton, New Jersey

Authors
K. Clark, A. Flacco,
P. Kaskiewicz, and
K. Lebsack



Contract No. 956291, Modification No. 1
May 27, 1983

Excess Science Accommodation Capabilities and Excess Performance Capabilities Assessment for Mars Geoscience and Climatology Orbiter

Extended Study - Final Report

Prepared for

Jet Propulsion Laboratory
California Institute of Technology
Sponsored by the National Aeronautics
and Space Administration under
Contract NAS7-918

Prepared by

RCA Government Systems Division
Astro-Electronics
Princeton, New Jersey

Authors

K. Clark, A. Flacco,
P. Kaskiewicz, and
K. Lebsack

Contract No. 956291, Modification No. 1

May 27, 1983

ABSTRACT

This report contains an assessment of the excess science accommodation and excess performance capabilities of a candidate spacecraft bus for the MGCO mission. The appendices are included to support the conclusions obtained during this contract extension. The appendices address the mission analysis, the attitude determination and control, the propulsion subsystem, and the spacecraft configuration.

TABLE OF CONTENTS

<u>Section</u>	<u>Page</u>
I. INTRODUCTION	I-1
II. CONFIGURATION CONSIDERATIONS	II-1
A. General	II-1
B. Science Instrument Accommodation	II-3
1. Science FOV Instrument Requirements	II-3
2. Science Instrument Constraints	II-4
III. SPACECRAFT BUS SUBSYSTEM ASSESSMENT	III-1
A. General	III-1
B. Spacecraft Bus Excess Capability	III-2
1. General	III-2
2. Power Subsystem	III-2
3. Command Control and Data Handling	III-2
4. Attitude Control Subsystem	III-3
5. Structure	III-4
6. Thermal	III-4
7. Propulsion Subsystem	III-4
IV. SUMMARY AND RECOMMENDATIONS	IV-1
APPENDICES	
A. Mission Analysis	A-1
B. Attitude Control System Overview	B-1
C. Propulsion Subsystem	C-1
D. Configuration Discussion	D-1

I. INTRODUCTION

This contract extension to the basic Mars Orbiter study addresses the identification of "excess capability" beyond the mission/system requirements, "excess capability" for science accommodation, and constraints on the accommodation of science instruments.

As this study effort progressed it became apparent that "excess capability" can be defined in a number of ways. It may be defined as (a) capability above the absolute minimum required to meet the mission requirements, or (b) the capability beyond the normal margins of performance included in an optimized spacecraft approach.

"Excess capability" in many cases cannot be defined solely by a numerical value (ex: extra instrument mounting space on the nadir facing side of the spacecraft, or "excess" instrument weight or power capacity has no meaning if an additional candidate instrument has cooler or viewing field-of-view (FOV) requirements that would be incompatible with an existing configuration). Further, "excess capability" may be available for only certain parts of a mission (as in portions of a power profile) and its utility depends on the use to which that "excess capability" can be put.

One of the TIROS series of spacecraft (TIROS-N) has been used as the baseline for the extended study effort. It was selected since it can provide sufficient bus performance for the Mars Orbiter mission. It does provide some excess capability (above the normal margins used on spacecraft designs) in certain subsystems. However, other spacecraft in the TIROS/DMSP series (ATN, SAATN, DMSP Block 5D-3, etc.) can provide significantly more "excess capability" if that is required for margin or growth (see Table 1).

The following factors have been kept in mind while performing that extended study.

- a. Applicability of the approach to the mission requirements
- b. Meeting payload and launch vehicle interfaces
- c. Improving reliability
- d. Consideration of cost factors
- e. Minimizing complexity
- f. Flexibility

During the extended study, the tasks that were emphasized, in addition to those of the modified contract requirements, were (a) reiteration of mission analysis, (b) review of the power requirements, (c) updating the instrument interface requirements, (d) detailing the attitude control approach, and (e) reviewing the candidate configurations. These tasks were oriented toward assessing the capabilities of the spacecraft approach against the standard requirements document and the science accommodation factors.

A summary of the results of these tasks is shown in the following appendices.

- Appendix A Mission Analysis
- Appendix B Attitude Control System Overview
- Appendix C Propulsion Subsystem
- Appendix D Configuration Discussion

TABLE 1. TIROS/DMSP SPACECRAFT GROWTH

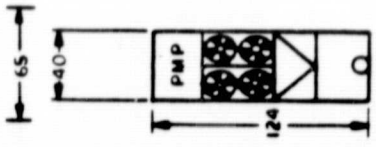
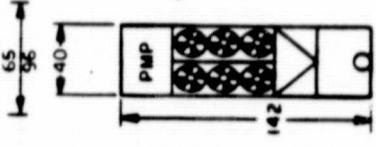
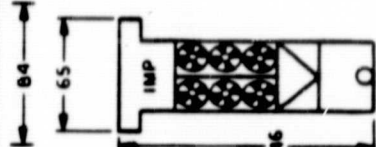
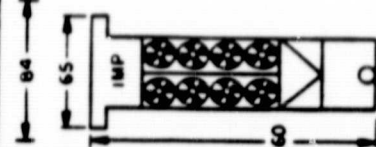

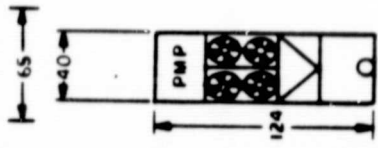
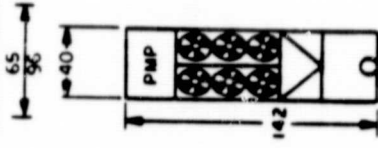
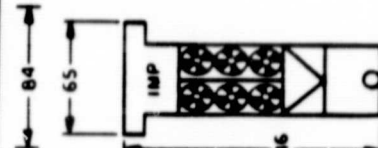
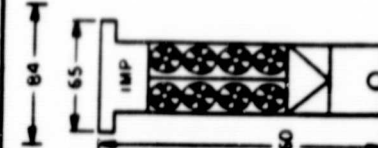

	 5D-1	 5D-2	 TIROS-H	 ATN/SAATN	 DMSPI(SD-3)/STS
TECO WEIGHT (LBS)	1131	1380 1850	1680	1835-2250 2470-2900	ELV STS 1697 1833 2470 2900
FIRST STAGE	LV-2F	ATLAS F	ATLAS F	ATLAS F/STS	SLV-3A/STS
SECOND STAGE	TE-M-364-4	NONE	NONE	NONE	364-4 NONE
THIRD STAGE	TE-M-364-15	TE-M-364-15	TE-M-364-15	TE-M-364-15/ N ₂ H ₄	N ₂ H ₄
N ₂ H ₄ (LBS)	35	35	35	35/1500	1500
POWER (WATTS)					
• BOL (ARRAY OUTPUT)	770	910	1095	1270/1486	1100
• EOL (LOAD CAPABILITY)	307	400	465	520/608	482
SUN ANGLE	0°-55°	0°-95°	0°-68°	0°-68°	0°-95°
PAYLOAD WEIGHT (LBS)	300	400 650	650	808	472/570 1285/1687

TABLE 1. TIROS/DOSP SPACECRAFT GROWTH (Continued)

	5D-1	5D-2	TIROS-N	ATN/SAATN	DOSP(5D-3)/STS
					
ADACS ●PRINTING & CONTROL ●CONTROL METHOD ●DETERMINATION SENSORS ●MODES	0.01° RWA & COILS CSA, SSA ESA, IMU PRIMARY BACKUP GYRO COMPASS GN ₂ MULS	0.01° RWA & COILS CSA, SSA ESA, IMU PRIMARY BACKUP GYRO COMPASS GULS	0.1° RWA & COILS SSA ESA, IMU BASIC GYRO COMPASS GN ₂ MULS	0.1° RWA & COILS SSA ESA, IMU BASIC GYRO COMPASS GN ₂ MULS	0.01° RWA & COILS CSA, SSA ESA, IMU BASIC GYRO COMPASS GULS
COMPUTERS MEMORY TECH	2 16K WORDS CMOS BULK PMOS	2 28K WORDS CMOS BULK & SOS & PMOS*	2 18K WORDS CMOS BULK & SOS & PMOS	2 18K WORDS CMOS BULK & SOS & PMOS*	2 64K WORDS CMOS BULK & SOS

*REPLACED WITH CMOS

II. CONFIGURATION CONSIDERATIONS

A. GENERAL

The proposed complement of science instruments requires modification to the spacecraft configuration shown to JPL in the MGO/LGO presentation and the Asteroid Rendezvous Spacecraft report.

In addition to satisfying science instrument requirements, the spacecraft configuration and attitude in all mission phases must satisfy the requirements for solar array illumination for all phases of the mission as discussed in the Attitude Control section.

To assist in this discussion a sketch of the proposed deployed configuration is shown in Figure 1 (see Section D17 for acronyms). The basic spacecraft is the TIROS-N vehicle mentioned earlier. The main body of the spacecraft has 3 circular, 18-inch diameter thermal louvers along its side panels.

The array is shown in the deployed position. When stowed, it is wrapped around the main body. The earth facing dish antenna is mounted on the body opposite to the Mars facing instrument panel and is gimballed for earth tracking. In the stowed configuration in the STS during the launch phase, the antenna boom is folded along the peak of the spacecraft body. The extendable and retractable booms for the MAG and GRS are located on the side panels of the spacecraft body.

All other instruments are mounted on the Mars-facing panel of the spacecraft, allowing for the FOV's for data collection and cooling needs.

The viewing and cooling FOV requirements for the Mars Orbiter preclude the location of the solar array and the earth communications dish within the hemisphere at the space viewing edge of the spacecraft.

The bipropellant tanks and equipment are located at the opposite end of the spacecraft from the instruments. In the launch configuration, the TOS stage is mounted beyond the bipropellant tank housing.

ORIGINAL PAGE IS
OF POOR QUALITY

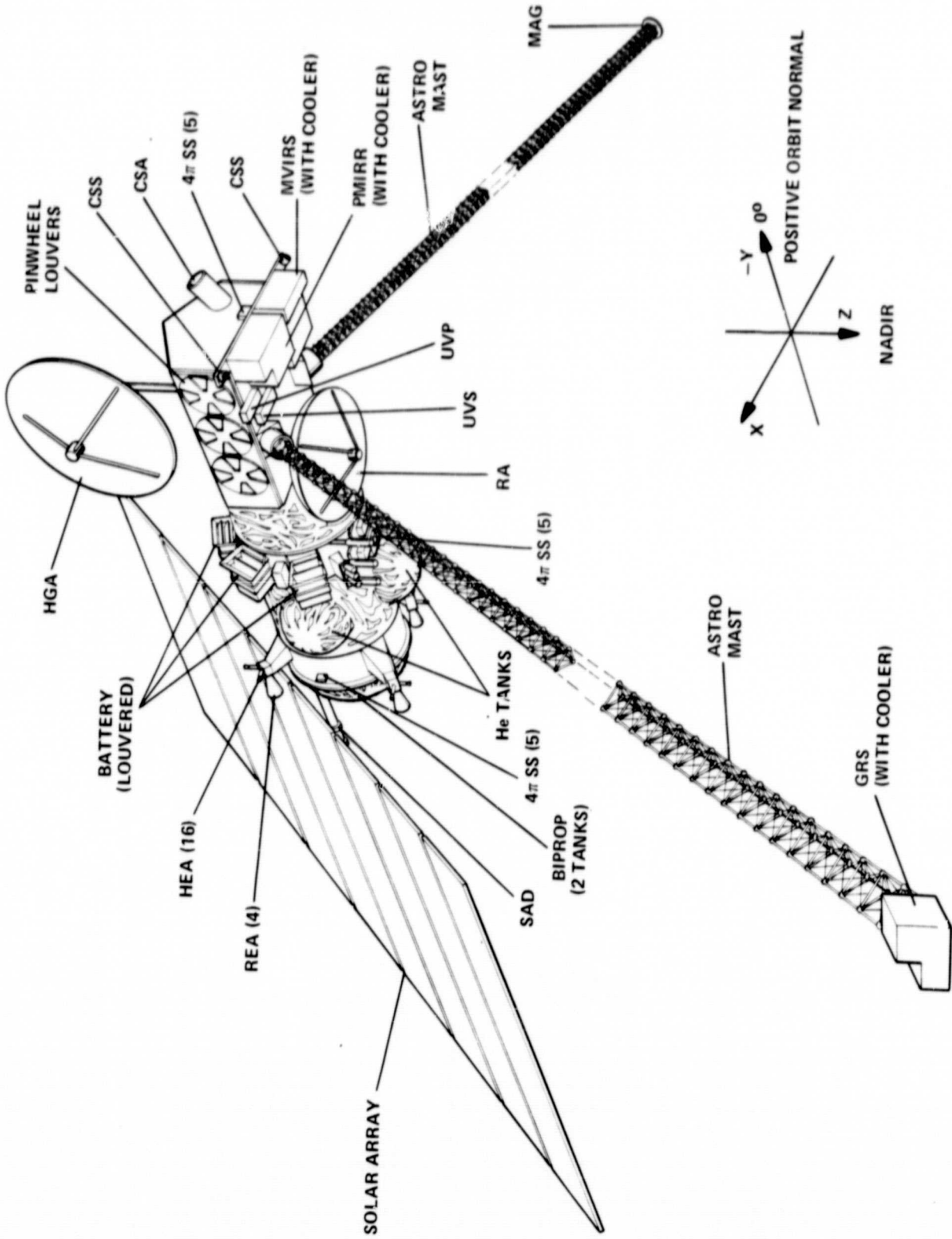


Figure 1. MCOO Spacecraft Configuration

Additional information on the configuration including FOV considerations are included in Appendix D.

B. SCIENCE INSTRUMENT ACCOMMODATION

1. Science FOV Instrument Requirements

As noted in the introduction, (a) one of the series of TIROS/ DMSP series (TIROS-N) is used as a baseline and (b) there are spacecraft in the series which can accommodate additional instruments and have added capability in almost all subsystem areas (Table 1). The identification of "excess capability" therefore, is limited to the TIROS-N type of spacecraft since it was selected as the candidate which most closely meets the Mars Orbiter requirements with sufficient margin to guarantee mission performance.

The science instruments were divided into three categories for configuration considerations.

- (1) Those which must be segregated from the spacecraft itself (GRS and MAG)
- (2) Those which require large FOV's for viewing and cooling (PMIRR, UVS and UVP)
- (3) Those which need a relatively narrow FOV (RA, MVIRS and possibly Radio Science)

The configuration studies completed to date on the Mars Orbiter, Lunar Orbiter, and Asteroid Rendezvous studies have shown that the science instrument complement can be physically accommodated on the TIROS-N bus. The sketch in Figure 1 shows the diagrammatic layout.

The GRS requires an unobstructed 2π Sr view of the nadir point. The magnetometer (MAG) must be kept free from magnetic fields of strength that interfere with its measurement capability. They are, therefore, located on extendable booms which are retractable for those thruster firing periods that would apply undue stress to the booms. Consideration has been given to mounting both on the same boom but insufficient knowledge is available at this time to make a firm decision. The GRS will require a view of space and sun shield to provide cooling.

The instrument mounting panel has been lengthened for two reasons.

- (1) To provide a mounting platform for coolers
- (2) To locate the PMIRR, UVS, and UVP where they have an unobstructed view for their particular FOV's (especially the UVP which must observe the zenith region)

Since the RA need only view the nadir, it is mounted at a convenient point between the other instruments on the Mars facing panel and the bipropellant system housing.

2. Science Instrument Constraints

Because of past experience in mounting many types of instruments on TIROS/DMSP spacecraft of several different configurations (over 60 spacecraft to date, few of which carry identical instrument groups), it appears that no major physical constraints result from mounting them on the TIROS-N spacecraft. When additional data becomes available (the large instrument contingency power figure in the standard requirements document suggest that added requirements are forthcoming) further refinement of these conclusions will be possible.

The requirements of the science instrument have been reviewed during the extended study. This review has resulted in the following conclusions.

- (1) The instruments can be accommodated on the TIROS spacecraft.
- (2) The combined FOV requirements for instrument viewing and coolers put some constraints on the candidate configurations, however, if these are considered of major consequence to JPL, these can be accommodated by the advanced TIROS-N spacecraft.
- (3) Science data can be collected in accordance with the various mission phases as defined by JPL with the constraints that the most of the image data collection during the phasing orbit is restricted to the polar region. However, all other instruments can be operated selectively during this phase.

III. SPACECRAFT BUS SUBSYSTEM ASSESSMENT

A. GENERAL

The first assessment of the ability of TIROS-N spacecraft bus to accommodate the science instrument payload needs resulted in the following overall evaluation.

<u>Subsystem</u>	<u>Preliminary Assessment of Margin</u>
Power	Sufficient - have some margin in the cruise mode and also in phasing orbit (if all instruments are not used full time in every orbit)
Command	Sufficient - requires interface matching, but exceeds needs
Data Handling	Basic elements meet requirements, after removing some tape recorders from TIROS-N spacecraft
Structure	Sufficient area for instruments. Can go to larger ATN body if added mounting area is required
Thermal	Sufficient - adapts to mission requirements
Attitude Control	Probably exceeds pointing accuracy requirement, depending on accuracy of ephemeris data at Mars
Propulsion	
Reaction Control	Sufficient propellant and margin for use in attitude control
TOS engine	Approximately 10% margin for 500 kg TIROS-N baseline
Biprop System	Sized for mission, can add propellant
Communications	Sufficient. Antenna pointing to DSN meets requirements

(See following discussion and attachments for further details.)

B. SPACECRAFT BUS EXCESS CAPABILITY

1. General

The basic ground rule for the selection of the spacecraft to meet the Mars Orbiter mission has been to maintain the flight-proven integrity of all equipment to assure mission success (see Figure 2).

The TIROS-N bus was selected for this application since the science instrument mounting could be accommodated on an existing structure, the command and data handling and attitude control subsystems have the flexibility to adapt to mission requirements through the addition or deletion of flight-proven equipment.

No new significant unproven component design or techniques are required to accommodate this mission.

2. Power Subsystem

The power requirements of the TIROS series of operational satellites vary with the payload needs. As a result, the solar array area and the numbers of batteries have been increased as mission demands grew. The power supply electronics design which have been qualified and/or flown span the mission requirements for the Mars mission. Therefore, in the event the science instrument contingency factors in the JPL standard requirements document are invoked, the TIROS-N bus can be upgraded to the advanced TIROS-N or, as in the past, an ATN power subsystem can be adapted to the TIROS-N bus.

With regard to "excess capability", adequate margins have been included to provide the required power for the mission. However, an excess in power capability is available during the cruise phase and during the phasing orbit, if the full science instrument payload is not required for the total orbit time.

3. Command Control and Data Handling

Although some additional functions may be required such as a command formatting unit to convert DSN uplink to ternary form required by the spacecraft command

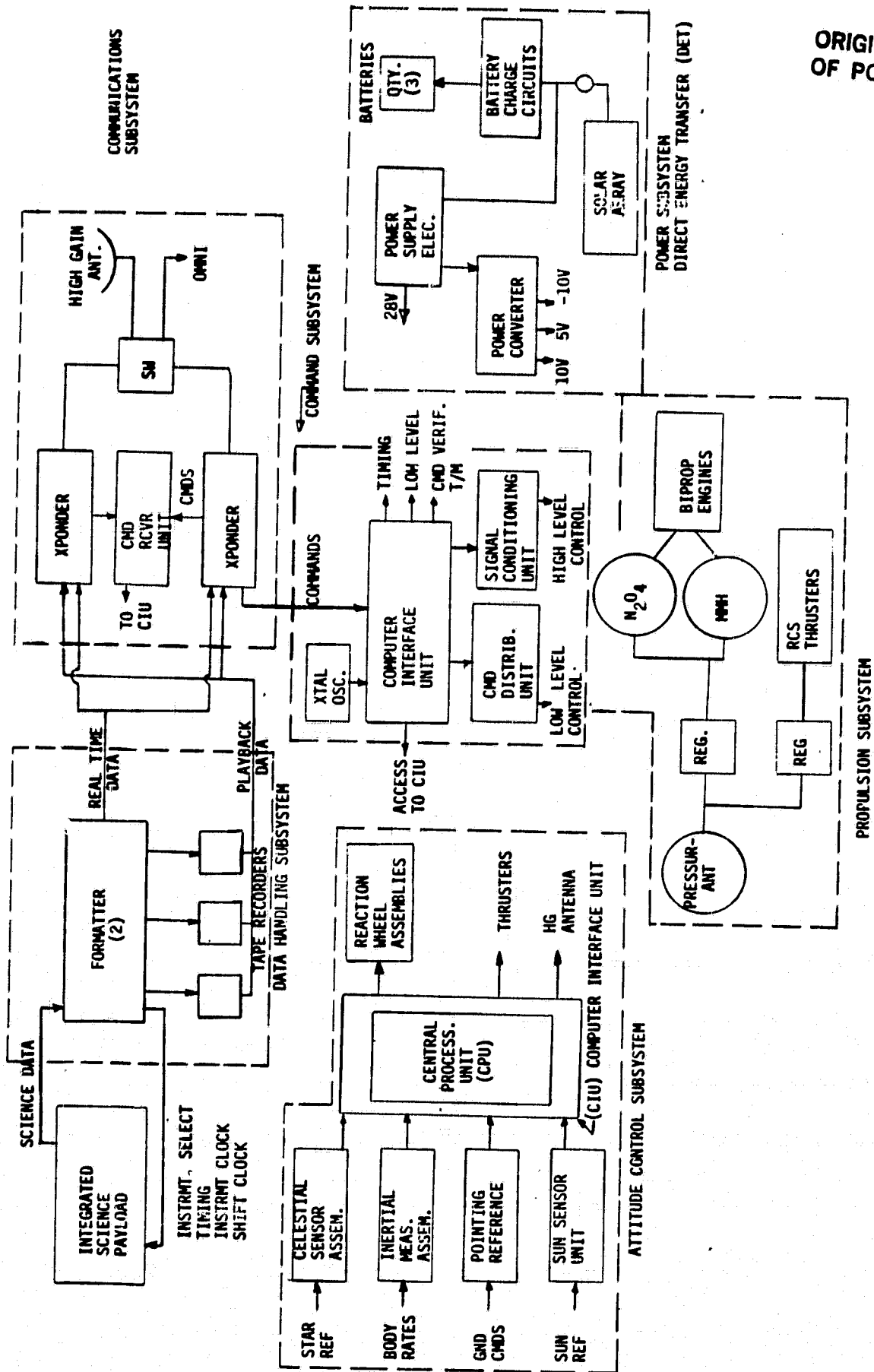


Figure 2. MGCO Spacecraft Block Diagram

distribution unit, the basic command system meets the command requirements. However, control signals to meet STS safety requirements and to accommodate relay drive or switched power requirements must be included. The telemetry handling and formatting system of the TIROS information processor (TIP) can be used to accommodate the ranges of digital data required for the mission.

Defining "excess capability" in the command and controls subsystem is difficult since the details of the command structure requirements have not been identified in detail. However, the SCP-234 computer utilized with the launch and orbit phases of the TIROS-N/DMSP spacecraft has a 32K read/write memory with single error correction/multiple-error detection capability and should provide extra capability for the mission if configured as on TIROS-N/DMSP where two computers provide either redundancy or additional performance as desired. The TIROS system provides a master clock at 5.12 MHz at one part in 10^8 per day, and two parts in 10^6 per year. If more precise clocking signals are required, the clock included by RCA in the NOVA satellites provide selectable increments to one part in 10^{10} per day.

The information processing capability of the TIROS information processor (TIP) can handle rates up to 16 kbps which can be supplemented to provide the 32 kbps rates desired. The DMSP system includes a programmable information processor (PIP) which may be considered for use here.

The TIROS system includes more tape recorder capacity than required, therefore, three recorders would probably be removed, providing additional power, space, and weight for other purposes.

4. Attitude Control Subsystem

The attitude control subsystem (see Appendix B) meets the mission requirements and may provide excess capability in its ability to orient the spacecraft, so as to provide both attitude knowledge and pointing accuracy up to five times the requirements for the data collection phases of the orbiting mission provided that the ephemeris data is known to the required accuracies. JPL may have the information from past Mars missions which may permit a better assessment of this added capability.

5. Structure

The structure of the TIROS-N spacecraft was designed to provide a variety of instrument complements, with the capacity for growth along the major axis of the spacecraft (see Table 1). An optimized layout for instruments on a particular spacecraft selected from the TIROS series should not include "excess capability" per se. However, added space for instruments can be had by selecting a later TIROS or DMSP spacecraft shown in Table 1.

6. Thermal

The thermal subsystem is also optimized to satisfy analytical results and predictions for thermal requirements for the mission. Added blankets, louvers, etc., that require little or no power can be added at a weight penalty. Added heaters cause a penalty in both weight and power. No effort was expended on this effort to provide "excess capability" beyond that which can be selected in tradeoffs against weight, power, and unique instrument requirements.

7. Propulsion Subsystem

The TOS stage, the bipropellant MOI subsystem, and other subsystem elements required for attitude control, momentum dumping, etc., are included in this section under propulsion.

A margin of 10% or so has been allotted within the TOS stage figures, so that some additional weight margin is available for assuring mission success for a 500 kg bogey.

The bipropellant liquid propulsion system was sized to provide the capability for Mars Orbit Insertion with margin to assure mission success. Here, too, this subsystem was sized for an optimized design with margins, as is true for the in-orbit propellant requirements.

Sufficient propellant can be included to permit JPL to elect to extend the mission for an additional Mars year (see Appendix C).

IV. SUMMARY AND RECOMMENDATIONS

- A. The TIROS-N spacecraft bus can satisfy the science instrument interfaces and the mission requirements of the Mars Orbiter mission.
- B. Some "excess capability" exists on the TIROS-N bus in its ability to provide knowledge of orientation of the spacecraft and pointing accuracy. In addition, the command, control and data handling subsystems appear to have extra capability beyond the requirements defined to date. However, since the cost impact of this extra capability is reflected only in recurring costs which are not significant, removal of this capability would only increase program costs.
- C. If added capability is required because of the addition of more science instruments or for other mission functions, this can be achieved by modification to the existing design or choosing another TIROS series spacecraft (Advanced TIROS-N or SAATN, see Table 1).

APPENDIX A
MISSION ANALYSIS

APPENDIX A
MISSION ANALYSIS

A1. ORBIT ACHIEVEMENT OUTLINE

For the purpose of introducing the mission analysis for MGCO it is worthwhile outlining the baseline orbit-achievement scheme. In effect this outline will summarize the results of the various sections of the orbit achievement analysis which are discussed in the later sections of this appendix.

In the baseline mission, launch of the MGCO spacecraft will be performed by the STS and the TOS (Transfer Orbit Stage). The type II Earth-Mars transfer, launching in 1990 within a 20 day launch window, has been considered. This is the reference Earth-Mars transfer for which data has been supplied by JPL. The combination of this launch system and transfer trajectory yields a high launch weight margin over the lift off weight of the proposed modified TIROS spacecraft design for the MGCO.

Injection onto the interplanetary cruise trajectory will be co-planar with the STS parking orbit. Following separation from the Shuttle, the attitude of the TOS will be controlled through its burn out by its own attitude determination and control subsystem (ADACS). Separation from the TOS will occur at burn out. The expended TOS will not be targeted accurately enough at this time to impact Mars, and therefore is of no concern regarding planetary quarantine. It may be positively biased in order to assuredly miss Mars.

Trajectory trim maneuvers, for launch error correction and for later precision targeting as Mars is approached, will be performed by the integrated bipropellant propulsion subsystem under command of the spacecraft computer in accordance with DSN-based tracking for navigation. The budget allowance for trajectory trims is 100 m/s.

Within minutes of injection onto the cruise trajectory the solar array will be deployed in order to avail the spacecraft of sufficient solar energy. The solar array boom, however, will remain folded and captive along the top of the electronics support module (ESM) throughout the cruise phase. In addition,

the booms for the GRS and MAG instruments will be deployed during the cruise, for calibration purposes. The solar array will survive Mars orbit insertion (MOI) in this configuration, though the instrument booms will be fully retracted, to be re-deployed later.

MOI into an initially highly elliptical capture orbit will be achieved by using the biprop system to perform a long duration burn, at a low thrust to mass ratio, along the approach trajectory, which will pass over the North Pole. The capture periapsis will be targeted to be at an altitude of approximately 360 km. The capture apoapsis altitude may well range between 8000 and 23000 km, depending upon the final nature of the capture burn. The capture burn is not critical throughout a wide range and thus allows contingency orbit-achievement strategies. The inclination of the capture orbit will be 90° as a result of the precise targeting of the arrival asymptotic trajectory; and no plane change will occur on insertion.

Through use of the biprop system around apsidal passes, the insertion orbit will be adjusted until it is approximately circular at 350 km altitude. Great flexibility in orbit control will result from this multiple burn insertion strategy.

The initial o'clock positions for the ascending nodes of the insertion and the mapping orbits are nominally 4 a.m. and 2 a.m., respectively. Following insertion, therefore, a drift phase lasting 59 days will ensue, during which the heliocentric motion of Mars will effect a change in the node o'clock position between these values. This type of node-changing drift phase has been proposed previously by RCA for the future STS launched versions of the TIROS and DMSP spacecraft. In the drift phase, the solar array boom and possibly the GRS and MAG booms may be deployed in order that science measurements may be made, especially over the polar regions of Mars, and transmitted to Earth.

At the end of the drift phase, the biprop system will be used to change the orbital inclination to 92.87° , and thereby achieve nominal Sun synchronism of the orbit plane.

During the drift and mapping phases of the mission, the eccentricity of the orbit will vary periodically due principally to the asymmetry of the gravitational field of Mars and also to a lesser extent due to solar gravity perturbations. Cyclical variations in the eccentricity will result in excursions of the periapsis to lower altitude and associated increases in atmospheric drag. Drag will be especially significant during passages through the dayside bulge of the atmosphere around the time of the solar maximum. The biprop system and possibly the use of a frozen orbit will be employed to limit these variations of the orbit within acceptable bounds throughout the mapping phase (≥ 1 Mars year).

It is necessary to ensure that neither the spacecraft nor any other hardware/debris impacts the surface of Mars prior to the expiration date of the NASA planetary quarantine policy, at the end of the year 2018. At the chosen end of life (EOL) of the mission, the orbit will be raised, using the biprop system, into a stable, initially circular orbit at an altitude of at least 525 km, in order to ensure compliance with the planetary quarantine requirements.

A2. EARTH-MARS CRUISE TRAJECTORY

The reference Earth-Mars trajectory supplied by JPL has been used to define the baseline MGCO spacecraft design. This trajectory requires a two impulse type II transfer; i.e., an injection maneuver for departure from the STS parking orbit followed by passage through a heliocentric angle greater than 180° and an insertion maneuver for MOI.

Realistic launch considerations dictate that at least 20 consecutive days be available for launching an interplanetary mission. The principal characteristic features of this transfer, incorporating a 20-day launch window, are shown in Table A-1.

This trajectory is optimum in the sense of allowing delivery of the maximum mass into orbit around Mars. In fact, however, the results of the "excess performance capabilities" study reported for the propulsion system in Appendix C has identified some margin in useful spacecraft weight (currently estimated to correspond to 111 kg for the maximum TOS capability) over the minimum spacecraft weight necessary to perform the reference extended mission. As one possibility, it is feasible that this margin could be traded off against

widening the set of possible Earth-Mars trajectories, e.g., to reduce the insertion retro-velocity requirement.

The worst-case values of C_3 and V_∞ for the reference trajectory and a 20-day launch window, i.e., $16.29 \text{ km}^2/\text{s}^2$ and 2.954 km/s , have been taken together as a pair in order to define the baseline spacecraft design. In fact, as shown in Table A-1, these worst-case values do not occur simultaneously. Taking the two as a pair, therefore, introduces conservatism into the design. When the actual combinations of C_3 and V_∞ are considered in the next study phase, the weight margin will undoubtedly be higher than reported herein.

The value of declination of launch asymptote, DLA, varies between 4.8° and -0.2° over the launch window. The relevance of DLA is illustrated in Figure A-1.

TABLE A-1. TWENTY-DAY LAUNCH PERIOD FOR 1990 MGCO REFERENCE MISSION

	First Launch Date	Last Launch Date	Units
<u>Launch Date (1990)</u> ¹	August 20	September 9	
Launch Energy - C_3	16.29	15.81	(km/sec) ²
Launch Declination ²	4.8	-0.2	deg
<u>Arrival Date (1991)</u> ¹	August 12	August 30	
Flight Time	357	355	days
Arrival V-infinity	2.712	2.954	km/sec
Arrival Declination ³	33.3	34.8	deg
ZAP Angle ⁴	55.1	53.4	deg

¹Launch and arrival times assumed at 0000 Hours UT.
²Earth Equator and Equinox of 1950.
³Mars Equator and Equinox of Date.
⁴Sun - Mars - V-infinity Angle.

ORIGINAL PAGE IS
OF POOR QUALITY

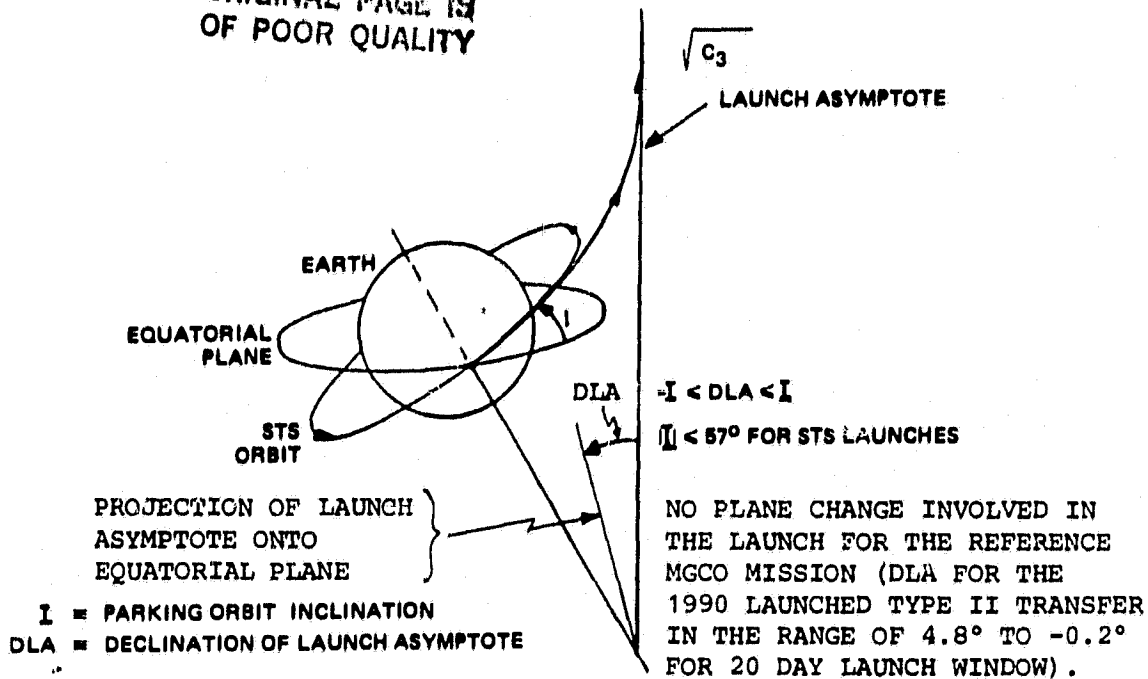


Figure A-1. STS Launch Geometry

If the inclination of the parking orbit is denoted by I , it may be seen from the figure that any value of DLA satisfying the relationship $-I < DLA < I$ may be achieved without a plane change being effected by the upper stage. All that is required is injection at the appropriate time and position in the parking orbit. Of course the correct alignment of the launch asymptote must be ensured by correct orientation of the STS parking orbit, which is determined through STS launch window selection.

Further regarding DLA, it may be shown that for MOI into near-polar orbits, no plane change will be necessary at Mars, any necessary plane-orientation adjustment being achievable at very little propulsive cost by one or more mid-course maneuvers. This would not be the case were the Mars insertion orbit required to be near-equatorial. The value of DLA, therefore, is not very significant in regard to MOI for the MGCO mission.

A3. LAUNCH SYSTEM SELECTION

A group of twelve launch systems below, are either currently available, soon to be available, or are conceptual were considered for the MGCO launch.

1. STS/PAM-D
2. STS/PAM-A
3. STS/IUS Two-Stage
4. STS/Centaur F
5. STS/Injection Module (IM)
6. STS/PAM-D2
7. STS/TOS
8. STS/IUS-1/PAM-D
9. STS/IUS-1/IM
10. TITAN 34/IUS Two-Stage (w/o EEC)
11. Delta 3920/PAM-D
12. Delta 2914

Feasibly, this listing could have been extended to include combinations of rocket motors, such as the SRM-1, acquired separately and integrated by RCA. Superficially this approach would seem to allow significant cost reductions, at the expense of increased complexity and risk.

As a result of these considerations JPL has specified the TOS as the transfer orbit stage for the MGCO mission. The TOS will be commercially available from Boeing and possibly Orbital Systems Corporation, Inc.

The engineering rationale behind this selection may be seen in Figure A-2. In this figure the payload weight at liftoff for performing the minimum required MGCO mission, i.e., 1755 kg as detailed in Table C-1, is shown against the planetary performance curves of the twelve launch systems.

The launch mass of 1755 kg was calculated starting from the end of life (EOL) "useful-mass" of the MGCO spacecraft of 500 kg (excluding propulsion system mass). The requirements and constraints that were figured into the calculation are:

- Bipropellant I_{sp} = 312 seconds through MOI, and is conservatively estimated thereafter
- EOL maneuver to achieve quarantine orbit, $\Delta V = 82.3^*$ m/s
- Orbit maintenance maneuvers, $\Delta V = 151^*$ m/s
- Inclination change (phasing-mapping orbit), $\Delta V = 168.5^*$ m/s
- MOI maneuvers (divers scenarios), $\Delta V = 2365^*$ m/s
- Trajectory correction maneuvers, $\Delta V = 100$ m/s
- helium mass = 4 kg
- TOS adapter mass = 100 kg

*includes inefficiencies due to low thrust and also to the predicted performance dispersions

- 1 STS/PAM-D
- 2 STS/PAM-A
- 3 STS/IUS TWO-STAGE
- 4 STS/CENTAUR F
- 5 STS/IM
- 6 STS/PAM-D2
- 7 STS/TOS
- 8 STS/IUS-1/PAM-D
- 9 STS/IUS-1/IM
- 10 TITAN 34/IUS TWO-STAGE (W/O EEC)
- 11 DELTA 3920/PAM-D
- 12 DELTA 2914

▲ JPL SELECTED REFERENCE OPPORTUNITY SHOWN - VALUE OF C₃ IS MAXIMUM OF 16.29 km²/s² ON FIRST DAY OF 20 DAY LAUNCH WINDOW (I.E. 8/20/99)

† INCLUDES 100 kg LAUNCH ADAPTER

* EOL S/C MASS MINUS PROPULSION SYSTEM MASS

— CURRENT OR UNDER DEVELOPMENT

- - - PROPOSED CONCEPT (DATA ARE PRELIMINARY ESTIMATES)

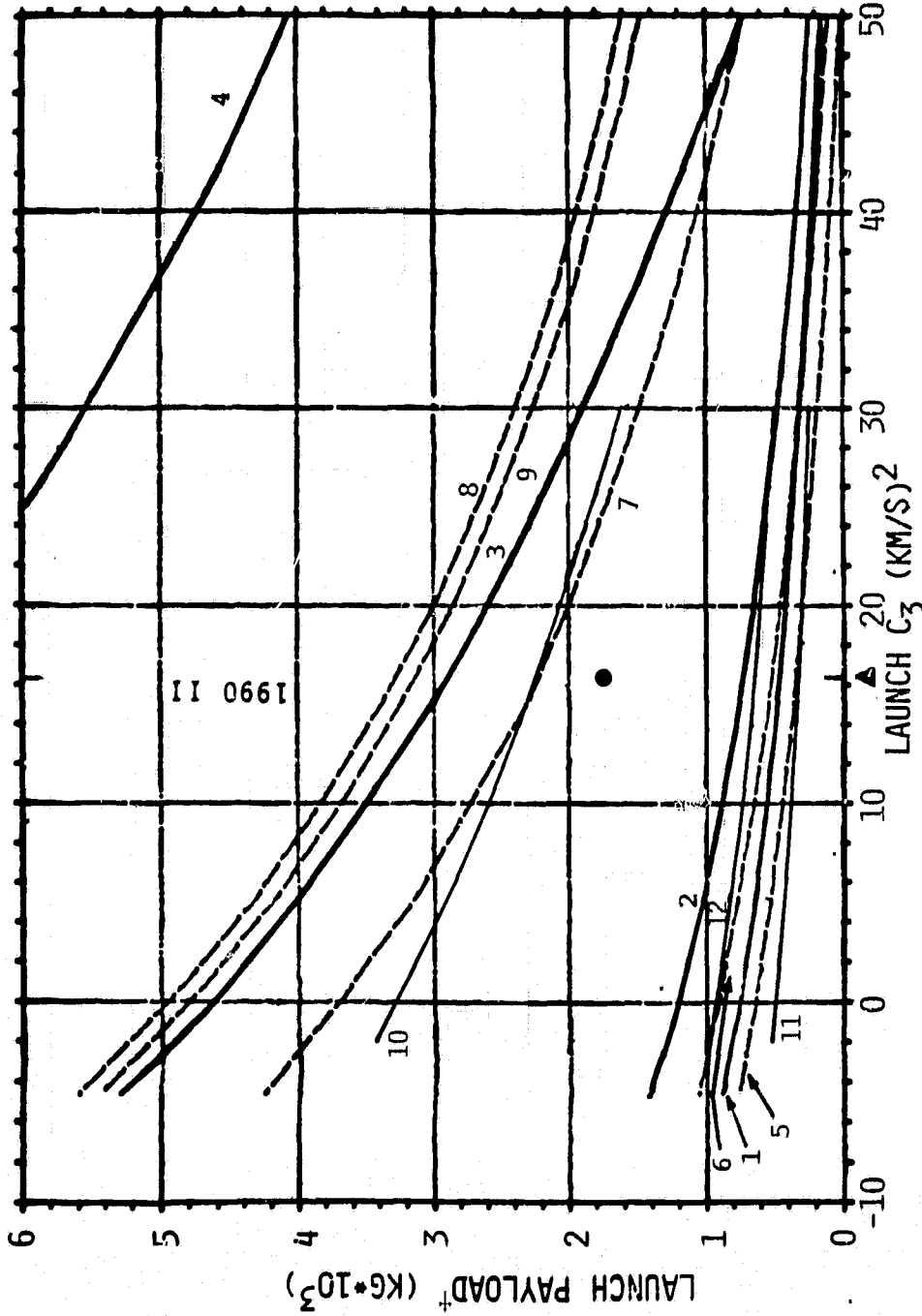


FIGURE A-2. MATCH OF TWELVE LAUNCH SYSTEMS AND THE MASS OF THE TOTAL LAUNCH PAYLOAD†, FOR THE 500 KG CLASS* TIROS-BASED MICO SPACECRAFT

Figure A-2. Match of Twelve Launch Systems and the Mass of the Total Launch Payload† for the 500 kg Class* TIROS-Based MICO Spacecraft

Note that the term "launch mass" as used here includes the mass of the adapter between the TOS and the MGCO spacecraft, which is currently estimated to be 100 kg.

It is clear that even the minimum throw mass of the MGCO spacecraft is beyond the capability of the STS/PAM-A and all less capable systems.

The next more powerful launch system beyond the STS/PAM-A is the Titan 34/IUS Two-Stage. This is not a favored launch system for several reasons. First, both the Titan 34 booster and the IUS Two-Stage will be much more expensive than the baseline choices, which are the STS and the TOS upper stage. Second, the IUS Two-Stage has a limited expected production run, especially now that the development of the STS/Centaur F has been recommended. Third, by the time of the MGCO mission launch, 1990, the STS will be fully operational.

For the minimum throw mass of 1755 kg, the TOS would be offloaded by approximately 10%. It may be seen in both Figure A-2 and Table C-1 that the maximum throw mass capability for the TOS is approximately 2080 kg. Appendix C describes how this throw mass margin of 325 kg corresponds to an increase in the "useful" spacecraft mass of 111 kg.

A4. LAUNCH PHASE

The launch phase of the mission will consist of boost from the Kennedy Space Center on board the Shuttle into a circular parking orbit at 296 km altitude, followed by deployment from the cargo bay and injection onto the interplanetary cruise trajectory.

The MGCO spacecraft, being evolved from TIROS spacecraft launched by expendable launch vehicles, will fit easily into the Shuttle cargo bay, even with a Sun/contamination shield should one be necessary. The spacecraft will be supported in the cargo bay by a special cradle structure which may have some commonality with the cradle for proposed STS launched TIROS and DMSP spacecraft. A conical adapter will mount the spacecraft to the TOS. The structure will be capable of handling the specified physical environments, the most severe of which will probably be those during emergency landing of the Shuttle and during TOS firing. Shuttle emergency landing load factors may typically be ~ 4.5 g in the Shuttle X

and Z directions. By comparison, the maximum acceleration of the TOS, with a payload of 1755 kg, will be ~ 4.6 g.

While the spacecraft is inside the cargo bay it will probably require thermal and contamination shielding. Before deployment the spacecraft will be in a quiescent, but powered-up state; and some internal heat dissipation will occur. A full thermal analysis will be necessary in further studies. Preferably, the design will be made to feature passive thermal control only.

The injection stack will be deployed from the Shuttle by the standard spring actuated TOS deployment system. The Shuttle orientation at separation may be held so that the orientation of the stack will be as close as possible to that required at ignition. The attitude determination system of the TOS will be initialized while still inside the Shuttle. Following separation and through the TOS burn the attitude of the stack will be controlled by the RCS and gimbaled thrust nozzle of the TOS. It is worth mentioning here that since the TIROS-based MGCO spacecraft will have its own attitude determination and control subsystem (ADACS), of a different injection stack (e.g., a stack incorporating the SRM-1 integrated by RCA) by the spacecraft is feasible.

Following separation, there will be a period of between approximately a half to one orbit during which the stack will drift to a clearance distance from the Shuttle that is safe for ignition.

At the appropriate moment, the TOS is ignited. The nominal burn time is 146 seconds. At burn out the orbital velocity (with respect to the Earth) will have been increased from 7.728 km/s to the value corresponding to the desired C_3 . For the 1990 launch, type II reference transfer, the maximum value of C_3 during the 20-day launch window, i.e., on 20th August (the first day), is $16.29 \text{ km}^2/\text{s}^2$.

Accordingly the relationship

$$V_{\text{injection}} = \left[C_3 + \frac{2\mu_E}{r_0} \right]^{1/2}$$

where C_3 = square of the departure hyperbolic excess velocity
 μ_E = gravitational constant for Earth = $398,601 \text{ km}^2/\text{s}^2$
 r_0 = initial orbit radius = 6,674 km

gives the injection velocity of 11.651 km/s. The TOS, therefore, imparts a velocity increment of 3.923 km/s to the stack. The geometry of the injection is shown in Figure A-1 and has been discussed in Section A2.

A5. EARTH-MARS CRUISE PHASE

The type II Earth-Mars transfer of the reference mission features a "coasting" trajectory which is essentially a section of an elliptical orbit around the Sun through a heliocentric angle of approximately 250°.

For the reference 20-day launch window the transfer time is almost constant at 357 to 355 days.

Plots of the development of pertinent spatial relationships relating to the geometry between the spacecraft, Mars, the Earth and the Sun, are shown in Figures A-3 through A-11 for the reference cruise trajectory launching at the opening of the window (i.e. cruise phase between 8/20/90 and 8/12/91). Figures A-12 through A-20 are the analogs of Figures A-3 through A-11 for the reference cruise trajectory launching at the closing of the window, (i.e., cruise phase between 9/9/90 and 8/3/91). Figures A-3 and A-12, the chase diagrams, are useful in aiding visualization of the relative orientations of the spacecraft and these celestial bodies. Note that the Sun angle referred to in Figures A-7 and A-16 is the angle between the Sun direction and the normal to the Earth-Mars transfer plane. It is shown here to indicate how far the cruise trajectory departs from the ecliptic plane, and how the Sun incidence angle would vary if the spacecraft were held inertially fixed, aligned with the normal to the cruise trajectory. The information shown graphically in these figures has been incorporated into the analyses of the configuration and of the communications, power and thermal subsystems for the MGCO spacecraft.

Figures A-8, A-9, A-17, and A-18 show that for trajectories following launches through the 20 day reference launch window, there are no conjunctions, or close conjunctions, of the Sun and spacecraft as seen from the Earth, nor of the Earth and the Sun as seen from the spacecraft, to cause degradation or interruption of communications.

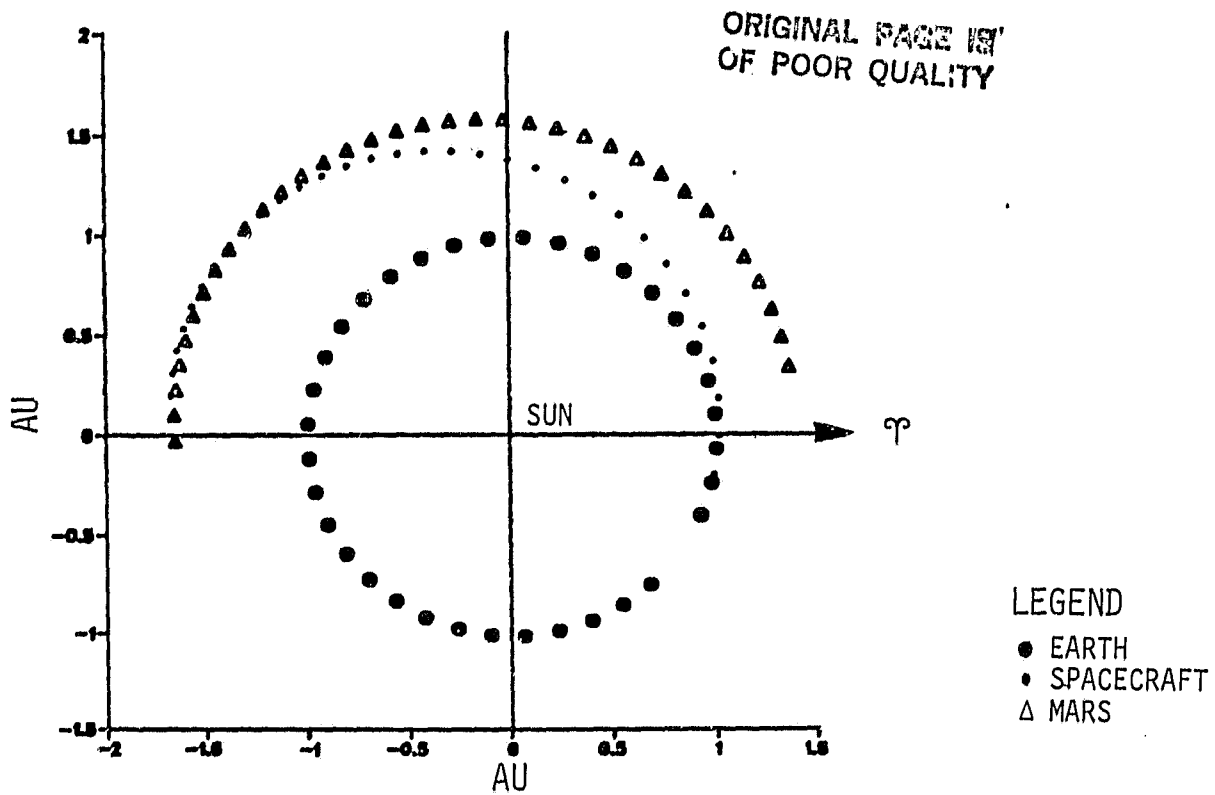


Figure A-3. 1990-91 Type II Mars Transfer Body Ephemerides -
10-Day Step (Opening of 20-Day Launch Window)

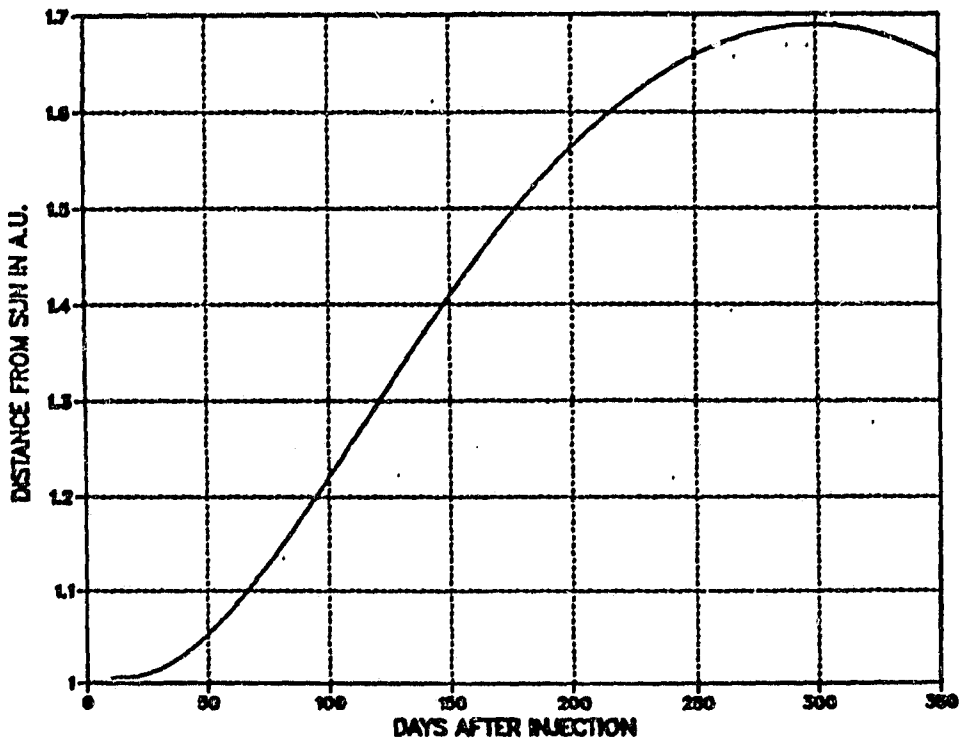


Figure A-4. 1990-91 Type II Mars Transfer Solar Distance
(Opening of 20-Day Launch Window)

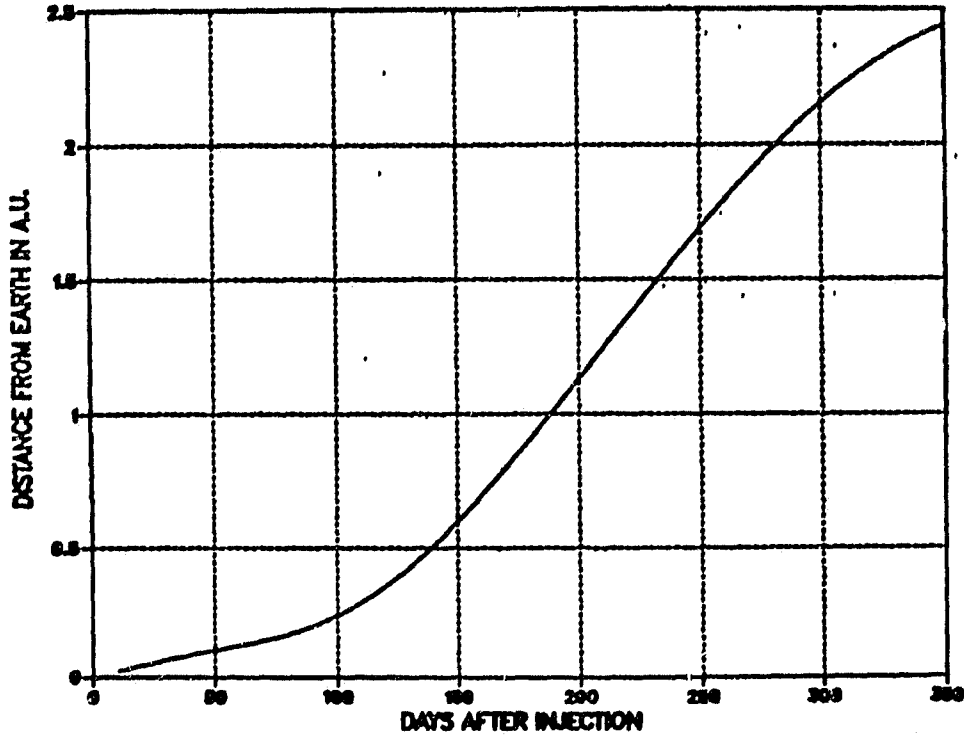


Figure A-5. 1990-91 Type II Mars Transfer Communications Distance
(Opening of 20-Day Launch Window)

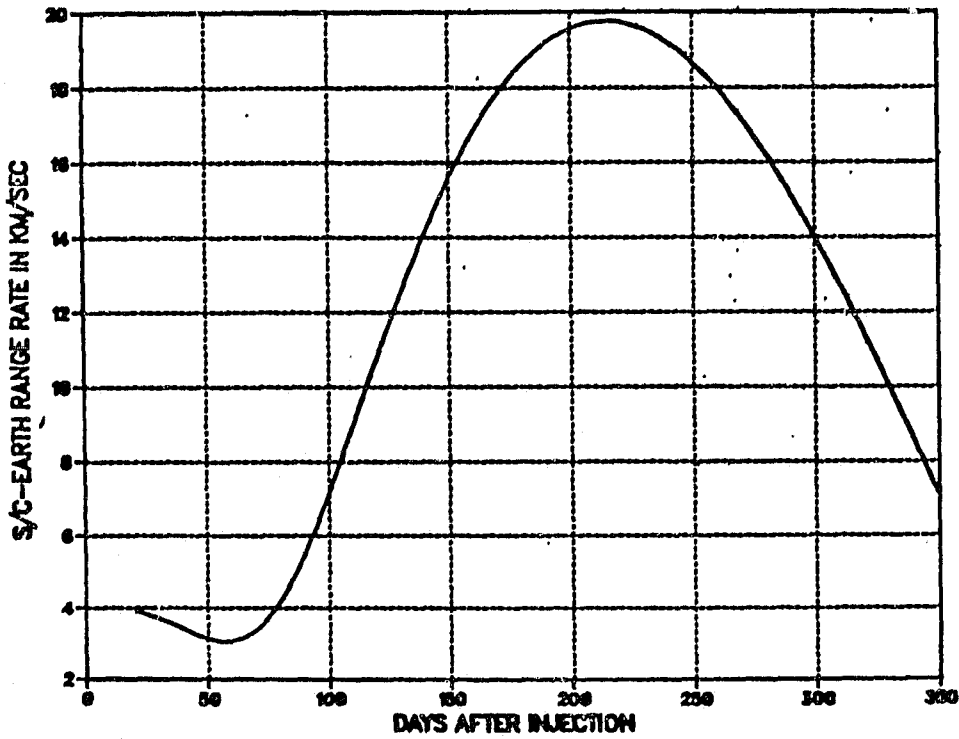
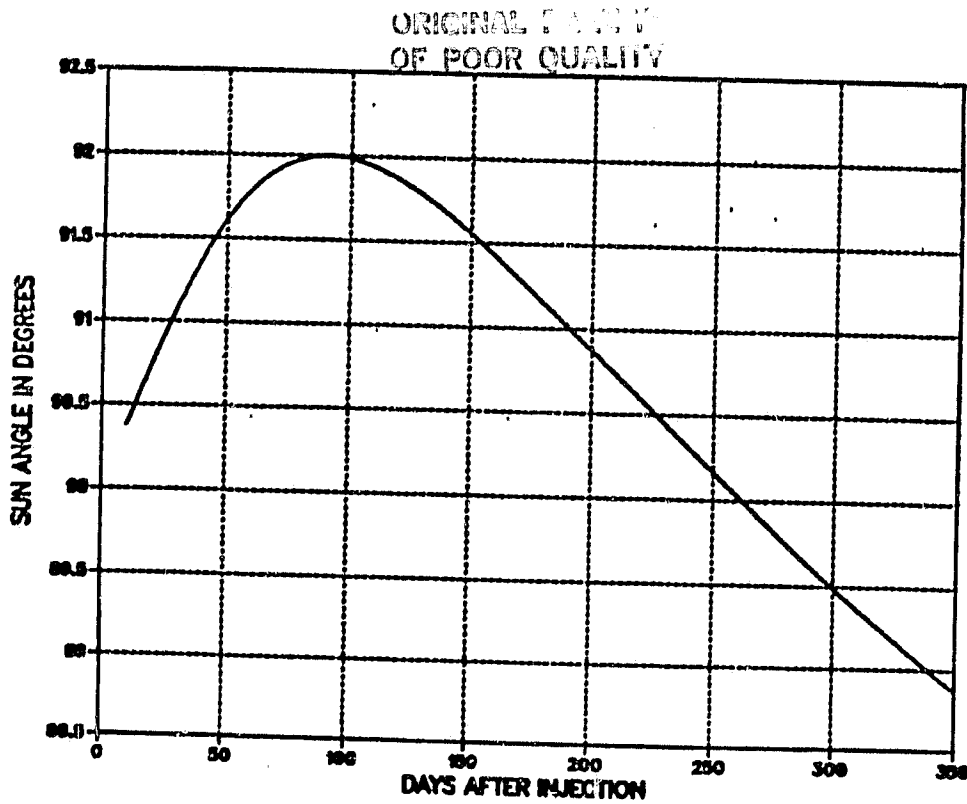


Figure A-6. 1990-91 Type II Mars Transfer S/C - Earth Range Rate
(Opening of 20-Day Launch Window)



*ANGLE BETWEEN SUN DIRECTION AND NORMAL TO CRUISE TRAJECTORY

Figure A-7. 1990-91 Type II Mars Transfer Sun Angle History*
(Opening of 20-Day Launch Window)

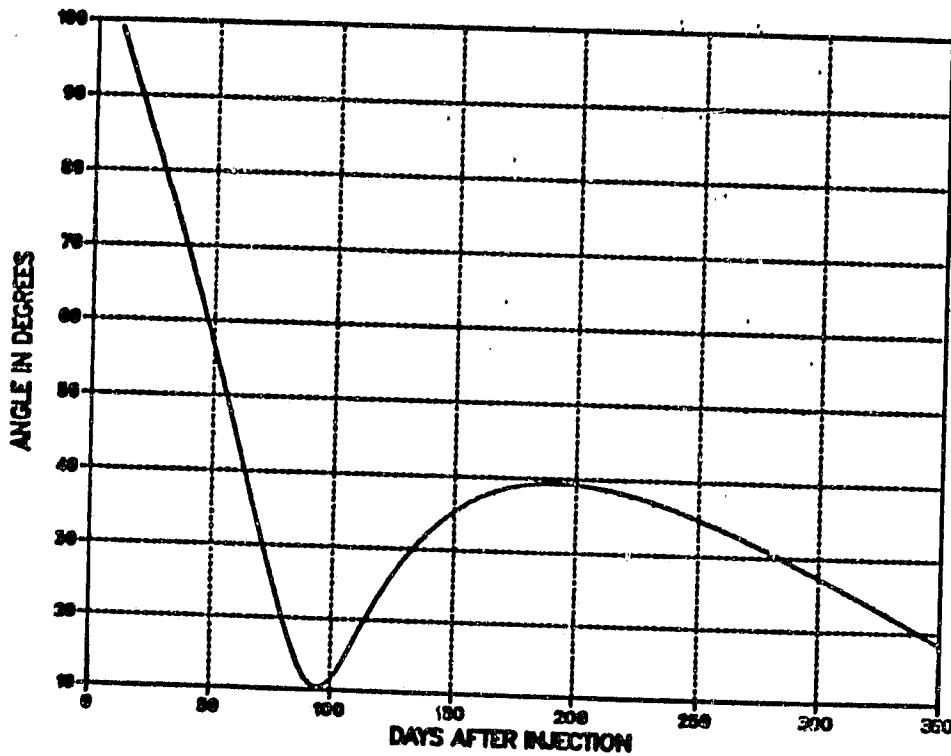


Figure A-8. 1990-91 Type II Mars Transfer Sun-S/C-Earth Angle History
(Opening of 20-Day Launch Window)

ORIGINAL PAGE IS
OF POOR QUALITY

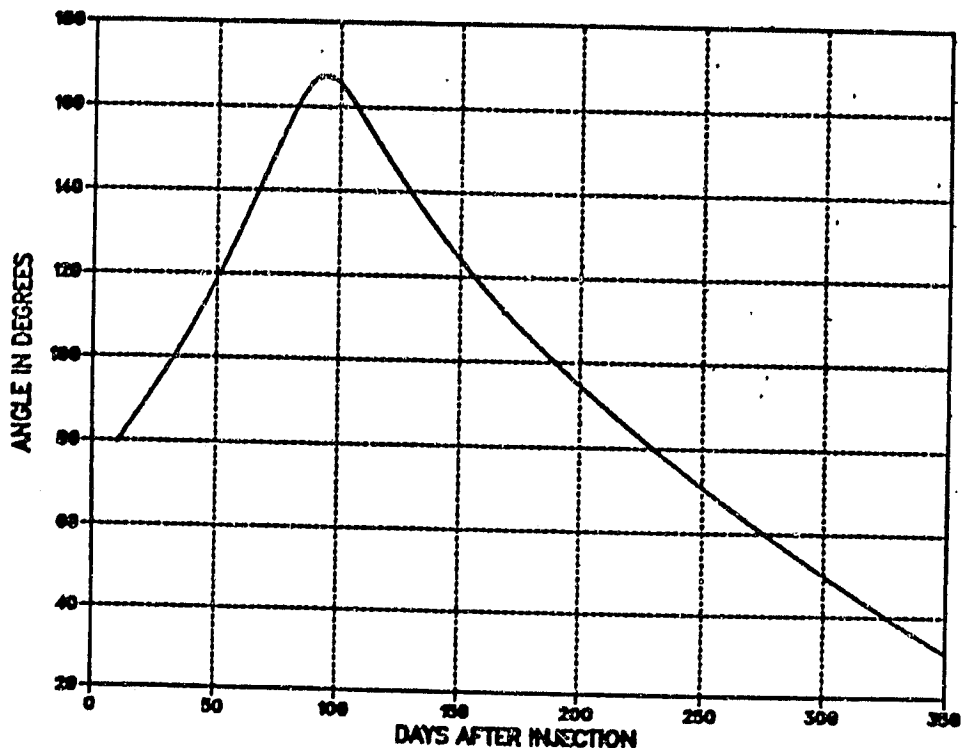


Figure A-9. 1990-91 Type II Mars Transfer Sun-Earth-S/C Angle History (Opening of 20-Day Launch Window)

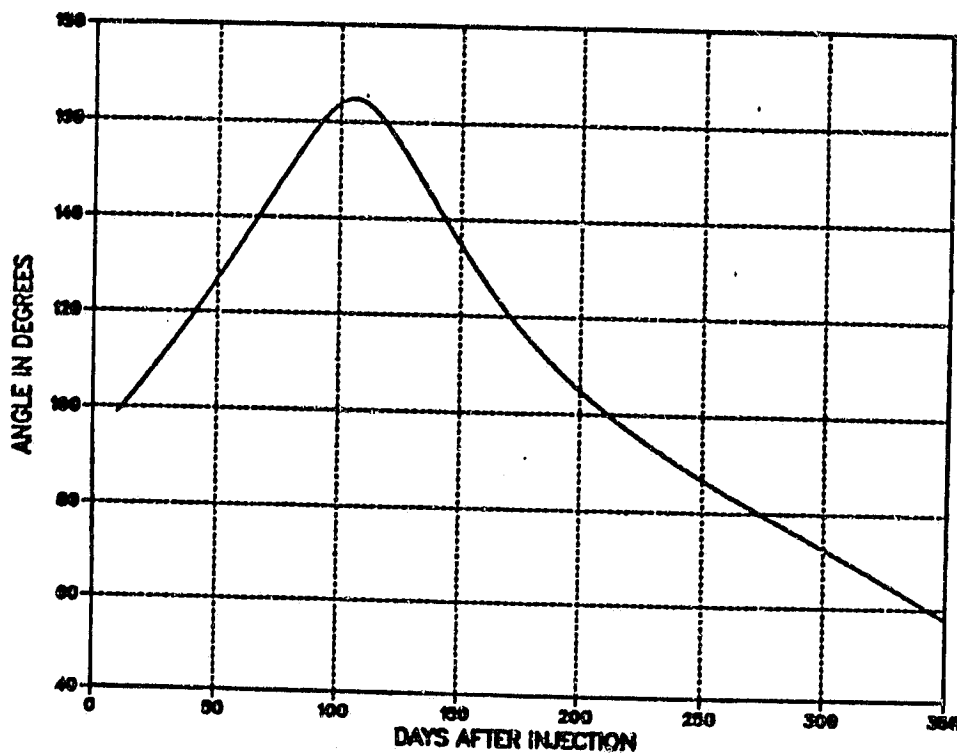


Figure A-10. 1990-91 Type II Mars Transfer Sun-S/C-Mars Angle History (Opening of 20-Day Launch Window)

OPTIMIZATION OF FOUR QUANTITIES

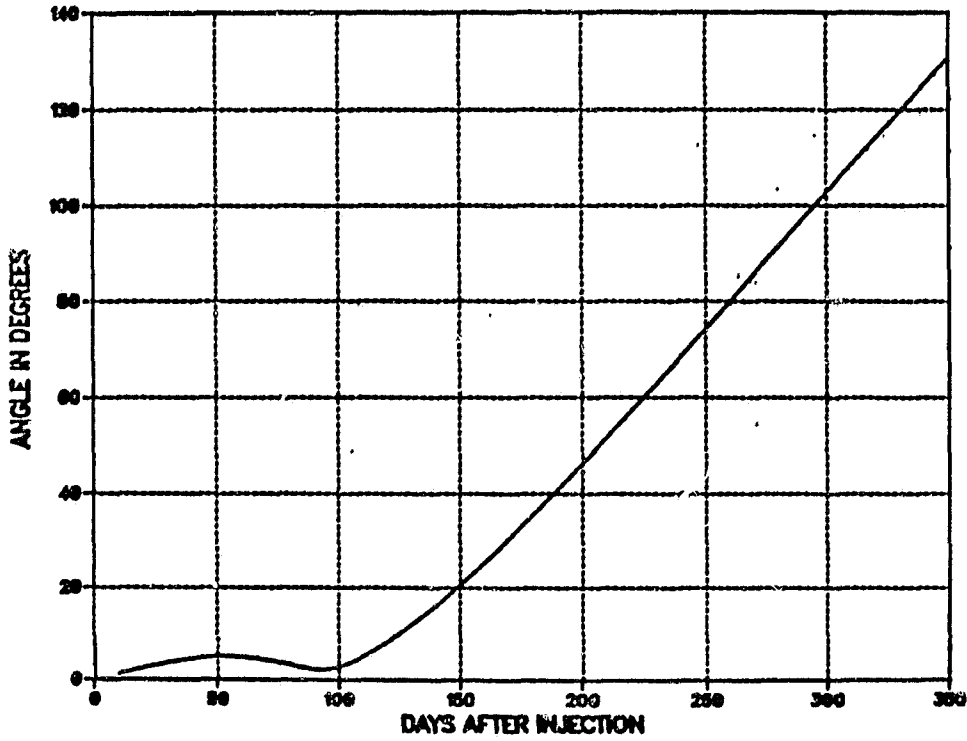


Figure A-11. 1990-91 Type II Mars Transfer Earth-Sun-S/C Angle History (Opening of 20-Day Launch Window)

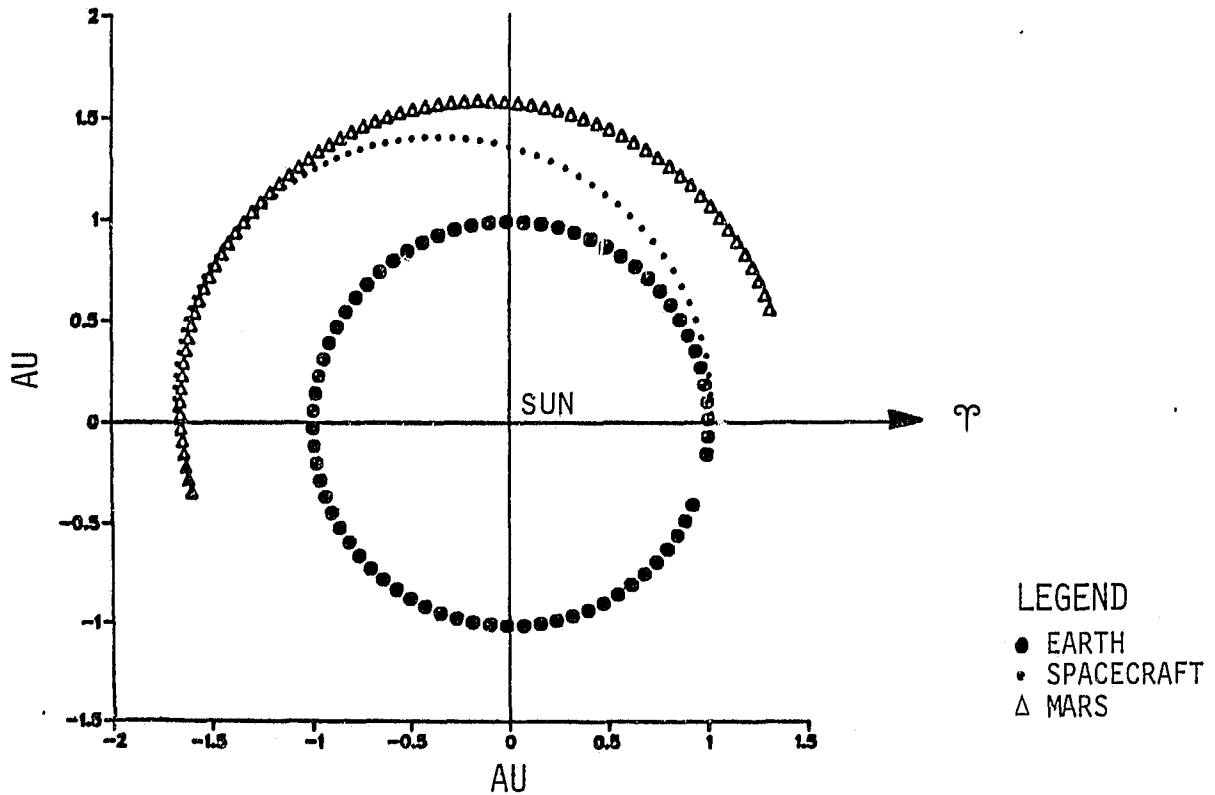


Figure A-12. 1990-91 Type II Mars Transfer Body Ephemerides - 5 Day Step (Closing of 20-Day Launch Window)

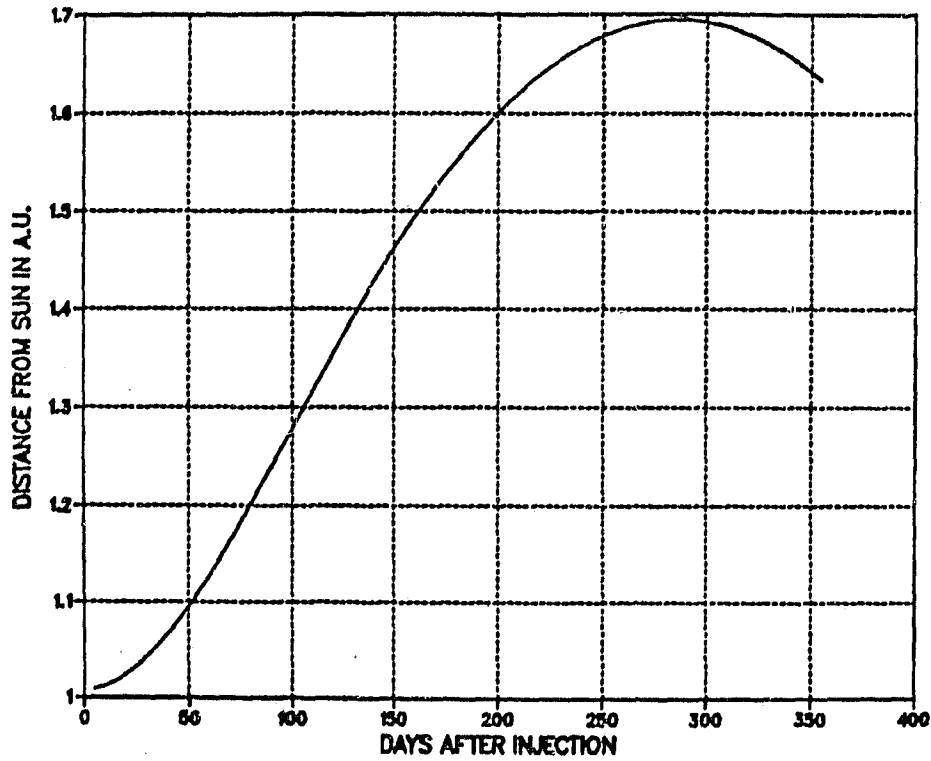


Figure A-13. 1990-91 Type II Mars Transfer Solar Distance
(Closing of 20-Day Launch Window)

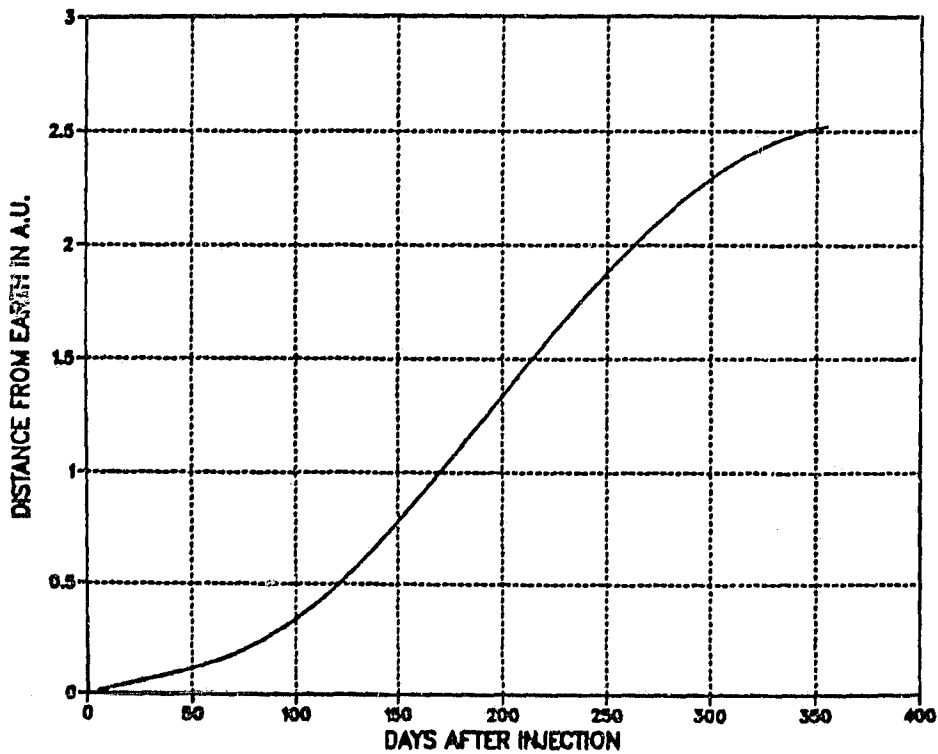


Figure A-14. 1990-91 Type II Mars Transfer Communications Distance
(Closing of 20-Day Launch Window)

ORIGINAL PAGE IS
OF POOR QUALITY

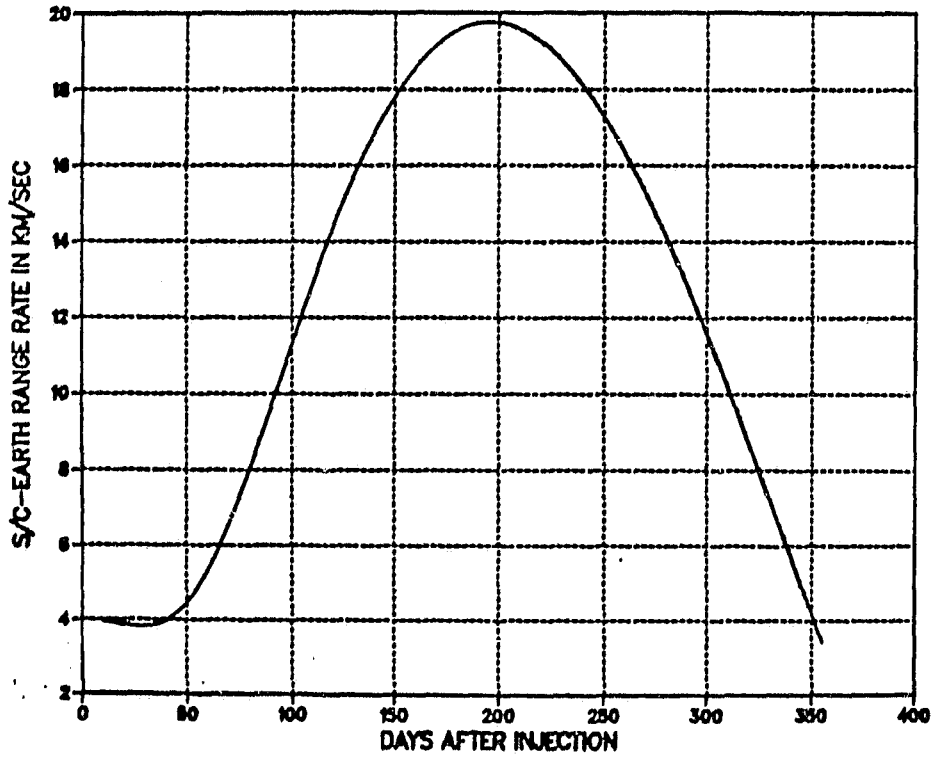
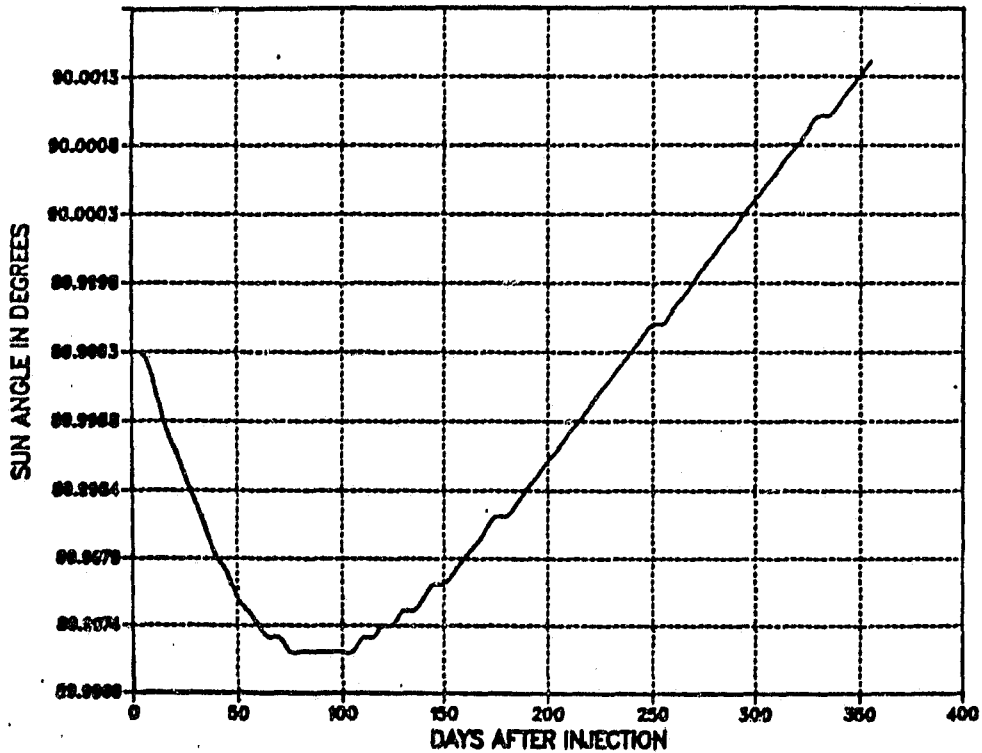


Figure A-15. 1990-91 Type II Mars Transfer S/C-Earth Range Rate (Closing of 20-Day Launch Window)



*angle between Sun direction and normal to cruise trajectory.

Figure A-16. 1990-91 Type II Mars Transfer Sun Angle History* (Closing of 20-Day Launch Window)

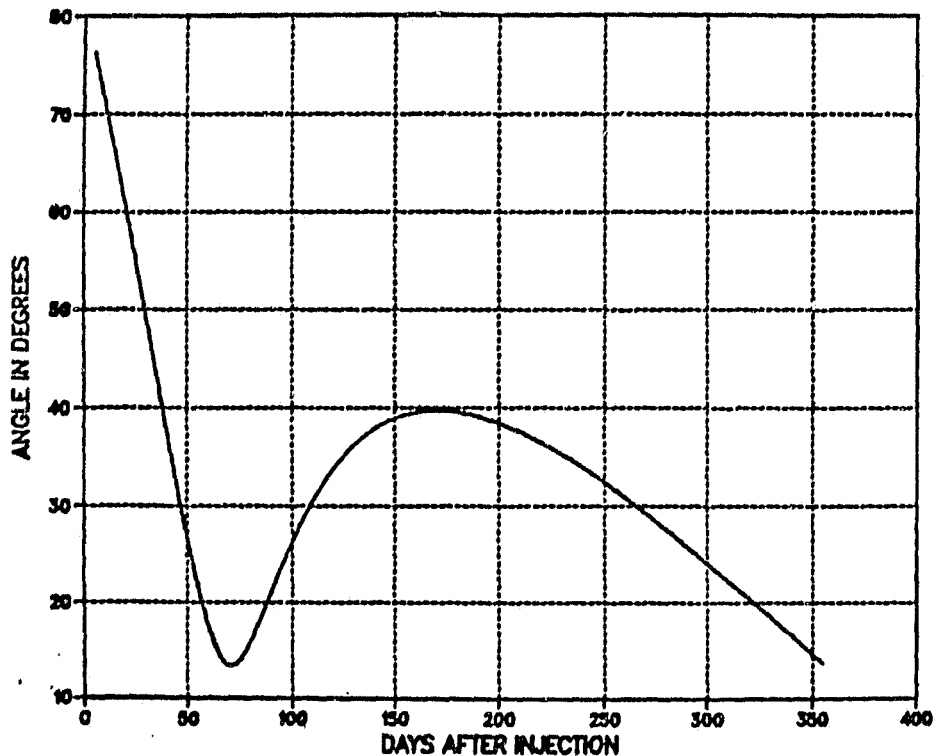


Figure A-17. 1990-91 Type II Mars Transfer Sun-S/C-Earth Angle History (Closing of 20-Day Launch Window)

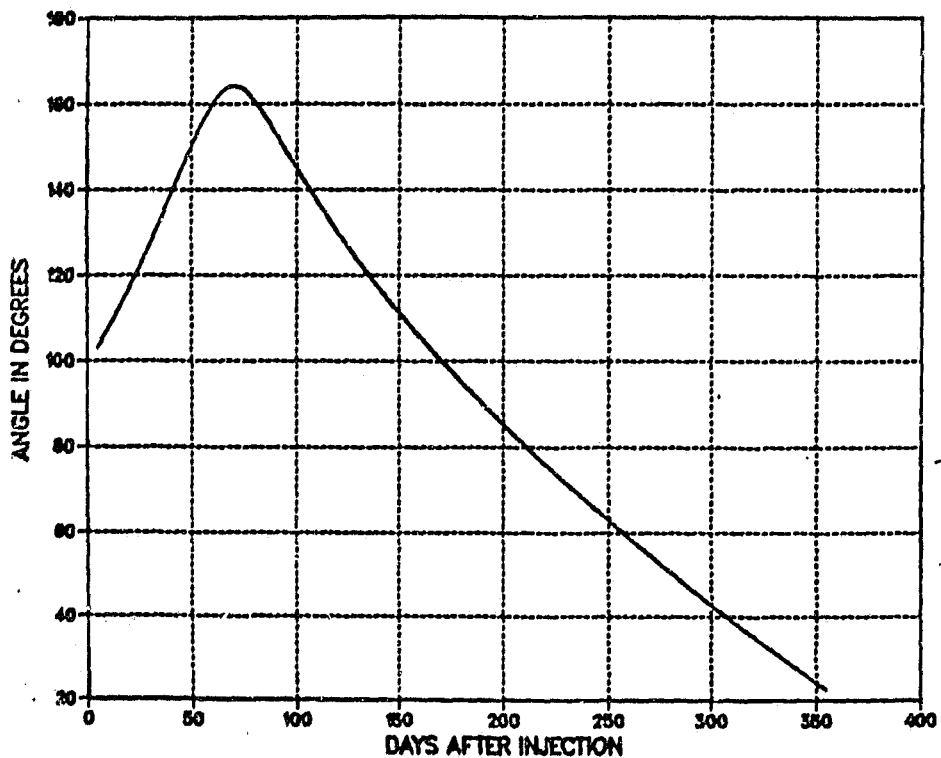


Figure A-18. 1990-91 Type II Mars Transfer Sun-Earth-S/C Angle History (Closing of 20-Day Launch Window)

ORIGINAL PART IS
OF POOR QUALITY

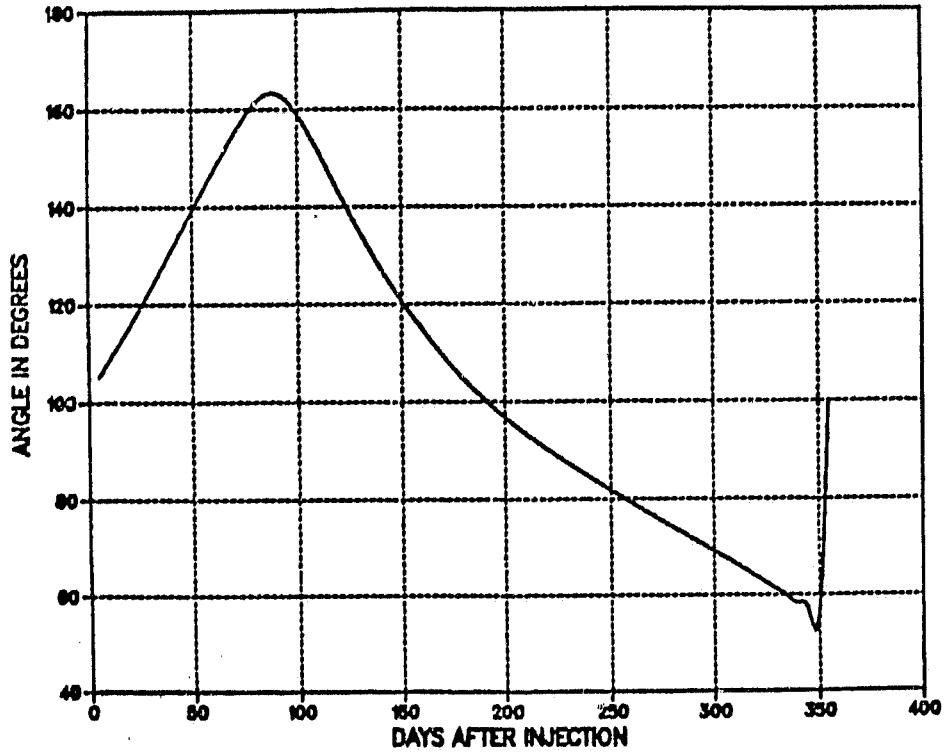


Figure A-19. 1990-91 Type II Mars Transfer Sun-S/C-Mars Angle History (Closing of 20-Day Launch Window)

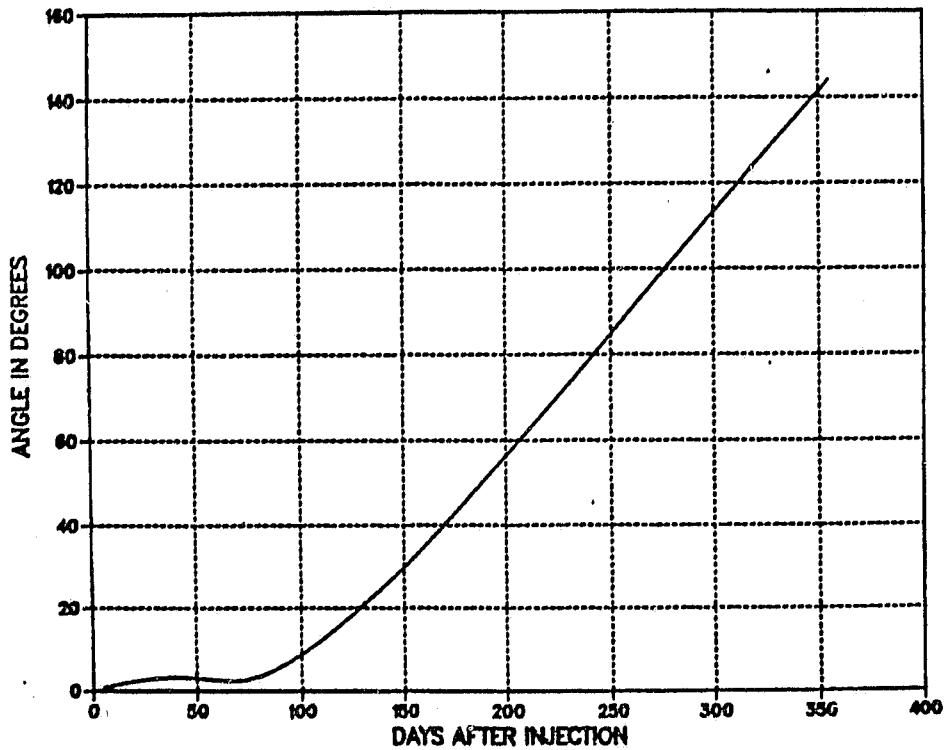


Figure A-20. 1990-91 Type II Mars Transfer Earth-Sun-S/C Angle History (Closing of 20-Day Launch Window)

Following very soon after burn out of the TOS, the spacecraft will separate from the spent TOS and the launch adapter. The jettisoned stage will not be targeted accurately enough at this time to intercept Mars, and will not be of concern regarding planetary quarantine.

At this time the ADACS of the MGCO spacecraft, which are described in Appendix B, will be initialized by the celestial sensor and will take over control of spacecraft attitude.

Within approximately ten minutes, the solar array will be fully deployed, like a wing along the apex of the ESM, in order to avail the spacecraft of sufficient solar power during the cruise phase. The solar array boom will remain folded and captive until after MOI in order that the solar array and the thruster plumes of the on board bipropellant propulsion system will not interfere with each other during MOI.

During the cruise phase, the spacecraft will be oriented according to considerations arising chiefly from power management and thermal control. Adequate viewing of the Sun and reference stars by the sensors of the on board attitude determination system in all spacecraft orientations will be ensured by the spacecraft configuration design and use of a 4π steradian Sun sensor. Basically, the normal to the plane of the solar array will be aligned with the Sun direction in order to achieve maximum generation of solar power. As discussed in Section III B2 of the attached main document, however, the demand for power will be low compared to that available, except during the infrequent and short duration periods of science-instrument checkouts. Freedom to align the solar array normal away from the Sun, therefore, will exist and will be used to aid in thermal control and to obviate the shunting of large electrical currents to dissipate excess solar power. Relative freedom of the orientation of the spacecraft about the line towards the Sun will exist during most of the cruise phase (cf. Appendix B).

While the spacecraft is within TDS km of the Earth during the cruise phase, down links via the X-band omni antenna will be strong enough for the planned science and spacecraft functions check outs. For these high data-rate checkouts at greater distances, however, use of the X-band high gain antenna (HGA) will be necessary. The configuration design of the 2-axis gimballed mounting

for the HGA will ensure Earth pointing capability of the HGA without disturbance of the orientation of the spacecraft set by power and thermal considerations.

It is feasible to incorporate any or all of several techniques for the establishment of the HGA link with the Earth at any time in unpowered flight including potential loss of lock situations. The proposed X-band omni antenna will permit the receipt of commands from the Earth regardless of the orientation of the spacecraft. In addition, several Earth search strategies may be programmed into the spacecraft computer for application should no commands from the Earth have been received within a preselected, commandable length of time.

Occasional minor "mid-course" trajectory correction maneuvers (TCMs) will be performed using the on-board bipropellant system under control of the velocity-metering guidance system acting upon stored commands uplinked from the Earth via the DSN. These TCMs will ensure the correct geometry for the arrival hyperbolic asymptote at Mars. In the reference mission, these TCMs involve a total of ΔV of 100 m/s (impulsive), which for the minimum mass spacecraft capable of fulfilling the extended-mission requirements, i.e. an initial cruise phase mass of 1655 kg (separated), corresponds to the expenditure of approximately 53 kg of MON-3+MMH bipropellant and helium pressurant, as indicated in Table C-2. For the TCMs, the spacecraft will be reoriented for correct pointing of the RCS thrusters under control of the on board ADACS.

At some preselected time during the cruise phase, the GRS and MAG instruments will be deployed on their respective booms. This deployment may occur in step fashion in order to allow the use of differential calibration techniques for these instruments. Since these booms will be TBS meters long, they will almost certainly have to be retracted prior to any propulsive maneuvers, i.e. TCM's, the MOI maneuvers and orbit maintenance maneuvers, in order to permit fast slew rate performance by the helium attitude control system and to ensure survival of the booms. The TCMs and orbit maintenance maneuvers may be performed using smaller thrusters than those used for MOI.

Several hours prior to commencement of the MOI maneuvers, the spacecraft will be re-oriented and held so that the resultant thrust vector of the low main

biprop engines will be aligned tangential to the hyperbolic arrival trajectory at the scheduled time of commencement of the first MOI maneuver, i.e., the capture maneuver. This reorientation will be performed open-loop, and a trim maneuver will then be made under ground command. It will be performed early enough that thorough verification of its accuracy may be made using the on-board attitude determination system. Pointing control during the burn will be performed by the on-board CPU using information from the on-board guidance system. The requirement for thruster pointing prior to and during propulsive maneuvers still allows freedom of orientation about the thrust axis and, therefore, allows maintenance of the HGA link and of power and thermal control.

A6. MARS ORBIT INSERTION

A6.1 Arrival Conditions

The geometry, timing and ΔV for the Earth departure maneuver effectively determine the Earth-Mars transfer trajectory. In turn, this trajectory, refined by TCMs, determines the conditions of arrival at Mars.

Before entering the gravitational sphere of influence of Mars, the spacecraft will have an arrival hyperbolic excess velocity (relative to Mars), V_{∞} , of between 2.714 km/s and 2.954 km/s, for launches at the opening and closing of the 20-day launch window of the reference mission respectively. This is shown in Table A-1. It can be seen easily, therefore, that the spacecraft will have positive energy in the Mars reference frame when one considers that, by comparison, a body with zero energy in the Mars reference frame, ejected from the planet at the escape velocity, would arrive at infinity with zero velocity relative to Mars. Accordingly, the spacecraft will follow a planar, hyperbolic trajectory around Mars unless it is either targeted to impact the planet or is acted upon by the on board propulsion system. The angle between the notional undisturbed arrival and departure asymptotes would depend upon the closeness of approach to Mars of the arrival asymptote.

In the proposed baseline MGC0 spacecraft design, the thrust level of the biprop system is low, being produced by four 490 N engines, in order that the deployed solar array will survive the shock and acceleration levels of propulsive maneuvers. In comparison it may be seen from Table C-2, as

examples, the masses of the spacecraft at the beginning and end of MOI for the extended mission are 1916 kg and 883 kg. The corresponding range of deceleration during thrusting is 0.23 g to 0.10 g. The choice of a low thrust to mass ratio for the TIROS-based MGCO spacecraft causes a inefficiency penalty of only ~5% in the MOI maneuvers and yet adds great flexibility to the orbit achievement scenarios, as described in Section A6.2.

The spacecraft will be targeted to enter an elliptical capture orbit with a periapsis altitude of approximately 350 km. The capture orbit will be coplanar with the hyperbolic arrival trajectory, which will have been arranged through TCMs to produce a precisely polar orbit, i.e., at 90° inclination. As indicated in Figure A-21, in the Mars reference frame the arrival asymptote for the reference mission approaches from the dawn sector, at an hour angle of approximately 0400 hours. In the reference mission the desired initial orbit has an early morning ascending node. Accordingly, the arrival asymptote will be targeted over the North Pole of Mars. Since the capture burn will be of long duration, the initial periapsis will be approximately over the equator, i.e., will have an argument of approximately 180°.

A6.2 Selection of Mars Insertion Scenarios

A6.2.1 INTRODUCTION

The selection of the elements of the Mars insertion orbit involves the careful matching of many constraints and requirements such as arrival geometry, propulsion system type and capability, mission science requirements, spacecraft requirements (e.g., power), planetary quarantine restrictions, etc. The interactive process is illustrated schematically in Figure A-22 and is discussed in this section. The basic geometry of the MOI is shown in Figure A-23.

A preliminary analysis of the MOI scenario for the low thrust to mass ratio of the TIROS-based MGCO and the corresponding propulsion requirements are presented in Section, A6.2. Since the navigation function will be performed by JPL, only certain aspects of the attitude control required for the insertion burns are discussed here, as they pertain to the nominal phasing orbit for the

ORIGINAL PAGE 19
OF POOR QUALITY

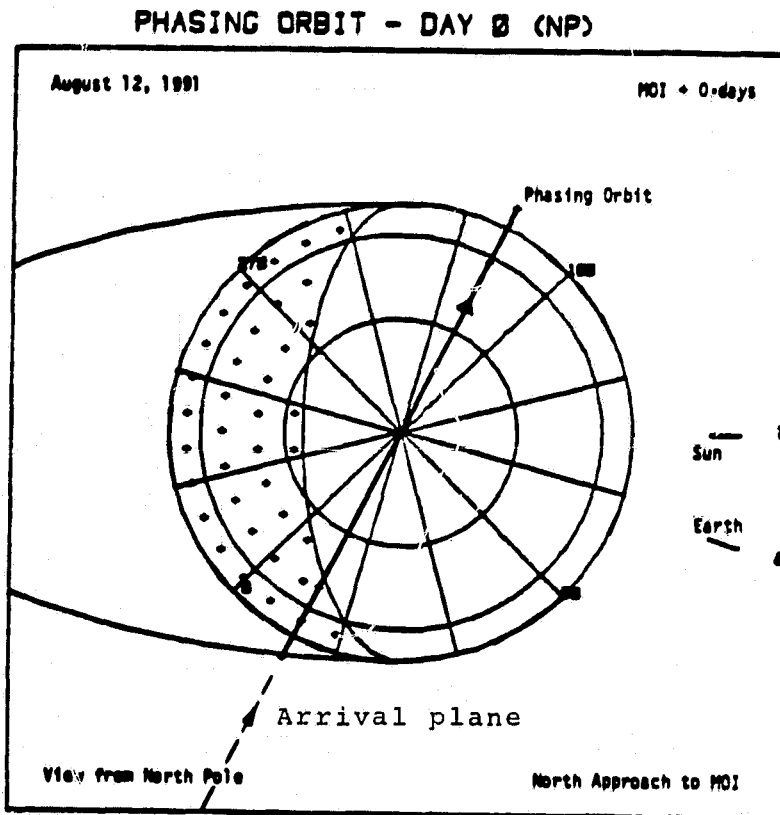


Figure A-21. Phasing Orbit after Mars Orbit Insertion

reference mission, which is polar and circular at 350 km altitude. The impulsive ΔV requirement for direct insertion has a maximum value of 2240 m/s, corresponding to launch on the last day of the 20-day launch window.

As described in Appendix C, the total thrust level for the TIROS-based MGCO spacecraft design is limited to approximately 1980 N. Using this value of thrust together with the other characteristics of the payload and the baseline propulsion subsystem design, it may be calculated that a burn duration of between 20 and 30 minutes is required to produce the necessary ΔV for direct insertion into a circular orbit at 350 km altitude above Mars. Such an insertion would involve a ΔV penalty of 175 m/s over the impulsive requirement.

Better performance could be obtained by splitting up the burn into say two parts. The first burn would capture the spacecraft around Mars and take it into an intermediate elliptical orbit. The second burn, at a later periapsis passage, would circularize the orbit at 350 km altitude.

For an impulsive direct insertion at a periapsis altitude of 350 km the approach hyperbola would be targeted so as to also feature an altitude of closest approach of 350 km. For the proposed low thrust level insertion of the TIROS based MGCO, however, the altitude of closest approach of the notional undisturbed approach hyperbola would be targeted higher in order to compensate for the reduction in periapsis altitude due to the long duration of the burn. The estimated increase in altitude necessary is approximately 250 km, as discussed in Section A6.2.2.

A6.2.2 SIMULATION OF TWO BURN SEQUENCES

Simulations of the orbit insertion have been performed to the preliminary analysis level for the two cases of:

- (1) maximum capability of the TOS, and
- (2) minimum spacecraft mass necessary to fulfill the requirements of the reference extended mission

For the maximum TOS capability the mass of the spacecraft on arrival at Mars is 1916 kg, as shown in Table C-2. The corresponding required altitude of closest approach for the notional undisturbed hyperbolic trajectory is 600 km (raised from the 350 km for the impulsive insertion). Table A-2 shows the details of the scenario as obtained from the simulation. The first burn results in a 8348 x 361 km altitude orbit. On the next periapsis passage, approximately 5.5 hours later, the second burn takes the spacecraft into the desired circular orbit at 350 km altitude.

For the minimum-mass spacecraft fulfilling the reference extended mission requirements, the mass of the spacecraft on arrival at Mars is 1598 kg, as shown in Table C-2. The altitude of the notional undisturbed approach is again 600 km, as in the case of the first simulation. Table A-3 shows the first burn results in a 6426 x 356 km altitude orbit, and the second burn circularizes at 350 km altitude.

In both simulations, the ΔV penalty for the low thrust insertion (over the impulsive requirement) is approximately 100 m/s i.e. $\sim 4.5\%$. In the actual event of thruster firings, there will be a small additional penalty due to dispersions in the performance of the components of the propulsion system about their nominal performance levels. For the maximum TOS capability case presented in Table A-2, the dispersion penalty has been estimated at ~ 25 m/s. The estimated total thrust penalty (over impulsive) for the MOI maneuvers, therefore, is estimated at approximately 125 m/s, i.e. $\sim 5.6\%$.

In the proposed baseline scheme the total thrust is produced by a set of four thrusters, acting as two opposed pairs. In the case of failure of a one or both thrusters of a pair, only the unaffected pair would be allowed to operate; and consequently the thrust level would be reduced by half. This contingency/ "failure" insertion mode will require very long burns, but is entirely acceptable. If such a malfunction were detected early enough, the hyperbolic approach trajectory would be retargeted, the commencement of the burn would be advanced, and the number of burns would be increased. Table A-4 shows the results of the simulation of such a scenario. Apportioning the total velocity decrement between four shorter burns compensates the higher inefficiency

TABLE A-2. ORBIT INSERTION SCENARIO - 1

Mass: 1916 kg
 Thrust: 1780 N (400 lb_f)
 Propellant: Bipropellant, I_{sp} = 310 s
 Hyperbolic Excess Velocity V_∞ = 2.954 km/s
 Closest Approach to Mars of Hyperbolic Orbit: 600 km

Burn No.	Burn Time (Min)	ΔV (m/s)	Spacecraft Mass in Insertion Orbit (kg)	Resulting Orbit Altitude (km)	
				Apoapsis	Periapsis
1	21.7	1544	1153.6	8347.6	361
2	7.5	795	892	350	350
Total	29.2	2339			

Impulsive ΔV: 2240 m/s
 Finite Burn ΔV Penalty: 99 m/s
 Max. Spacecraft Acceleration: 1.99 m/s² (0.2 g)

TABLE A-3. ORBIT INSERTION SCENARIO - 2

Mass: 1598 kg
 Thrust: 1780 N (400 lb_f)
 Propellant: Bipropellant, I^{sp} = 310 s
 Hyperbolic Excess Velocity V_∞ = 2.954 km/s
 Closest Approach to Mars of Hyperbolic Orbit: 600 km

Burn No.	Time (min)	ΔV (m/s)	Spacecraft Mass In Insertion Orbit (kg)	Resulting Orbit Altitude (km)	
				Apoapsis	Periapsis
1	19	1643.8	931.1	6425.8	356.2
2	5.4	629.9	742	350	350
Total	24.4	2273.7			

Impulsive ΔV: 2240 m/s
 Finite Burn ΔV Penalty: 96.7 m/s
 Max. Spacecraft Acceleration: 2.40 m/s² (0.24 g)

TABLE A-4. ORBIT INSERTION SCENARIO WITH HALF THRUST LEVEL - 3

Mass: 1916 kg

Thrust: 890 N (200 lb_f)

Propellant: Bipropellant, I_{sp} = 310 s

Hyperbolic Excess Velocity V_∞ = 2.954 km/s

Closest Approach to Mars of Hyperbolic Orbit: 600 km

Burn No.	Burn Time (Min)	ΔV (m/s)	Spacecraft Mass in Insertion Orbit (kg)	Resulting Orbit Altitude (km)	
				Apoapsis	Periapsis
1	35.4	1195	1290	26666.5	405.7
2	10	445	1120	6478.6	386.1
3	10.8	565	930	993.6	360
4	2.2	135	880	350	350
Total	58.4	2340			

Impulsive ΔV: 2240 m/s

Finite Burn ΔV Penalty: 100 m/s

Max. Spacecraft Acceleration: 1.01 m/s² (0.1 g)

otherwise associated with the lower thrust level. The corresponding ΔV penalty (compared to impulsive) is the same as that shown in Table A-2. Contingency plans for other failure modes will be examined in later study phases.

It should be noted that the nominal pitch and yaw controls during thrusting for TIROS/DMSP spacecraft are achieved by off-pulsing one or more of the set of four thrusters. Hence, with a half-system operation, this primary control is lost about the corresponding axis, and the backup pitch/yaw control is provided by the gas thrusters, which are helium engines in the proposed MGCO design.

For the thrust characteristics of the proposed design, the MOI simulations presented in this section represent reasonable, though not optimized scenarios. Considering the smallness of the calculated ΔV penalties compared to the impulsive case, however, optimization would not yield a substantial improvement.

A6.2.3 GUIDANCE AND CONTROL CONSIDERATIONS

Splitting up the orbit insertion burn is preferable not only because it reduces the finite burn ΔV penalty, as described in the previous section (A6.2.2), but also on grounds of guidance considerations. An intermediate elliptical orbit would permit accurate orbit determination; and any deviation from the nominal could be ascertained and then corrected in the next burn. An intermediate orbit would also permit calibration of the effective thrust level, which would be off from nominal due to the off-pulsing of the thrusters for steering. Hence, the next burn could be targeted more accurately.

The simulations described in Section A6.2.2 assumed tangential thrust. Programmed pitch-over would therefore be required for steering during the burn. Pitch and yaw control during the burns may be done by off-pulsing one or more of the four thrusters. Off-pulsing the main thrusters, however, would reduce the effective thrust level and make the burns a little longer. Roll control is achieved by use of the helium thrusters.

Some amount of backup pitch and yaw control during burns may be achieved by use of the helium thrusters. This would be necessary if one of the main thrusters failed and consequently a half-system had to be used.

Prior to a burn, the spacecraft will slew from its cruise attitude into the required initial burn attitude. After the burn, the spacecraft will slew back to the cruise attitude. This will minimize the duration of possible communication and power losses.

Checking the orientation of the Sun and the Earth in relation to the capture orbit, however, the Sun and the Earth make angles of approximately 172° and 155° with the normal to the insertion orbit. With the antenna located on top of the "ESM", on the same side as the solar array (with boom retracted), and with freedom in choice of roll attitude during burn, there may be little or no disruption in communication and power due to the re-orientations of the spacecraft for the MOI burns.

The GRS and MAG booms will be retracted during the burn sequences. This will be done even if they can withstand the shock and acceleration levels, since retraction will reduce the moments of inertia and so speed up the slew maneuvers.

Attitude update prior to burns will be done in the same manner as during the interplanetary cruise. For each maneuver, velocity gained will be controlled by the on-board velocity metering guidance system.

A7. DRIFT ORBIT PHASE

Following MOI, the spacecraft will be slewed into an orientation similar to that in which the Earth orbiting TIROS and DMSP spacecraft fly during their operational phases, i.e. with the pitch axis along the long axis of the spacecraft and the bottom face of the ESM held nadir-pointing. Attitude determination and control during the orbital phases around Mars are described in Appendix B. If Earth lock of the HGA is not maintained during MOI and the associated re-orientations, it will be re-established either upon ground commands via the omni antenna or under control of the stored Earth-search command sequence whenever necessary.

Within minutes of re-orientation, the solar array boom will be fully deployed and the cant angle will be adjusted to achieve normal incidence of sunlight on the solar array and, thereby, maximum power generation.

At this point in the mission, the high pressure helium tanks will be isolated from the propulsion system by a pyrotechnic valve. This isolation of the high pressure helium will reduce the potential for pressure loss through leakage during the mapping phases of the mission, which may extend to two Mars years or further. The propulsion system will be capable of operation from then on in the blow-down mode, under the pressure of the helium already inside the propellant tanks. Since a redundant pair of pyrotechnic valves is featured in the design (cf. Appendix C) the helium pressure in the propellant tanks could be restored at least once, if necessitated by say a small gas leak on the low pressure side.

Since the minimum energy Earth-Mars transfer is used in the reference mission, the phase angle of the insertion orbit will be approximately 60° . The requirement that the initial orbit phase angle of the mapping orbit shall be 30° , therefore, slightly complicates the orbit achievement strategy. The reference mission incorporates a drift/phasing orbit phase following MOI so that in the Mars reference frame the phase angle of the insertion orbit will precess from its arrival value, i.e. nominally 60° , to the desired value, i.e. nominally 30° , at which time the orbit will be adjusted to be Sun synchronous.

Since the inclination of the insertion orbit for the reference mission is 90° , the orbital plane will be virtually inertially fixed in the celestial reference frame. Consequently, in the Mars reference frame the orbit plane will precess at the same rate as that at which Mars orbits the Sun. The mean heliocentric rate for Mars is approximately $0.52^\circ/\text{day}$; but since arrival at Mars occurs near the aphelion of Mars, the precession rate over the first few months will be $\sim 0.43^\circ/\text{day}$. In the reference mission the drift phase lasts for 59 days, resulting in a final orbit phase angle of nominally 30° , i.e. an ascending node o'clock position of 0200 hours. The orbital geometry at the end of the drift phase is shown in Figure A-24.

Several alternative schemes for achieving the desired initial phase angle of the mapping orbit are more costly in terms of propulsion requirements, and have been rejected. For example, an Earth-Mars transfer could be selected such that the arrival plane and the desired initial orbit plane are coplanar. Another inefficient scheme involves arrival along the minimum energy Earth-Mars trajectory, just as in the reference mission, followed by propulsive changing of the plan of the resultant insertion orbit to the desired orientation. It is much more useful, however, to use any available margin to extend the lifetime and/or the orbital adjustment capability for the mapping phase and/or to increase the payload capability. Furthermore, operation of the spacecraft for the 59 days in a precisely polar drift orbit of the reference mission allows science measurements to be made over the polar regions. Since the inclination of the mapping orbit will be 92.87° , for Sun synchronism, the regions close to the poles will not be seen by the instruments during the mapping phase (cf. discussion in Section A8).

PHASING TO MAPPING ORBIT - DAY 59 (NP)

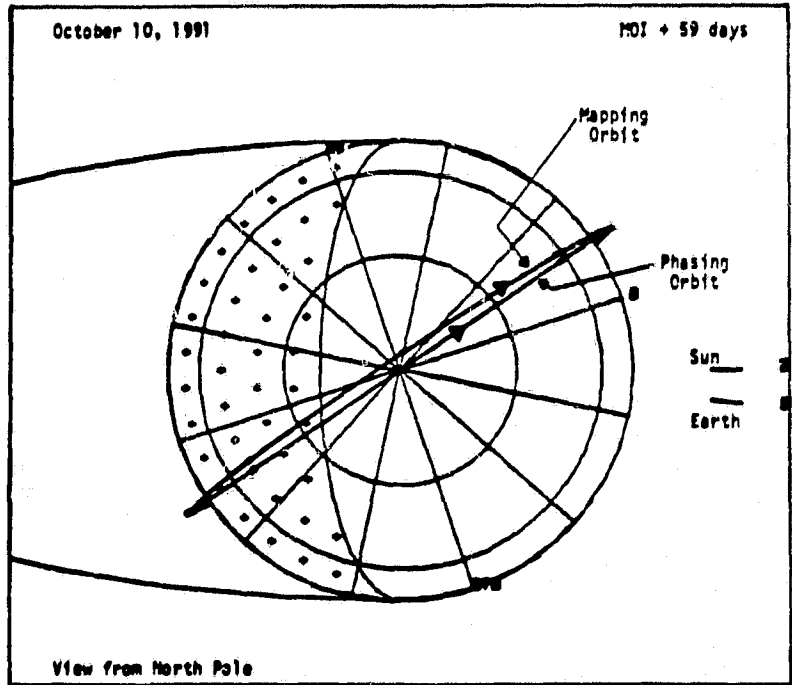
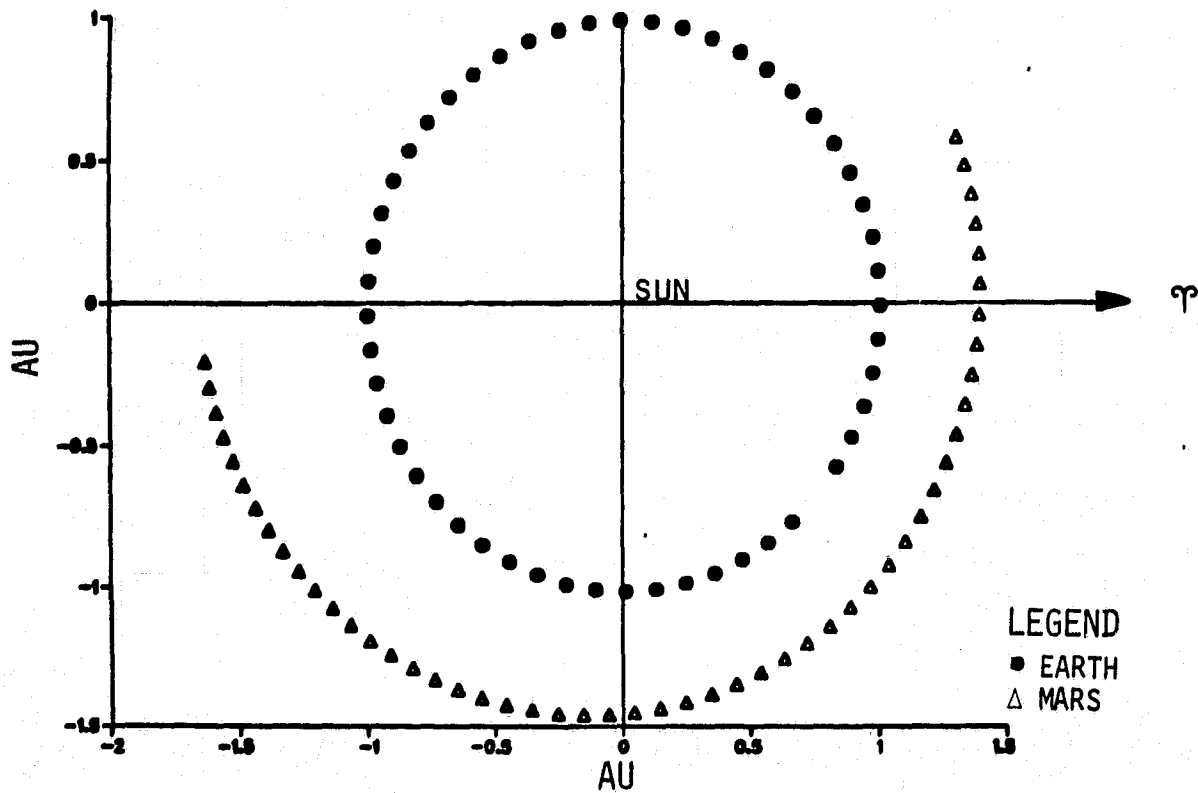


Figure A-24. Phasing Orbit to Mapping Orbit Transition



1990-91 TYPE II MARS TRANSFER

Figure A-25. Mars Orbiting Phase Chose Plot - 10 Day Step

In essence, the MGCO will function in the drift orbit just as it will in the mapping orbit, with the exception that the orbit phase angle will be changing continuously at a relatively high rate, as described in the second paragraph above.

Plots of the time development of several pertinent spatial relationships for the reference mission from the time of arrival at Mars are shown in Figures A-26 through A-29. These figures correspond to a launch at the opening of the 20-day launch window of the reference mission. Similar plots corresponding to a launch at the closing of this launch window would start 18 days later. These figures show several geometrical relationships between Mars, the Earth and the Sun for three Mars years after arrival. Figure A-25, however, shows the chase plot for only the first Earth year after arrival. The information shown graphically in these figures has been incorporated into the configuration, communications, power and thermal analyses.

It may be seen from Figures A-25 through A-29 that upon arrival of the spacecraft at Mars the relative positions of the Earth, Mars and the Sun are among the worst that occur during the mission. The solar range, at ≈ 1.65 AU, is close to its maximum value, though decreasing. The Earth range, at 2.5 AU, is close to its maximum value, and increasing.

In addition, conjunction (of Mars and the Sun) occurs approximately 80 days after arrival, i.e. approximately 20 days after the start of the mapping orbit. Temporal relationships between the different orbit phases, Martian seasons, Martian dust storms, and heliocentric coordinate references are shown in Figure A-30.

In order to tailor the mission to the varying mission geometry, the science measurement rates (and thereby the data handling, communications and power requirements) will be relaxed during adverse periods such as the arrival period. Furthermore, short shut down periods, typically of less than 20 days duration, will be unavoidable around conjunctions, as for the Viking mission.

During science measurement phases of the mission, the solar array will be oriented for normal incidence of the solar radiation, i.e. for maximum power output, by use of the proposed two-axis control of the array. The

1990-91 TYPE II MARS TRANSFER

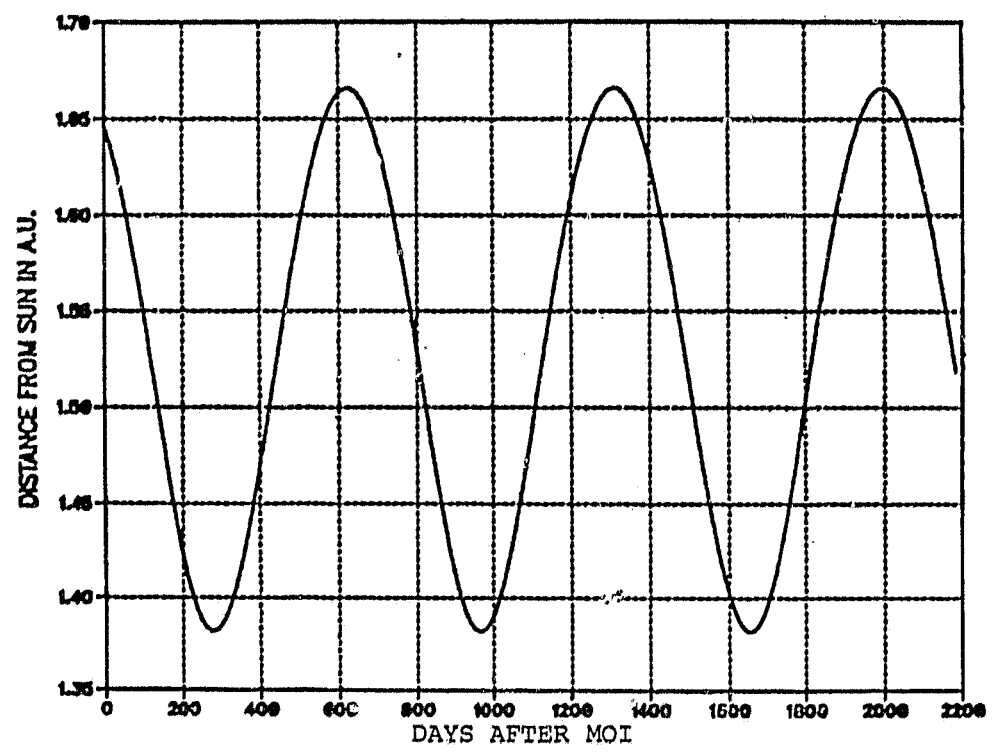


Figure A-26. Mars Orbiting Phase Sun-Mars Range

1990-91 TYPE II MARS TRANSFER

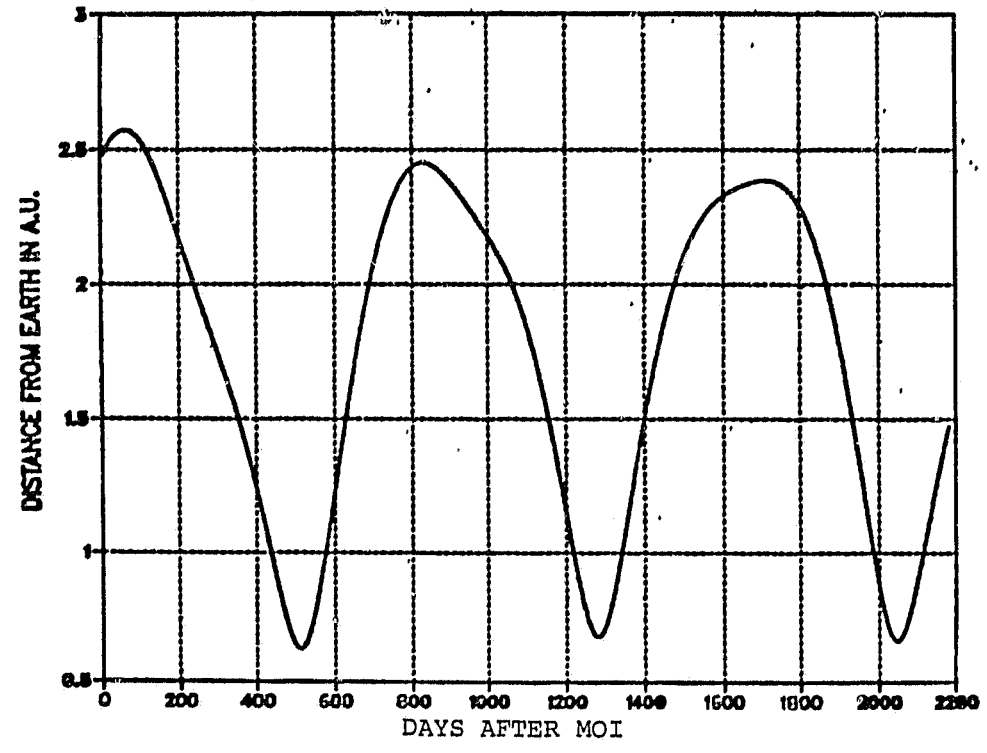


Figure A-27. Mars Orbiting Phase Earth-Mars Range

1990-91 TYPE II MARS TRANSFER

ORIGINAL DOCUMENT
OF POOR QUALITY

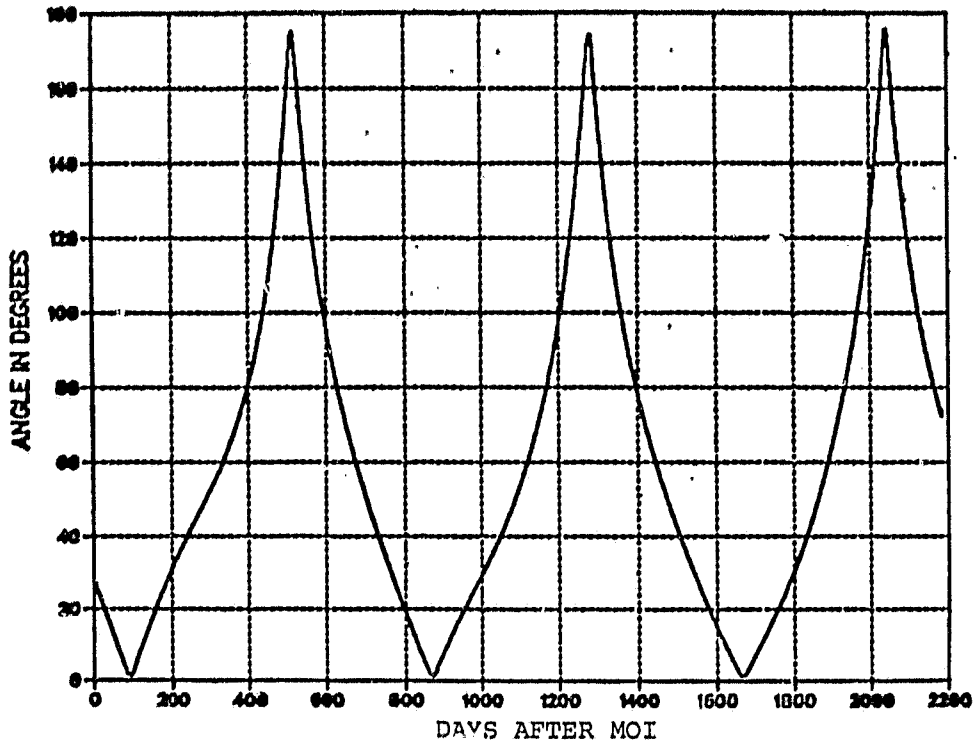


Figure A-28. Mars Orbiting Phase Sun=Earth=Mars Angle

1990-91 TYPE II MARS TRANSFER

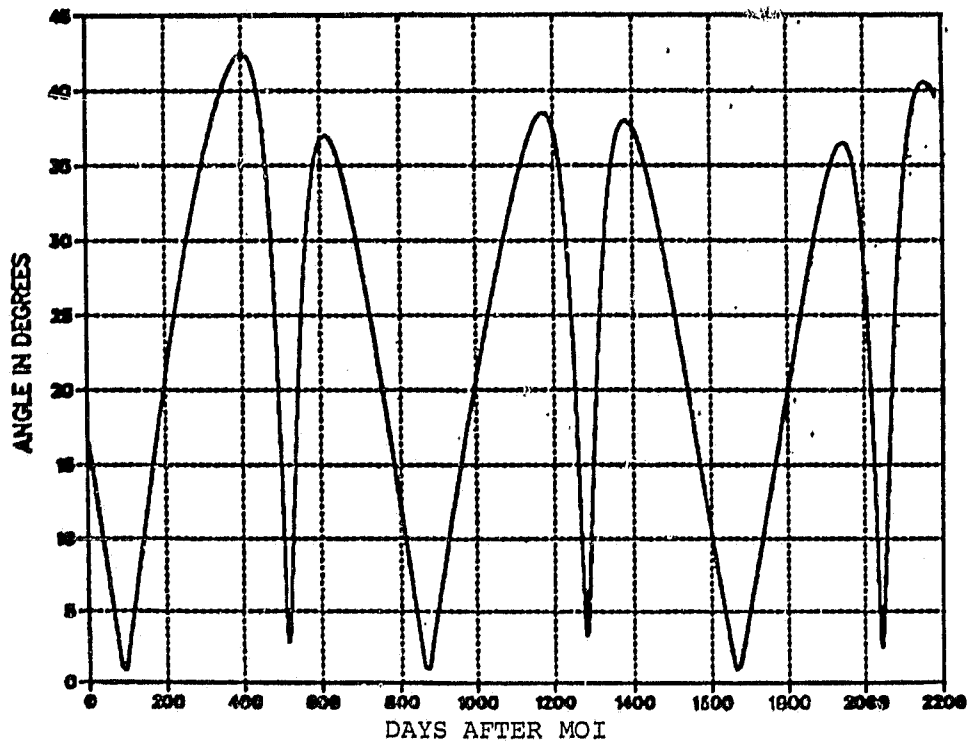


Figure A-29. Mars Orbiting Phase Sun-Mars-Earth Angle

▲ Mars Orbit Insertion
 ▲ Orbit Adjusted to Sun Synchronous
 (30° Phase Angle)

End of Reference Minimum-Mission
 EOL Raising of Spacecraft
 into Parking Orbit

Mapping Phase (1 Mars Year Minimum)

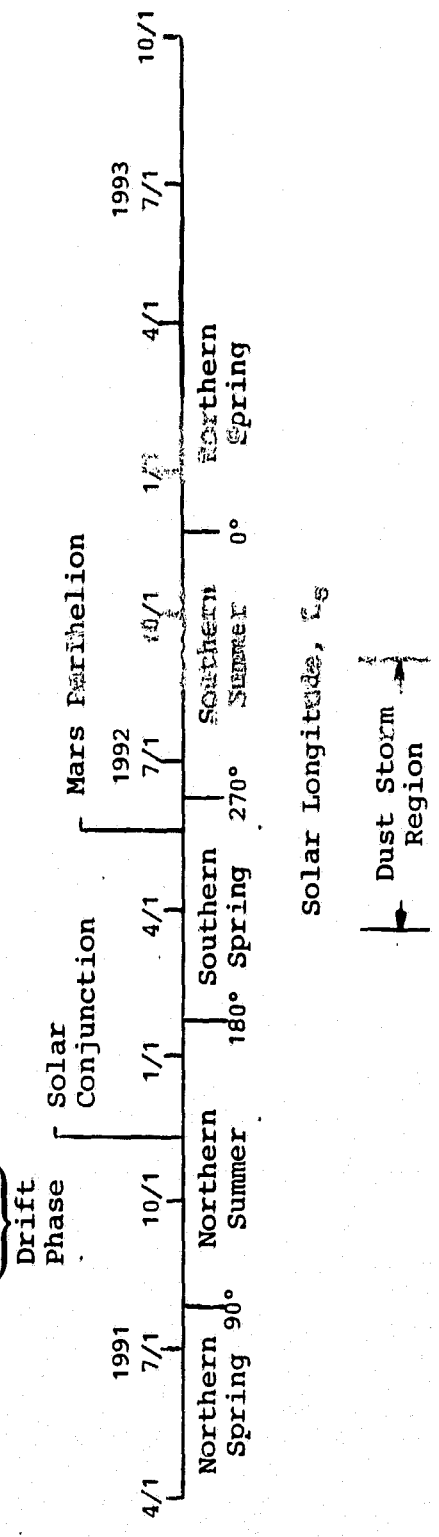


Figure A-30. Orbital Phase Timeline - Following Type II Minimum Energy Transfer with 1990 Launch

ORIGINAL COPY
 OF DOCUMENT

time development of the Sun angle throughout the drift phase is shown in Figure A-31. The Sun angle here is defined as the angle between the Sun direction and the positive orbit normal. Another important environmental factor affecting the power subsystem, the time in solar eclipse per orbit increases to 40 minutes from an initial value of 30 minutes during the drift phase, as shown in Figure A-32. Also of importance for power balance, as well as for communications planning, is the time of occultation of the Earth by Mars per orbit. This increases from approximately 10 to 40 minutes during the drift phase, as shown in Figure A-33.

Local time coverage of the drift orbit progresses uniformly from the initial 4 a.m. - 4 p.m. zone to the 2 a.m. - 2 p.m. zone, i.e. the ascending node drifts towards the midnight sector as shown in Figure A-34.

It may be seen from the orbit geometry that during the science measurement phases the HGA tracking will consist of rotation of the dish about the pitch axis at 1 rev per orbit, with a roll-yaw offset angle which varies slowly from day to day. The roll-yaw offset angle, measured with respect to the orbit normal, may be referred to as the antenna offset angle. Figure A-35 shows that the antenna offset angle changes almost linearly between approximately 155° and 125° during the drift phase of the reference mission. This excursion is within the range encountered during the mapping phase, and is compatible with the proposed two axis gimballed pointing control of the HGA described in Section A8.

During the drift phase, as much science data as possible will be collected and transmitted back to Earth. The GRS and MAG booms will probably be re-deployed for science measurements and may then be retracted for the inclination change maneuver.

The start of the reference MGCO mission occurs in the year of the solar maximum, i.e., 1991. The predicted orbit decay due to drag during the mission, therefore, is currently of significant concern. Even assuming the highest elevated Martian atmospheric densities thought possible, however, it is unlikely that orbit maintenance maneuvers will be necessary during the 59-day drift phase. It is more likely that the orbital decay occurring during

MGCO PHASING ORBIT EPOCH=91,8,12,0,0,0,0
RUN 003

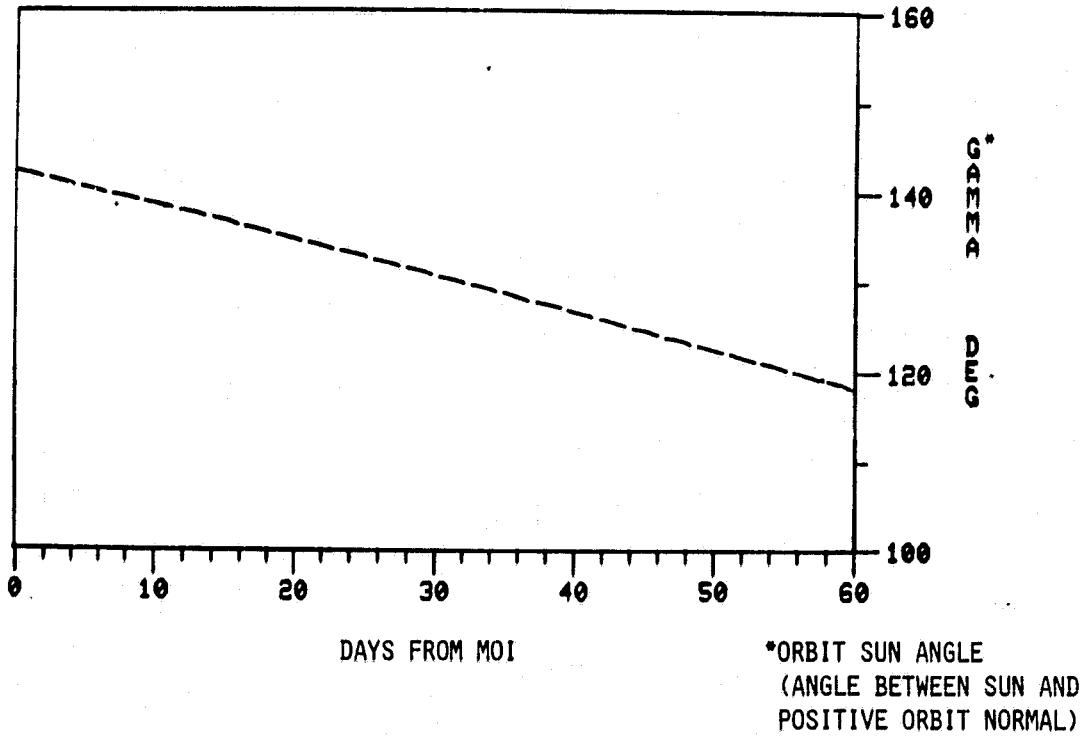


Figure A-31. MGCO Phasing Orbit - Sun Angle Throughout the Drift Phase

MGCO PHASING ORBIT EPOCH=91,8,12,0,0,0,0
RUN 004

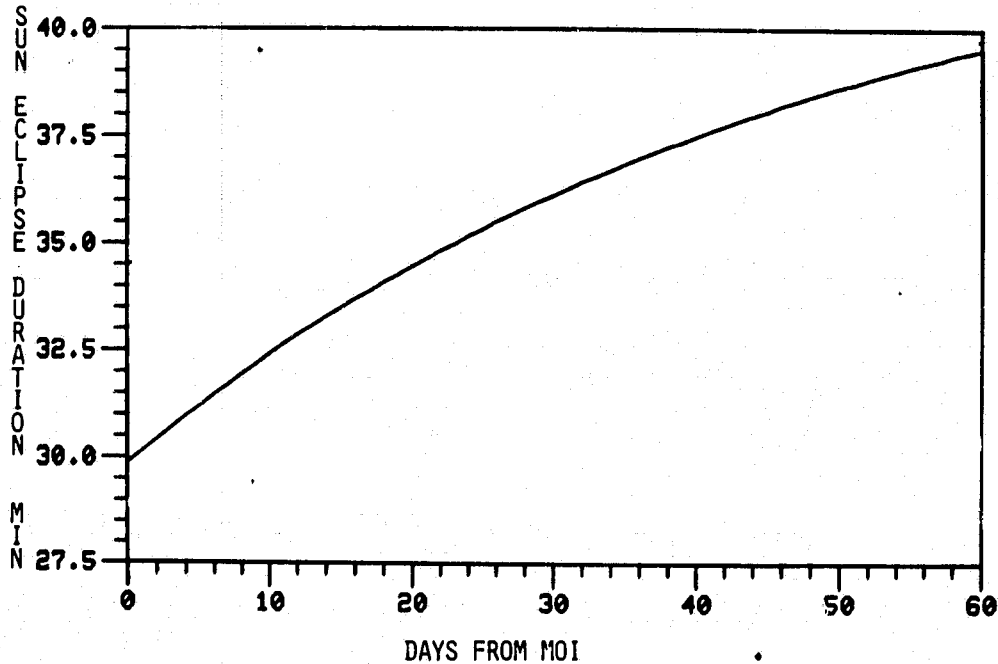


Figure A-32. MGCO Phasing Orbit - Eclipse Duration

ORIGINAL PAGE IS
OF POOR QUALITY

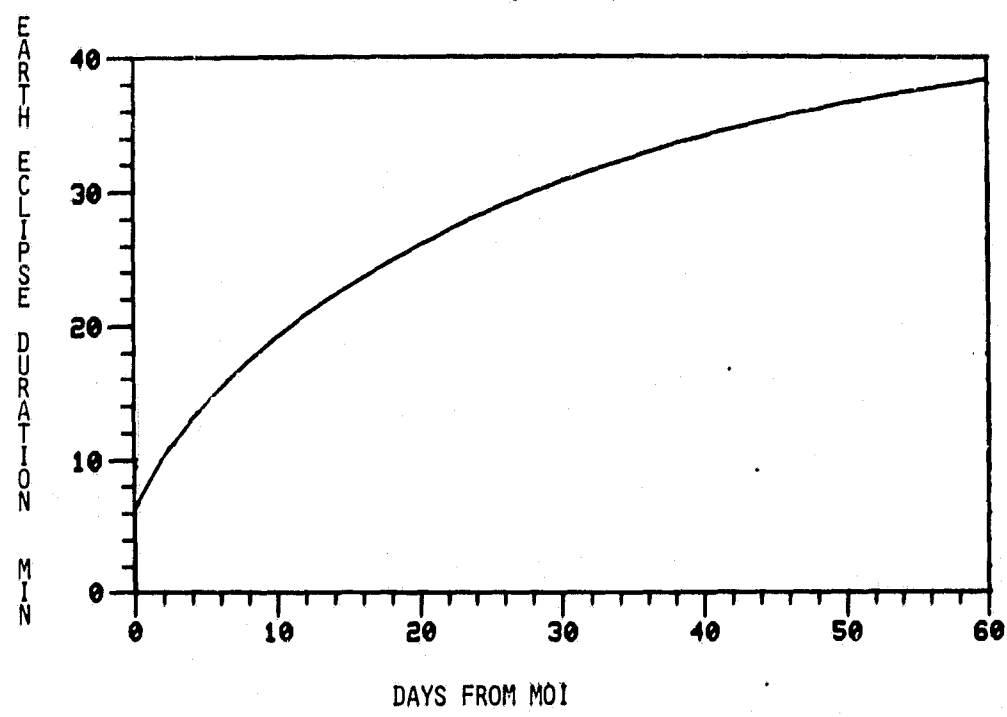


Figure A-33. Eclipse Duration Variation (Phasing Orbit)

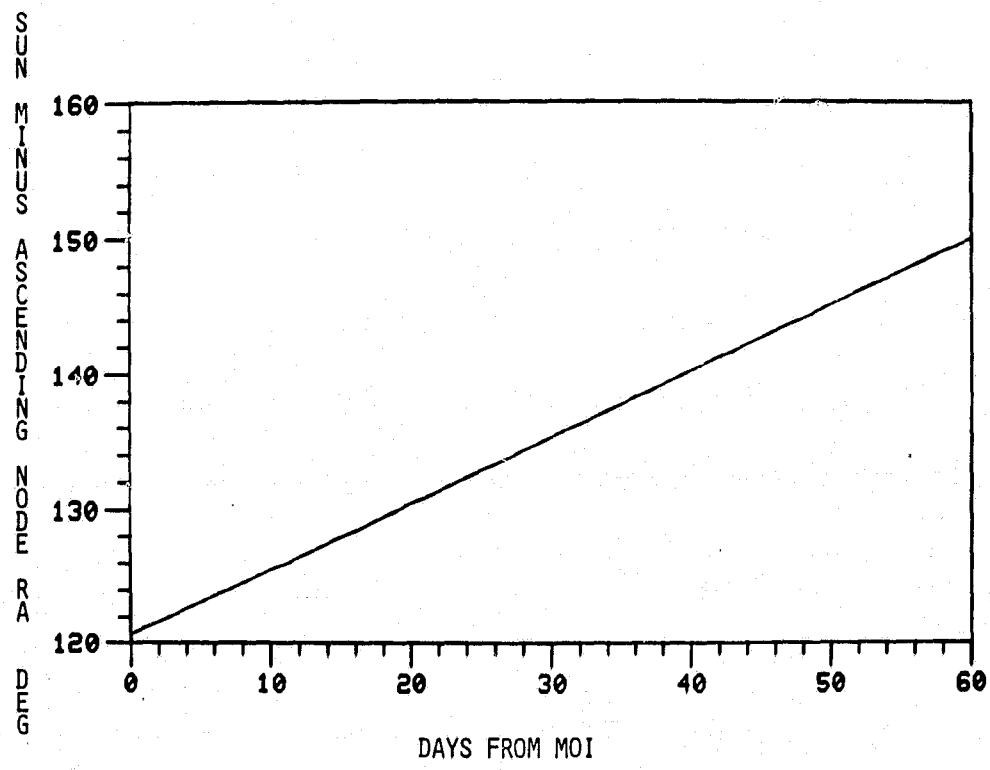


Figure A-34. Sun Right Ascension Minus Ascending Node Right Ascension Variation (Phasing Orbit)

ORIGINAL DRAFT
OF POOR QUALITY

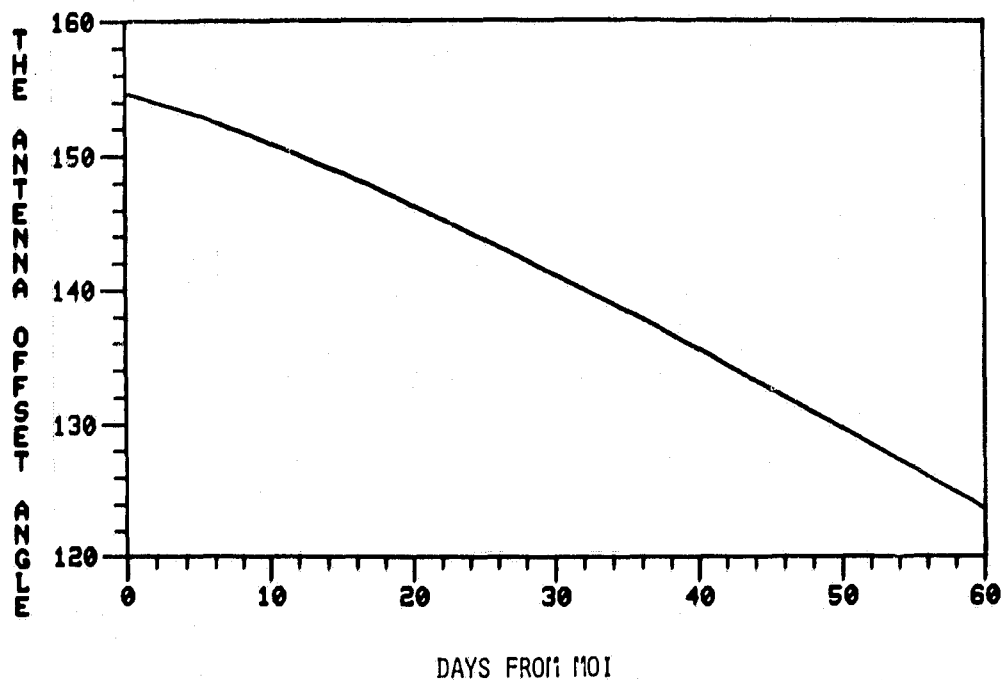


Figure A-35. Antenna Offset Angle Variation (Phasing Orbit)

the drift phase will be counteracted by the maneuver performed to also achieve the mapping orbit. In any case, redundant sets of small thrusters (probably $\sim 20\text{N}$ thrust level) will probably be included in the bipropellant propulsion system. These thrusters could be located to act parallel/antiparallel to the orbit velocity vector in the operational orientation of the spacecraft, to perform orbit maintenance maneuvers. The orbit maintenance maneuvers are predicted to involve ΔV increments of $\sim 18\text{m/s}$ and will certainly be necessary during the mapping phase, as described in section A8. These thrusters may also be used for the TCMs during the cruise phase. Thus, reorientations of the spacecraft for orbit maintenance maneuvers during the science measurement phases would be obviated. Preliminary considerations indicate that this is a viable and attractive approach to orbit maintenance. Further analysis will be performed in the next phase of the study.

Science duty-cycling is likely to be imposed during the drift phase because of aforementioned adverse arrival conditions, and will be used to restrict low to mid latitude coverage and to focus available capabilities on those polar regions which will not be sensed in the later mapping phase of the reference mission.

A8. MAPPING PHASE

At the end of the 59-day drift phase, the instrument booms will be retracted and the spacecraft will be reoriented for a plane change maneuver to achieve an inclination of 92.87° and nominal Sun synchronism. The o'clock position of the ascending node of the resultant initial mapping orbit for the reference mission is nominally 0200 hours. The orbit will be nominally circular at 350 km altitude.

The four main 490N thrust biopropellant engines will probably be used to produce the velocity change involved in this maneuver. The impulsive ΔV requirement for the reference mission would be 164 m/s. The "finite burn" penalty for this maneuver has been calculated at 3.3 m/r, and a further penalty of 1.2 m/s due to performance dispersions may be expected. The estimated total ΔV requirement for this maneuver by the TIROS-based MGCO spacecraft, therefore, is 168.5 m/s. Table C-2 indicates that this maneuver involves the expenditure of approximately 53 kg of propellant and hydrazine, for the maximum TOS capability spacecraft.

The maximum acceleration level, with all four thrusters firing, is approximately 0.1g, which is survivable by the fully deployed solar array for this thrust orientation.

Considerations of thrust control, attitude determination and control, power management, thermal control and communications for this maneuver are similar to those discussed in section A6 for the MOI maneuvers. This maneuver will involve a single burn only. Following the inclination-change maneuver, the spacecraft will be reoriented for its operational mode, and the booms will be redeployed.

Figures A-25 through A-29 show the spatial relationships between Mars, the Earth and the Sun through the extended mapping phase and have been discussed in Section A7. As discussed therein, the conjunction of Mars that will occur approximately 20 days after achievement of the mapping orbit will force a temporary shut down of communications, for a period up to three weeks. The next conjunction will occur one synodic period (i.e. 2 years and 2 months)

later, in the extended mapping phase of the reference mission, as shown in Figures A-28 and A-29.

The time development of the orbit Sun angle for the mapping orbit is shown in Figure A-36). This variation will be tracked by the proposed two-axis solar array drive, to ensure maximum solar power. Figure A-37 shows that the length of time in solar eclipse per orbit will always be within two minutes of 40 minutes. On the other hand, Figure A-38 shows that the time of Earth occultation by Mars per orbit will be approximately 42 minutes for periods of approximately 500 days, interspersed by periods of approximately 50 days when there will be no Earth occultation. The first period of no Earth occultation coincides with the period of minimum Mars-Earth range shown in Figure A-27; i.e., higher data-rate communications are favored at this time for given fixed communication system characteristics, though the peaking solar range at this time, shown in Figure A-26, limits the benefit. A detailed analysis of data retrieval capabilities throughout the orbital phases of the mission will be performed in the next study phase.

Although the mapping orbit is referred to as being Sun synchronous, the variation of the speed of Mars in its significantly elliptical orbit will cause the MGCO orbit to wander cyclically in Martian local time. As shown in Figure A-39 the corresponding angular range of the nodal positions will be approximately 22° , corresponding to ≈ 1.5 hours in local time. The initial ascending node position will first drift to the late extreme at approximately 0210 hours after approximately 100 days and then move towards its early extreme at approximately 0040 hours after approximately another 250 days, etc.

The antenna offset angle cycles between approximately 65° and 160° during the mapping phase, as shown in Figure A-40. The HGA tracking will consist of rotation of the HGA about the pitch axis at 1 rev per orbit, with the antenna offset angle (cf. the discussion in section A7) varying only slowly from day to day, as described in section A7. Occultation of the Earth by Mars will occur for those HGA pointing directions at angles greater than $\approx 5^\circ$ away from the zenith. With this knowledge, the spacecraft configuration will be developed to ensure that advantage may be taken of all opportunities for the HGA to see the Earth during the mapping phase, without obstruction by other parts of the spacecraft.

ORIGINAL PAGE IS
OF POOR QUALITY

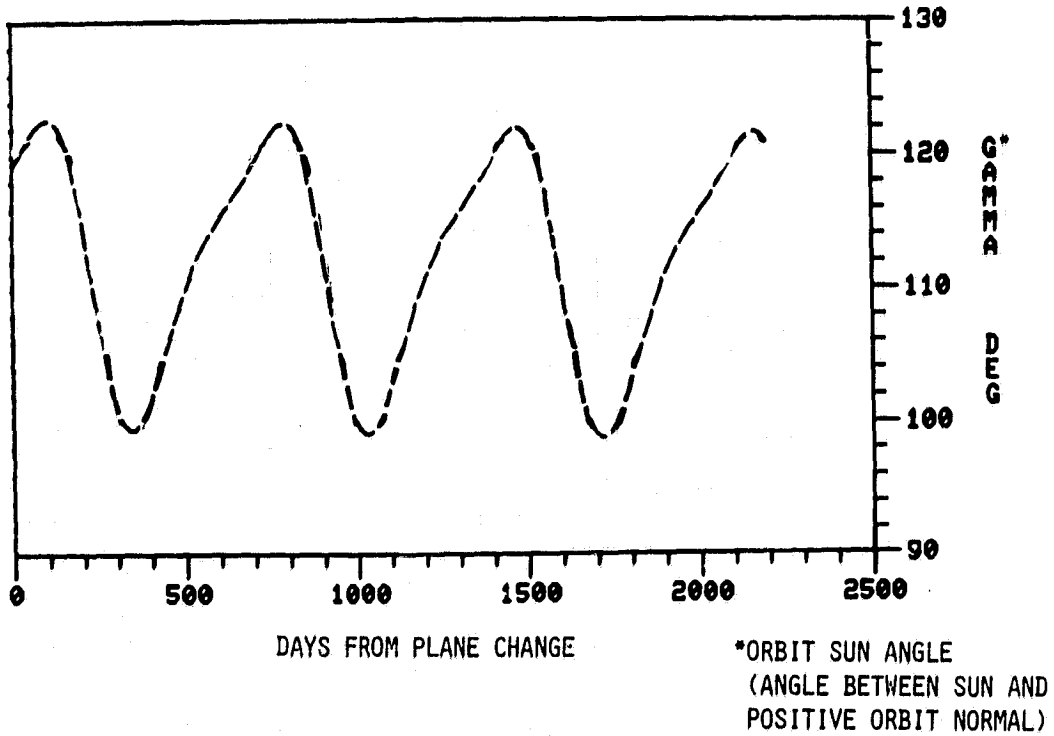


Figure A-36. Orbit Sun Angle Variation (Mapping Orbit)

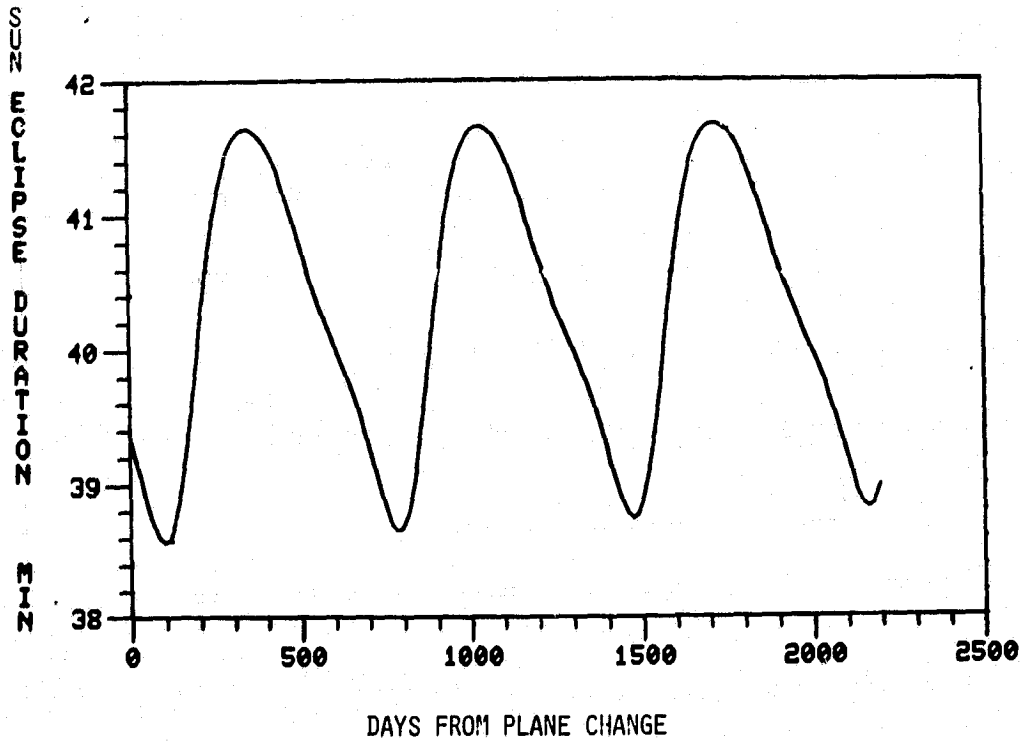


Figure A-37. Sun Eclipse Duration (Mapping Orbit)

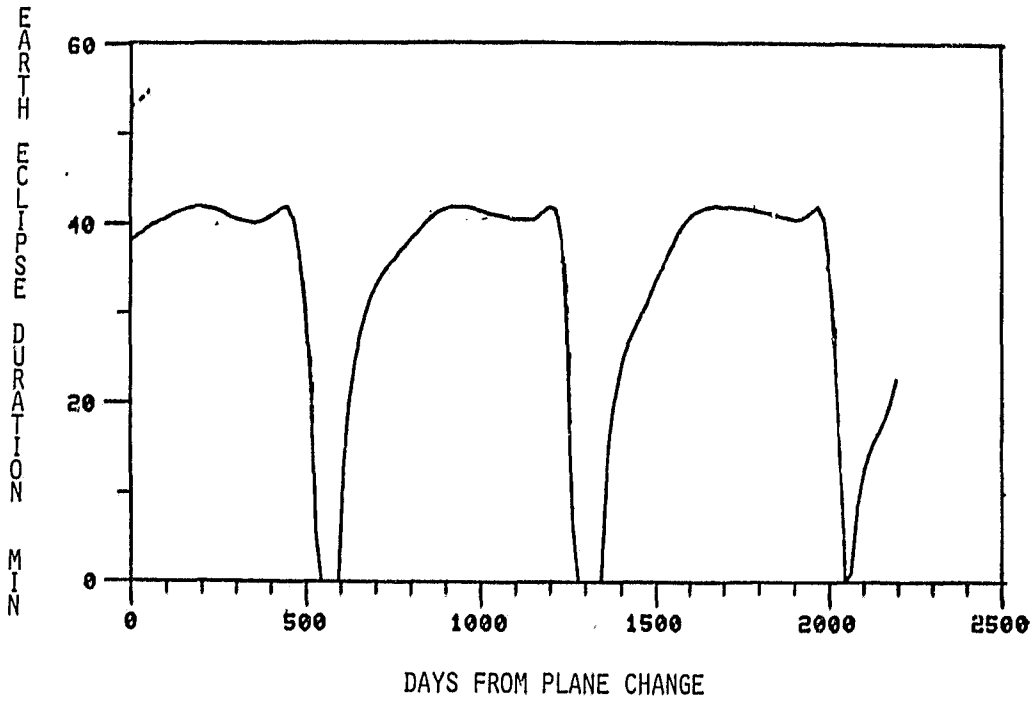


Figure A-38. Earth Eclipse Duration (Mapping Orbit)

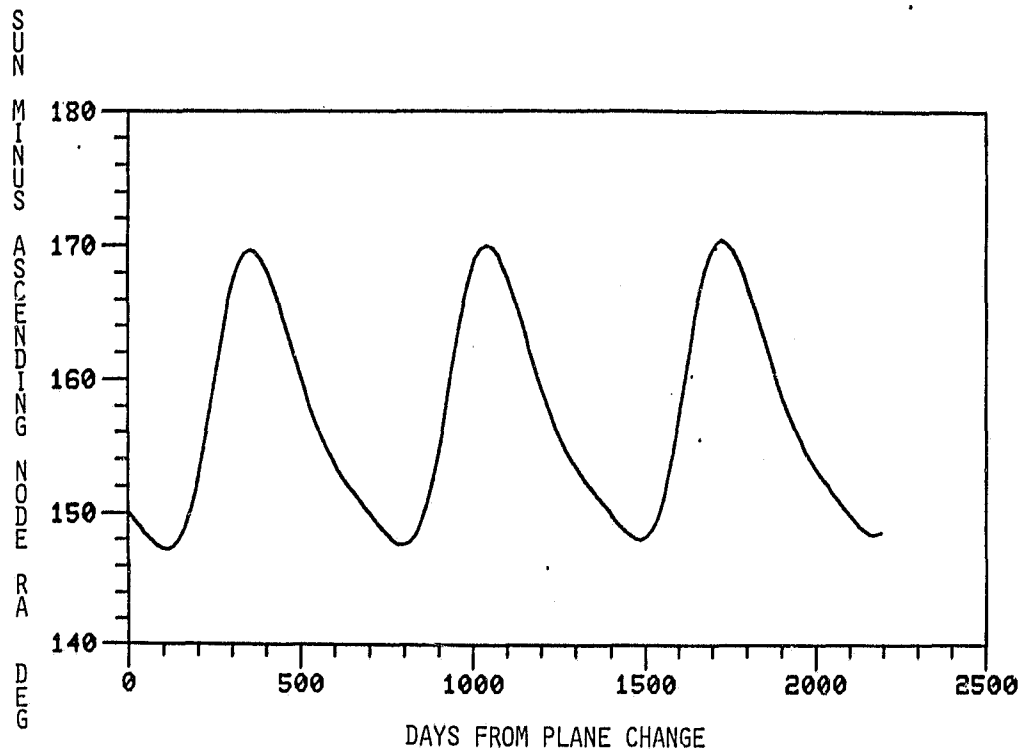


Figure A-39. Sun Right Ascension Minus Ascending Node Right Ascension Variation (Mapping Orbit)

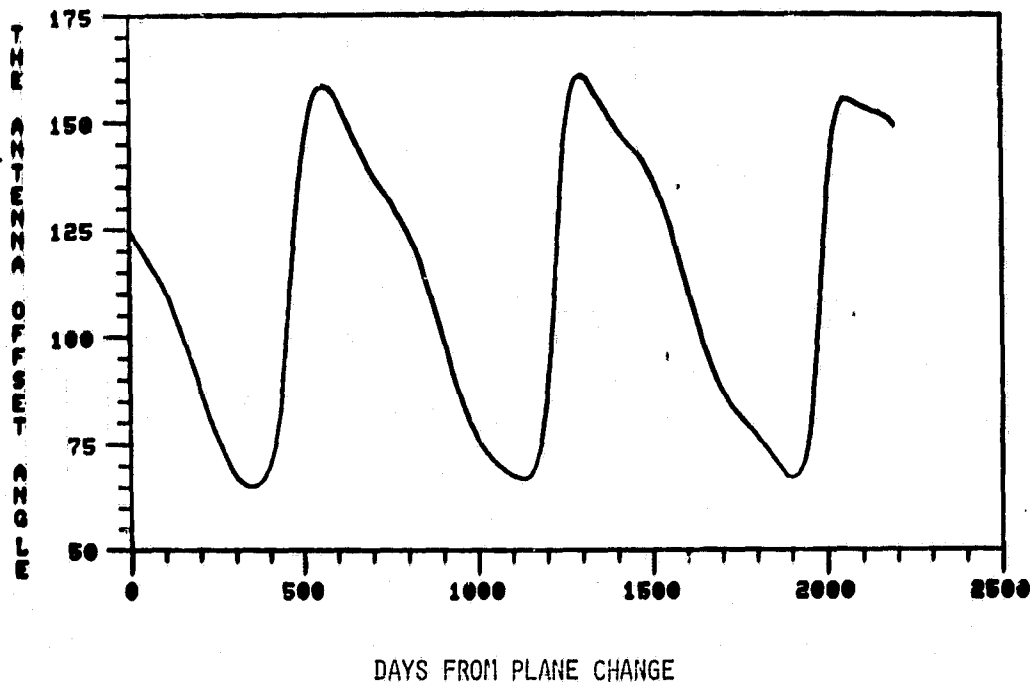


Figure A-40. Antenna Offset Angle Variation (Mapping Orbit)

It is worth noting that a beneficial alignment of the gimbal axes for the HGA would be one with one gimbal axis parallel to the spacecraft roll axis, to allow setting of the antenna offset angle, and the other gimbal axis parallel to the pitch axis, to allow tracking of the Earth at 1 rev per orbit. With this design, the dynamic performance requirement for the first gimbal axis, for offset-angle control, is very much less than that for the Earth-tracking axis. Furthermore, should the pitch-tracking gimbal control fail, the Earth tracking function could be duplicated by halting the 1 rpo pitch rotation of the spacecraft, with the pitch attitude of the spacecraft held inertially to maintain the pointing of the HGA towards the Earth. This back-up mode would involve the least possible disturbance to the normal operational attitude control of the spacecraft. Of course, nadir pointing is incompatible with this back-up mode, and science measurements would be temporarily restricted.

Orbit and altitude maintenance during the orbital phases of the MGCO mission will involve the counteracting of small perturbations due to the asphericity of Mars' gravitational field associated with the third and higher harmonics in the spherical harmonic expansion of the gravitational potential; aerodynamic

drag; solar, lunar, and planetary gravity; solar pressure; gravity gradient torques; RCS thrusting; etc. The spacecraft will be rotated about the pitch axis at 1 rev per orbit in order to maintain nadir pointing. The pitch axis itself will be precessed at an average rate of one revolution per Martian year (687 days) in order to maintain its alignment with the normal to the Sun synchronous orbit. These controls will be effected to the degree that the required operational lifetime of one to two Martian years is ensured, and that the required accuracy in pointing control of the instruments is maintained.

In the reference mission, the orbit will be allowed to decay under the influence of the aspherical gravitational field and the aerodynamic drag until the periapsis altitude falls to approximately 270 km. The aerodynamic drag will increase as the periapsis altitude decreases. Around the time of solar maximum (i.e. 1991) the 2σ high exospheric temperature at Mars is predicted to be approximately 400K, and the corresponding atmospheric density is predicted to be 6.6×10^{-11} kg/m³ at 250 km altitude and 1.5×10^{-11} kg/m³ at 300 km altitude at the peak of the dayside bulge, i.e., at approximately 1400 hours local time near the equator. Under the very worst conditions, the atmospheric density at these altitudes might be five times higher. Chauncey Uphoff, of JPL, has calculated that for a spacecraft with a ballistic coefficient ($C_D A/m$) equal to $0.02 \text{ m}^2/\text{kg}$ (where C_D is the drag coefficient ≈ 2 , A is the frontal area and m is the mass) the required orbit maintenance ΔV over 700 days in this 2σ high case is 50 m/s. Accordingly, 100 m/s would be required for the extended mapping phase of the reference mission which lasts two Mars years. In the worst-case (5X) atmosphere, the corresponding required orbit maintenance ΔV would be five times higher, i.e. 500 m/s. The orbit maintenance ΔV requirement (impulsive) specified for the reference extended mission is 150 m/s. It may be recalled from Section A3, however, that the conservative mass-margin analysis presented in Appendix C has identified a potential spacecraft growth margin of 111 kg for the maximum TOS capability mission' over the minimum spacecraft mass capable of performing the reference extended mission. Furthermore, recent discussions with Boeing indicate that RCA is currently underestimating the TOS capability. Even so, the 111 kg growth margin alone could be translated into additional propulsive (ΔV) capability of 614 m/s for the on board bipropellant system.

Circularization of a 270 x 430 km altitude orbit to 350 km altitude will require a two burn sequence involving ΔV s of 18 m/s and 17 m/s. These maneuvers may be performed using small biprop thrusters, e.g. 20 N thrusters, without reorientation of the spacecraft, as discussed in section A7.

The MGCO spacecraft will be designed to operate under the aerodynamic pressure to be expected at the lowest allowed periapsis altitude of 270 km. The atmospheric density at 270 km altitude consistent with the 2σ high dayside bulge values given above is approximately $4.56 \times 10^{-4} \text{ kg/m}^3$. Under these conditions, the aerodynamic pressure ($=1/2 \rho V^2$) at this altitude would be $2.7 \times 10^{-4} \text{ N/m}^2$. For a density five times higher, the aerodynamic pressure would be $\sim 1.4 \times 10^{-3} \text{ N/m}^2$. The effects of aerodynamic torque will be analyzed further during the next study phase.

In the reference mission it would be possible to insert the spacecraft into a frozen mapping orbit, with the periapsis over the South Pole of Mars. With the symbols e and ω representing the orbital eccentricity and argument of periapsis respectively, it may be noted that e and ω are interdependent. For the reference mission it is possible to select an initial, frozen mapping-orbit in e - ω space, in which the periapsis will librate around the South Pole of Mars. The corresponding atmospheric density at periapsis would be lower than that for a monotonically precessing mapping orbit, since the poles of Mars are flattened and since the dayside bulge is over the equator. Chauncey Uphoff estimates that for this frozen orbit the value of e would remain below 0.011, i.e., the periapsis would remain above approximately 310 km over 700 days. The potential use of a frozen orbit for the mapping phase will be examined in detail in the next study phase. The great flexibility in orbit adjustment capability afforded by the proposed on board low thrust bipropellant propulsion system certainly makes this strategy feasible.

Since the inclination of the mapping orbit will be 92.87° , the polar caps will be inaccessible for sensing by any nadir pointing sensor with a field of view less than approximately 6° (subtended at the center of Mars) across track. It is intended, therefore, that the drift orbit phase of the reference mission, in which the orbit will be precisely polar, will be used to advantage to provide science coverage of these polar regions, as discussed in Section A7.

Adequate thermal control and power management during all mission phases will be ensured by both the design and operation of the spacecraft.

For the nominal mapping orbit at 350 km mean altitude, the orbital period which is 116 minutes, there will be 8528 orbits during the reference minimum-duration mapping phase, which lasts one Mars year (687 days). If orbit control were possible so that no two sensor swaths overlapped at the Martian equator, then full equatorial coverage at the dayside node, for example, would be achieved with a swath width of 2.50 km, i.e. 0.042° or 0.74 milliradians subtended at the center of Mars and 0.41° or 7.1 milliradians subtended at the nominal mapping orbit altitude of 350 km. In comparison, the narrowest fields of view among the currently base lined nadir-pointing instruments for the MGCO mission are $0.2^\circ \times 0.7^\circ$ for the PMIRR and $0.1^\circ \times 1^\circ$ for the UVS and the UVP; and the inclusion of new instruments may not be ruled out at this time. Consequently, since perfect swath control is extremely unlikely, even if possible, the extent of global surface coverage particularly near the equator, by sensors with such narrow swaths, remains uncertain, pending estimates from future studies. The most practical way to achieve full global coverage may well be to extend the mission phase as long as possible and to favor the transmission of data taken in low latitude zones over redundant data from overlapping swaths at higher latitudes. This question of ground coverage is not pertinent to atmospheric sensing. In a similar vein, though, full seasonal climatological coverage over most surface regions will be achieved by taking measurements throughout a period of 1 and possibly 2 Martian year(s). Since the range of the ascending node o'clock position in local time, from MOI through the mapping phase will be 0400-0040 hours, the local time coverage at low latitudes for the reference mission will be confined approximately within the corresponding post midnight and post noon meridians. Local time coverage at higher latitudes will be through the transition regions between these two zones.

A9. MARS QUARANTINE

The NASA policy on planetary quarantine, as applied to the MGCO mission, requires that all spacecraft and associated equipment must be left in orbits that will survive the relevant expiration date of the policy, which in this case is the end of the year 2018.

Lightweight instrument hatches and covers would probably burn up before reaching the surface of Mars if they were jettisoned in the circular phasing or mapping orbit at 350 km altitude. This issue will be resolved through further study. In the unexpected event of the ejection of hatches and covers in these orbits not being allowed, the MOI scenario (described in Section A6) could easily be tailored to include an intermediate orbit which is sufficiently stable for hatch and cover ejection. This flexibility in orbit adjustment capability is afforded by the proposed on-board low-thrust bipropellant propulsion system, (as discussed in Section A6. Otherwise the hatches and covers could feasibly be designed to be captive.

In the reference mission, the mapping phase is terminated at the chosen end of life by raising the spacecraft into a coplanar, nominally circular orbit at an altitude of at least 525 km, using the on-board bipropellant propulsion system. The specified corresponding total impulsive ΔV required for a two burn sequence to perform this orbit raising is 80 m/s. In the propulsion summary of Appendix C an allowance of 82.3 m/s was budgeted, in order to include allowances for the estimated low thrust penalty and performance dispersions.

High altitude, circular orbits such as the proposed EOL parking orbit are the longest lived. The determination of the stability of an orbit around Mars, however, is a complicated process which must take into account several influencing factors. For example, the asphericity of Mars and its gravitational field and also third-body effects from the Sun are significant contributing factors. For low orbits, atmospheric drag is important. The study of the orbital motion of a satellite of Mars grows rapidly in complexity as one tries to generalize the situation, since the oblateness coefficient, J_2 , is twice as large as the similar coefficient for the Earth.

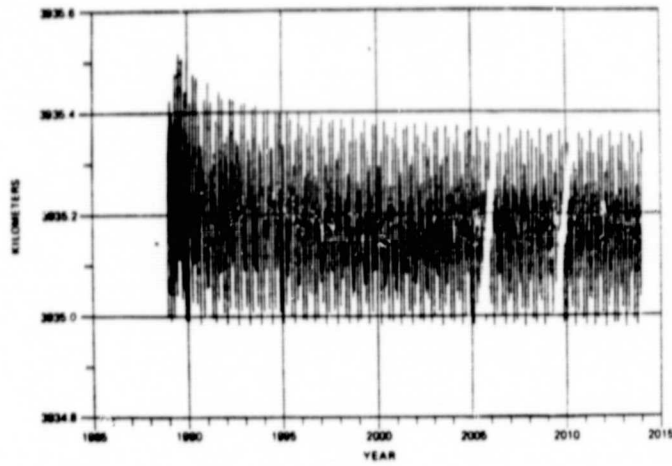
Researchers in the field have shown that resonant situations between oblateness and long-period third-body effects can occur at several orbit inclinations. The effect of this is to cause large variations in the periapsis altitude over short periods of time. A semi-analytic method of predicting the variation of a Mars orbit over long periods of time has been reported in the literature. It has been used to simulate the proposed EOL parking orbit, which is initially circular at 525 km altitude and 92.6° inclination, and also to simulate a potential Mars capture orbit which

initially has a periapsis altitude of 525 km, an inclination of 92.6° and a period of twelve hours (this simulation also serves as a sample potential failure-mode analysis). The results show that these orbits do not exhibit undesirable resonances.

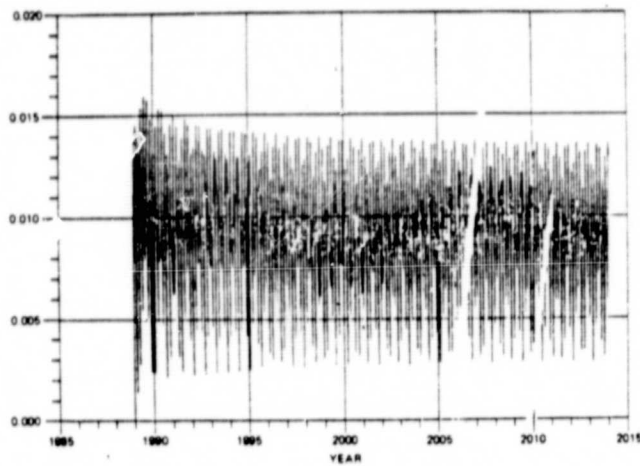
Results of the simulations for the initial circular orbit at 525 km altitude are displayed in Figure A-41. The variations of the semi-major axis, the eccentricity, and the inclination remain well bounded until the year 2014 at the earliest; and should remain so well beyond 2018. Specifically, the eccentricity ranges between 0.003 and 0.014. There are slight high-frequency oscillations but nothing of significance which might cause orbit decay. Based on these simulations, it is concluded that the selected EOL parking orbit is sufficiently stable to satisfy the NASA planetary quarantine policy requirements. On the other hand, elliptical orbits and circular orbits at around 300 km to 400 km altitude may decay too fast.

Results of the simulations for the elliptical orbit are illustrated in Figures A-42 and A-43. The difference between the two sets of results shown in these two figures is that Figure A-42 corresponds to a drag-free simulation while Figure A-43 corresponds to the model for the atmosphere of Mars contained in "Models of Mars Atmosphere (1967)", NASA Space Vehicle Design Criteria (Environment), NASA SP-8011, December 1968, which may be considered to represent the extreme, worst case. Figure A-43 indicates that this elliptical Mars orbit may not be stable until 2019, or may be only marginally stable. A more appropriate simulation in a follow-on MGCO study would clear this matter up.

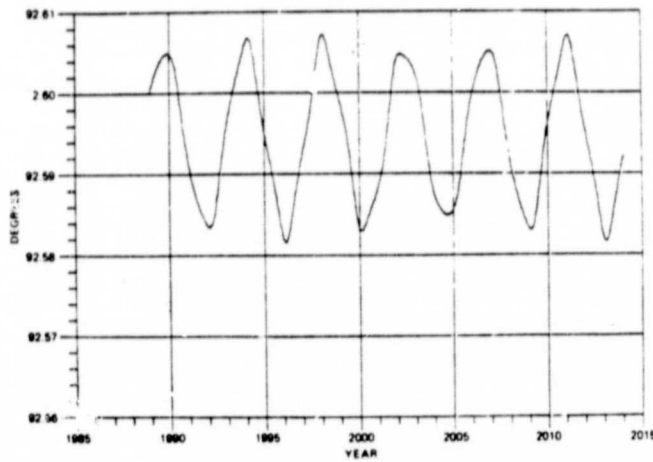
ORIGINAL PAGE IS
OF POOR QUALITY



A. SEMI-MAJOR AXIS



B. ECCENTRICITY



C. INCLINATION

Figure A-41. Stability of the EOL Parking Orbit around Mars, Initially Circular at 525 km Attitude and 92.6° Inclination

ZERO DRAG SIMULATION

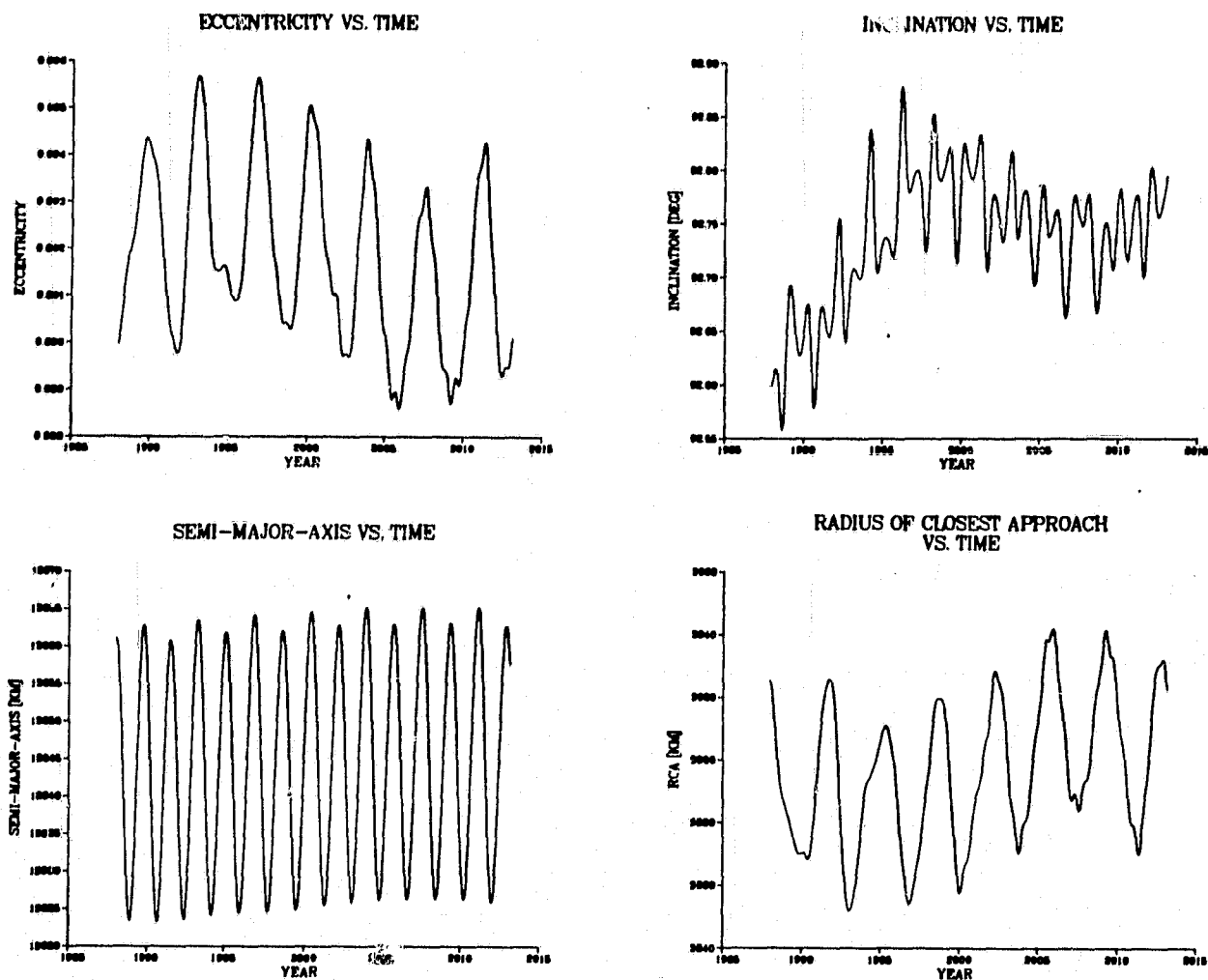


Figure A-42. Stability of a Potential Mars Orbit, Initially at 92.6° Inclination and Elliptical With a Periapsis Attitude of 525 km and a Period of 12 Hours for the Zero Drag Case

MAXIMUM DRAG SIMULATION

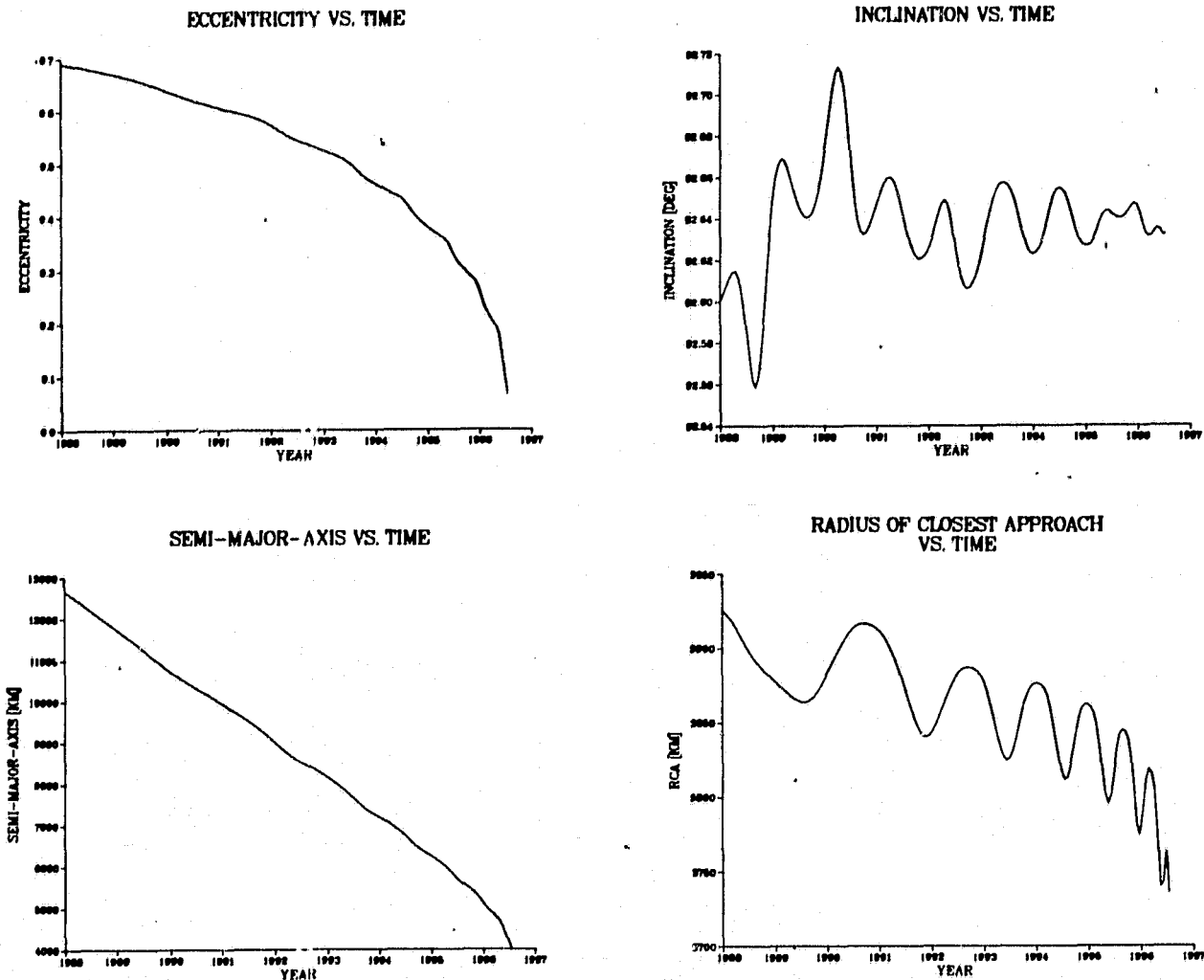


Figure A-43. Stability of a Potential Mars Orbit, Initially at 92.6° Inclination and Elliptical With a Periapsis Attitude of 525 km and a Period of 12 Hours for the Extreme Worst* Case of Drag.

APPENDIX B
ATTITUDE CONTROL SYSTEM OVERVIEW

APPENDIX B

ATTITUDE CONTROL SYSTEM OVERVIEW

B1. ATTITUDE CONTROL SYSTEM OVERVIEW

The baseline for the Attitude Determination and Control Subsystem (ADACS) is a zero momentum, four reaction wheel system using pressurized helium thrusters for momentum desaturation. Attitude control during thrusting maneuvers is provided by off-modulation of the four 100 pound bi-prop thrusters. Attitude reference measurements are provided by star sensors, a scanning horizon sensor, a 4π steradian Sun sensor assembly, and an inertial measurement unit. The functional requirements of the ADACS are summarized in Table B-1. The ADACS orients the spacecraft inertially during the cruise phase to provide illumination of the partially deployed solar array and points the high gain antenna (HGA) towards the earth to provide a secure high data rate communications link. The ADACS also points the spacecraft to commanded inertial orientations during trajectory correction maneuvers, Mars Orbit Insertion (MOI), and plane change maneuvers. The spacecraft is nadir-oriented during both the phasing orbit and mapping orbit. An autonomous solar re-acquisition capability to a safe-hold mode is provided to insure the safety of the spacecraft in the event that attitude lock is ever lost. The primary difference in hardware between the ADACS for the MGCO mission and the DMSP mission (as presented by the Block 5D-3 design) is that the MGCO system uses an additional star sensor during the cruise phase otherwise the systems are functionally equivalent as shown in Table B-2. Much of the ADACS software developed for the TIROS/DMSP spacecraft is transferable to the MGCO system. A simplified block diagram of the ADACS is shown in Figure B-1 and an equivalent summary is given in Table B-3.

The most significant attitude control system requirements are those imposed by the Pressure Modulated Infrared Radiometer (PMIRR) during the mapping orbit phase. The three signal pointing requirements (control/knowledge) in milliradians about each axis are as follows:

<u>Axis</u>	<u>Control Knowledge (mradians)</u>
Roll (X-Axis)	3/2
Pitch (Y-Axis)	9/2
Yaw (Z-Axis)	3/2

TABLE B-1. ADACS FUNCTIONAL REQUIREMENTS FOR MGCO MISSION

Mission Phase	Required Functions
Launch	All functions provided by STS/TOS.
Cruise	Control orientation of s/c to satisfy power/thermal constraints and open-loop pointing of HGA to earth. Reorient s/c to ground commanded inertial orientations for bi-prop motor firings.
Phasing Orbit/ Mapping Orbit	Three axis nadir orientation s/c with solar array illuminated by the sun and HGA pointed at earth. Re-orient s/c to ground commanded orientations for orbit adjust maneuvers.
Fail-Safe	Control orientation of s/c to satisfy emergency power/thermal/communications constraints.

TABLE B-2. FUNCTIONAL COMPARISON OF ADACS FOR MGCO AND DMSP

MGCO	DMSP
One revolution/120 minutes within 0.1° pointing accuracy with inertial/celestial reference.	One revolution/100 minutes within 0.1° pointing accuracy with inertial/celestial reference.
Maintenance of pitch axis to sun-synchronous orbit normal (one revolution/martian year).	Maintenance of pitch axis to sun-synchronous orbit normal (one revolution/earth year).
Inertial orientation and control during bi-prop ΔV maneuvers.	Inertial orientation and control during hydrazine ΔV maneuvers.
Open-loop pointing of appendages (solar array and HGA).	Open-loop pointing of appendage (solar array).
Backup nadir oriented ACS: Estimated accuracy of 0.25° using conical scan H/S.	Backup nadir oriented ACS: 5D-2 demonstrated accuracy of 0.12° using radiation balance H/S, 5D-3 predicted accuracy of 0.20° using conical scan H/S.
Momentum dumping (helium system)	Momentum dumping (magnetic system with backup nitrogen system).

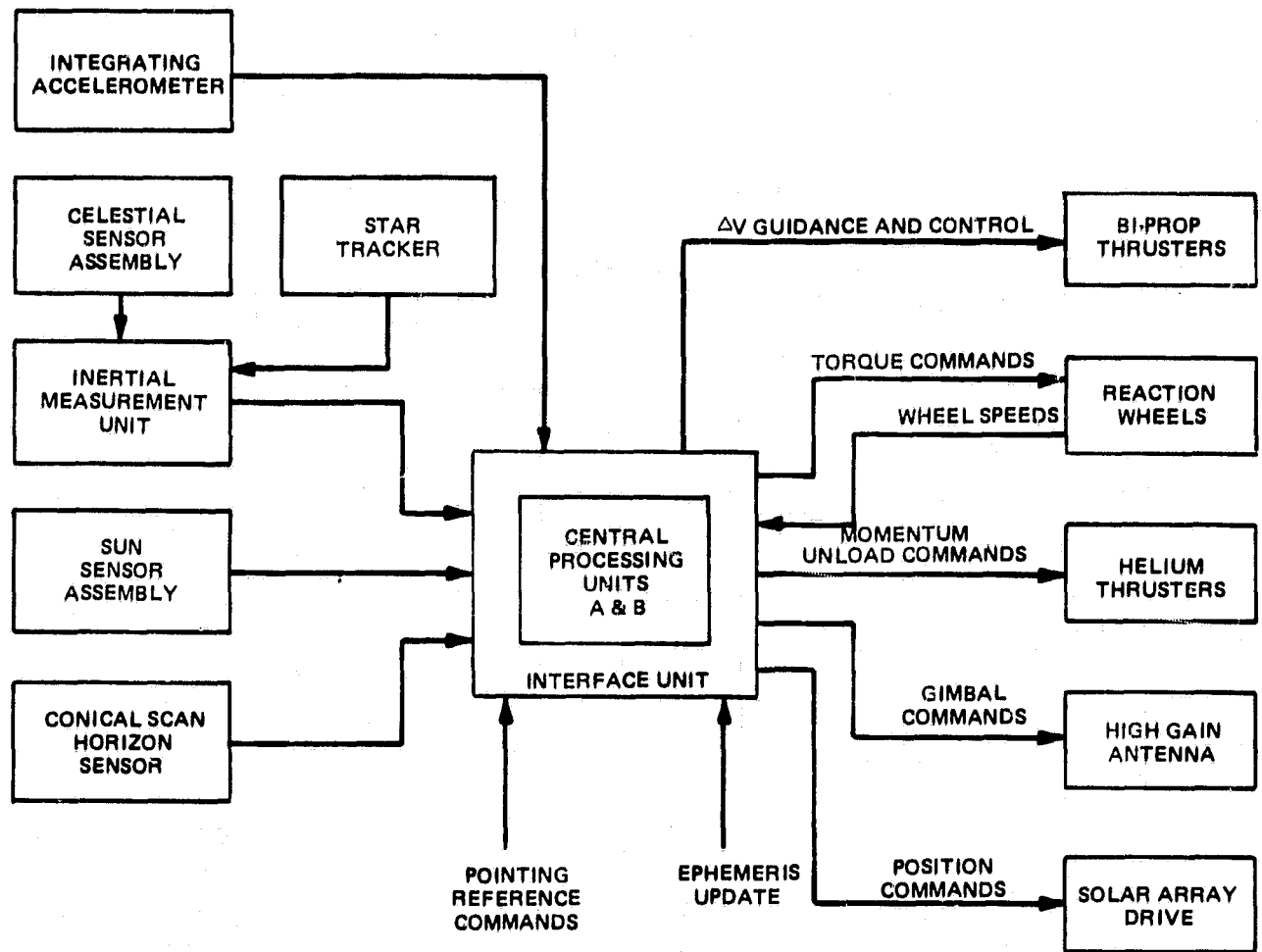


Figure B-1. Block Diagram of ADACS

TABLE B-3. ATTITUDE CONTROL SYSTEM EQUIPMENT SUMMARY

Equipment	Representative Supplier	Weight	Power	Heritage on RCA Programs
Inertial Measurement Unit	Honeywell	23 LB	41.6-5.60W	5D-2
Conical Scan Horizon Sensor	Barnes	15 LB	12W	SAATN, 5D-3
4π SR Sun Sensor	Adcole	3.5 LB	0.75W	SAATN, 5D-3
Star Tracker	Ball	17 LB	18W	NASA Standard
Reaction Wheel Assembly	Ball	4 LB	12W (Max) 3W (Avg)	TIROS/5D-2
Celestial Sensor Assembly	Honeywell	7.4 LB	1.5N	5D-2

B2. CRUISE CONTROL MODE

During the cruise phase of the mission, from Transfer Orbit Stage (TOS) separation to MOI, the spacecraft is inertially oriented to satisfy power, thermal, and communications requirements. The nominal orientation of the spacecraft is with the -Z (yaw) axis canted off from the sunline at a commanded angle to balance power and thermal loads, and with the rotation angle about the sunline commanded to insure appropriate star sensor and HGA viewing geometries. The measurements required for attitude determination are provided by the sun sensor assembly, star tracker, and IMU. Attitude control is achieved by varying the speed of the reaction wheels in response to inertial attitude error signals. Momentum desaturation is accomplished autonomously by pulsing the helium thrusters in response to reaction wheel tachometer signals.

Ground command of the helium thrusters is also possible in order to achieve manual momentum desaturation or to speed up reorientation maneuvers.

B3. VELOCITY CONTROL MODE

Changes in the velocity of the spacecraft are required for mid-course correction during cruise, Mars Orbit Insertion and circularization, plane change maneuvers, orbit adjust maneuvers, and boost to the quarantine orbit at the end of the mission. The velocity changes are accomplished using the four 100 pound bi-prop thrusters with the duration, inertial orientation, and velocity magnitude being commanded from the earth. The inertial attitude sensors, star tracker, and IMU used during cruise control also provide the attitude reference during the velocity control mode. Prior to ignition, attitude control about the thrust axis to ± 1.0 degree is provided by the helium thrusters, which are fired in couples. Attitude control about the two transverse axes to ± 0.2 degree is achieved by off-modulation of the bi-prop thrusters. Burn duration is controlled by a velocity metering system which employs an integrating accelerometer backed up by a burn duration timer which is set by ground command. The accelerometer is the Sunstrand Q-flex and is included as part of the TIROS/DMSF IMU with the integration being performed outside the IMU. This is functionally equivalent to that of the hydrazine trim burn attitude control system employed on TIROS-N/ATN and DMSF Block 5D-2.

B4. PRIMARY ON-ORBIT-CONTROL MODE

The primary control mode used during the phasing and mapping orbits is derived from the Primary Attitude Determination and Control System (PADACS) used on DMSP. This system generates the spacecraft attitude with respect to an orbital reference frame based upon inertial attitude measurements provided by the celestial sensor assembly and the IMU and a stored projected ephemeris. The ground generated ephemerides are computed from RF tracking and uplinked to the spacecraft approximately on the order of twice per week. Based upon DMSP experience, it is anticipated that the dominant error source in the attitude determination will be inaccuracies in the ephemeris. In-track and cross-track accuracies of the Mars Orbit of 7.36 kilometers will be required to insure attitude determination accuracy of 0.1 degree with respect to the orbital reference frame. The attitude determination accuracy scales nearly linearly with orbit determination accuracy down to approximately one kilometer. Below that level other error sources such as instrument errors and alignment errors need to be considered. Attitude control during PADACS operation is accomplished by varying the speed of the reaction wheels. Momentum desaturation is achieved by firing the helium thrusters.

B5. BACKUP ON-ORBIT CONTROL MODE

The backup attitude control mode used during the phasing and mapping orbits is derived from the backup attitude determination and control system used on DMSP Block 5D-2 and TIROS. It is identical with the proposed DMSP Block 5D-3 system since it also uses a conical scan horizon sensor for nadir oriented attitude determination. Yaw attitude is derived by gyrocompassing. BADACS will be used for initial acquisition to the orbital reference frame orientation and is a backup in the event of a failure in the primary system. It is estimated that the accuracy of the Martian BADACS system will be approximately 0.25 degree due to the uncertainty of the CO₂ defined horizon. Detailed analyses of the predicted radiance variations of the Martian atmosphere will be required in order to refine this estimate during the next phase of the study. Attitude control and momentum desaturation are achieved in the same manner for BADACS as for PADACS.

B6. FAIL SAFE CONTROL MODE

This sun oriented control mode is derived from the sun-safe mode proposed for DMSP Block 5D-3. This mode can be entered automatically at any time during the mission in order to provide a safe attitude that will insure solar power, adequate thermal control, and the opportunity to communicate with the earth. Five sensor heads provide full spherical coverage to determine the position of the sun to 0.25 degree accuracy. Gyros are used to provide rate damping and to control the spacecraft rate about the sun line to a predetermined value. Control torques are provided by the helium thrusters. The solar array and high gain antenna are commanded to selected reference positions upon entry into the fail-safe mode. The reaction wheels and the bi-prop thrusters are disabled during this mode. Rotation about the sunline can be stopped automatically either through receipt of a DSN signal by the HGA or by acquisition of a desired star by the celestial sensors. A wide variety of timed HGA search patterns can be implemented within this mode if future studies establish a requirement for them.

APPENDIX C

PROPULSION SUBSYSTEM

APPENDIX C
PROPULSION SUBSYSTEM

C1. PROPULSION SUBSYSTEM

The MGCO propulsion subsystem comprises the hardware and propellant to perform all propulsion functions following release from the shuttle bay. This includes insertion into the heliocentric transfer trajectory, mid-course trajectory corrections, Mars Orbit Insertion (MOI), plane change into the Mars mapping orbit, mapping orbit maintenance, final transfer into the quarantine orbit, and supplementary attitude control functions. In this section, the propulsion capability will be described for the MGCO Flight System, as defined by Figure 1.4-1 of JPL Attachment 1, Standard Mission/System Performance Requirements, reproduced here as Figure C-1.

C2. SYSTEM DESCRIPTION

Initial injection from the 296 km altitude STS parking orbit is performed using the TOS system, which is a commercial derivative of the IUS based on the SRM-1 solid propellant first stage motor. TOS is an autonomous stage which uses independent battery power, avionics and a reaction control system to provide 3-axis stabilization during the one-half to one orbit from STS release until TOS firing, and thrust vector control during the injection burn. Important motor characteristics include a maximum propellant load of 9705 kg and an effective specific impulse of 291.9 seconds. Following the injection burn, both the TOS and its adapter are separated from the MGCO Insertion System.

All propulsion functions following injection are performed with a pressure regulated, liquid bipropellant system using N_2O_4 and MMH as propellants. With reference to the schematic diagram shown in Figure C-2, helium is used as the system pressurant, as well as the supply for redundant sets of eight Reaction Control Subsystem (RCS) thrusters. These 8.9 N thrust helium engines provide impulse bits for spacecraft alignment before major burns, for roll control and back-up pitch and yaw control during the burns, for rapid orientation maneuvers, and for momentum unloading throughout the mission.

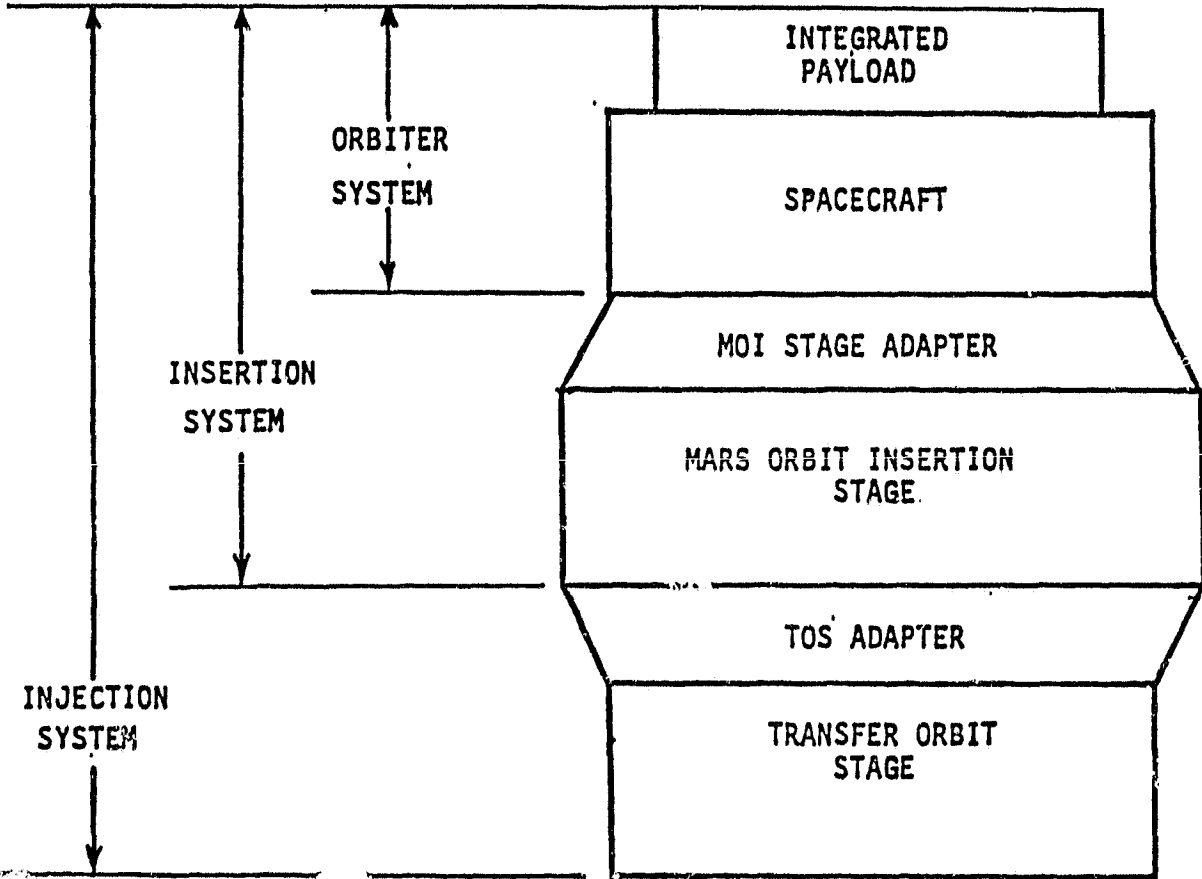


Figure C-1. MGCO Flight System

NOT FOR USE IN
OF POOR QUALITY

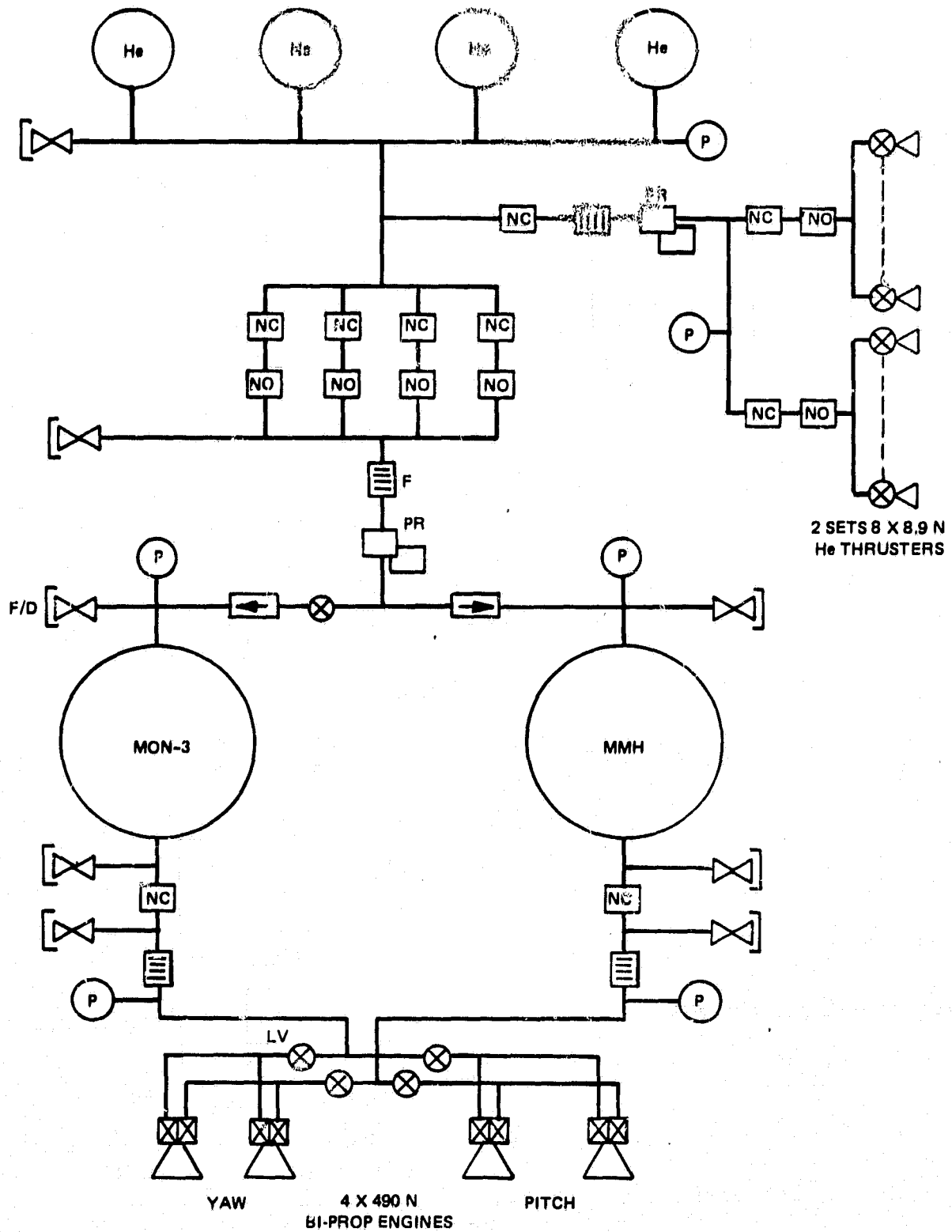


Figure C-2. Liquid Propulsion System Schematic

Primary thrust is generated by four, 490 N thrust Marquardt Model R-4D engines with a specific impulse of 312 seconds at a mixture ratio of 1.65. This flight qualified engine has been selected for several programs (LEASAT, L-SAT and INTELSAT VI) and has performed to specifications on INSAT, launched in 1982. On MGCO, the four engines are arranged in two opposing sets of two. In normal operation, the engines are off-pulsed to provide pitch and yaw control, with the RCS thrusters used for roll control about the thrust axis. In the event of an engine malfunction, one pair of engines is disabled, with the RCS thrusters providing back-up attitude control.

Two regulators are used in this system. The principal thrust regulator is fed through parallel sets of two series connected, explosively driven valves; one valve is normally closed, the other normally open. This arrangement allows the regulator to be isolated during extended periods when leakage and regulator drift could be a problem, e.g., during heliocentric cruise and the 59 day phasing orbit period. Following the final plane change maneuver to the mapping orbit, this regulator is permanently isolated from the pressurant, and the remaining propulsion functions (orbit maintenance and transfer to the quarantine orbit) are accomplished in the blowdown mode using the helium in the propellant tanks.

The second regulator is used to drop the stored helium pressure to a level compatible with the helium thrusters. Since impulse bits from these engines are required on a daily basis for momentum wheel unloading, this regulator is used continuously throughout the mission. Regulator drift is less important in this case since impulse bit changes due to off-design pressures can be compensated with duty cycle adjustments.

In order to preserve the natural environment on Mars, none of the components of this liquid propulsion system will be staged during the MGCO mission. Thus, in comparing this system to the JPL designed MGCO Flight System defined in Figure C-1, the present liquid system includes the Mars Orbit Insertion Stage, MOI Stage Adapter and the portion of the spacecraft mass which is attributed to burns for achievement of the phasing orbit, orbit maintenance and quarantine orbit. These portions will be identified in mass breakouts presented later in this section.

C3. CAPABILITY

The capability of the above system to perform the MGCO mission was established after various characteristics of the TOS and the bipropellant propulsion stage were evaluated. These have led to the following assumptions in the propulsion system assessment.

- TOS burn-out stage mass of 1224 kg
- TOS adapter mass of 100 kg
- Helium mass of 4 kg for all helium thruster functions, including an ample contingency allowance
- Total low thrust ΔV penalty of 105 m/s
- An estimated ΔV allowance of 28 m/s for thruster and injection dispersions

The low thrust ΔV penalty assumes two burns during MOI. The first of these achieves capture by Mars, leaving the spacecraft in a highly elliptical orbit, and the second circularizes this initial orbit at the desired 350 km altitude. This represents a substantial improvement over the penalty incurred for a single burn (about 175 m/s), but is still greater than that associated with a larger number of burns. Further study is required to identify the optimum burn schedule for the MOI maneuvers.

Multiple burn capability offers a further advantage. In the event of an engine malfunction during MOI, which in effect halves the thrust due to the necessity to shut down the opposite thruster, the burn schedule can be altered immediately to include a larger number of burns, thereby avoiding an increased ΔV penalty. For example, initial examination of this failure mode has shown that a four-burn sequence can maintain the ΔV penalty below the 100 m/s for the case of two engines out at the beginning of MOI.

Propulsion system capability for the MGCO mission, including the low thrust penalty and contingency allowances, is shown in Figure C-3, where useful spacecraft mass is plotted against TOS throw mass. Here, useful spacecraft mass is defined as end-of-life mass minus all propulsion hardware, residual propellant and pressurant. Hence, useful spacecraft mass represents the total non-propulsion related mass available to accomplish the mission objectives. Figure C-3 employs worst-case assumptions for required heliocentric injection

ORIGINAL PAGE IS
OF POOR QUALITY

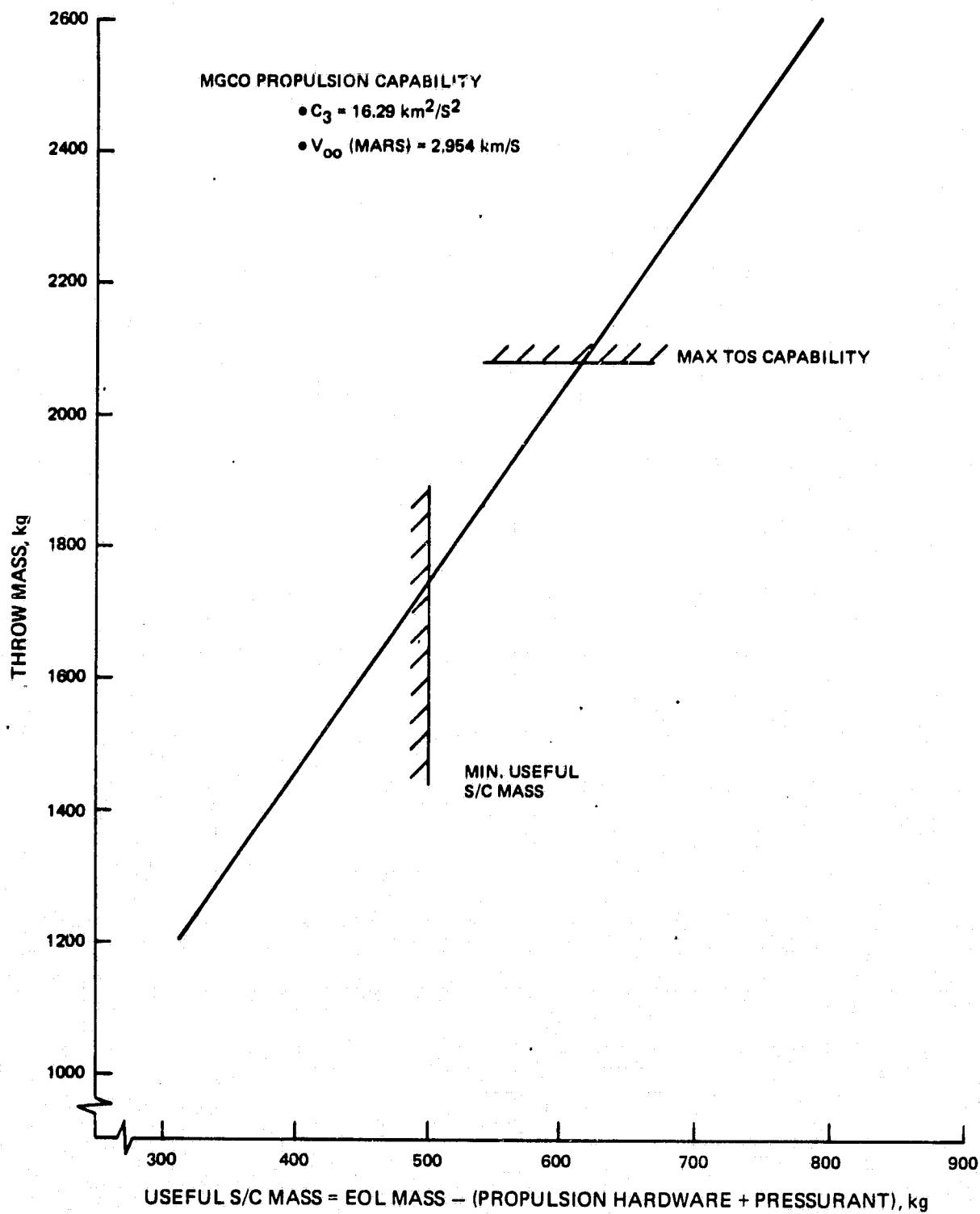


Figure C-3. MGCO Propulsion Capability

velocity and arrival hyperbolic excess velocity at Mars, even though these maxima occur at opposite extremes of the launch window. This introduces some conservatism, as for example in an early launch which requires the total planned TOS propellant while leaving an additional liquid propellant margin at Mars. Conversely, a late launch allows some on-loading of liquid propellant (consistent with tank capacity) in order to decrease the TOS injection velocity to the required value.

For the TIROS-N spacecraft considered for this mission, the minimum useful spacecraft mass that fulfills all the mission objectives is 500 kg. This spacecraft contains the full 80 kg instrument package, has ample propellant for the extended mapping mission, and has sufficient propellant margin and redundancy to guarantee mission success. Figure C-3 shows that this corresponds to a 1755 kg throw mass which implies that the TOS is off-loaded by approximately 10%.

Alternatively, the propellant load in the TOS can be increased up to the fully loaded condition, with the extra MGCO insertion system mass used for growth or "excess" capability. The extra capability can accommodate a heavier complement of instruments on the next larger spacecraft in the TIROS family, or it can be used to increase the liquid propellant load with the same spacecraft to provide even greater margins and extended life. Figure C-3 shows that the maximum useful spacecraft mass can be increased by greater than 20% to 611 kg.

Table C-1 compares propulsion masses for the baseline 500 kg case and a maximum throw mass case where the added capability is concentrated only on greater instrumentation mass. Since analysis shows that the change in ΔV penalty is insignificant for this larger spacecraft using the same thrust level, no increase in the ΔV budget is assumed. The table shows that the only significant growth in propulsion subsystem mass is in the required propellant.

Based on the assumed mission profile, a schedule of spacecraft mass at various stages in the MGCO mission is shown in Table C-2.

TABLE C-1. MGCO SYSTEM MASS (kg)

	Baseline	Extended Capability
Propellant	1017	1217
Propulsion Hardware	127	140
Helium Pressurant	<u>11</u>	<u>12</u>
Propulsion Subsystem	1155	1369
Useful Spacecraft	<u>500</u>	<u>611</u>
Insertion System	1655	1980
TOS Adapter	<u>100</u>	<u>100</u>
Throw Mass	1755	2080
Transfer Orbit Stage	<u>9973</u>	<u>10929</u>
Injection System	11,728	13,009

TABLE C-2. MGCO MISSION MASS PROFILE (kg)

	Baseline	Extended Capability
Throw Mass	1755	2080
Insertion System	1655	1980
Start MOI	1602	1916
Start Phasing Orbit	737	883
Start Mapping Mission	694	830
End Mapping Mission	653	782
EOL Mass in Quarantine	634	759
Useful Mass	500	611

APPENDIX D
CONFIGURATION DISCUSSION

APPENDIX D
CONFIGURATION DISCUSSION

D1. INTRODUCTION

The proposed MGCO spacecraft bus is based upon the TIROS and Block 5D series of RCA spacecraft. These spacecraft have been designed to carry diverse, complex payloads consisting of planetary and environmental sensors in Sun-synchronous Low Earth Orbit (LEO) at any local time. They are three axis stabilized and rotate at one revolution per orbit (rpo) about a body fixed pitch axis. The accommodation of the MGCO payload complement in a TIROS/Block 5D design is therefore well conceived and efficient. The environment and the corresponding operational requirements to be experienced are sufficiently similar to those for the TIROS/Block 5D missions that many of the TIROS/Block 5D design concepts are applicable either directly or with a similar degree of modification as is exhibited within the family of TIROS and Block 5D spacecraft.

Utilization of the basic designs of the RCA families of spacecraft with body-mounted solar arrays (e.g., Atmosphere Explorer and Dynamics Explorer) and three-axis stabilized geostationary communications spacecraft (e.g., Satcom, GSTAR, Spacenet, etc.) has been rejected after the analysis of fundamental capabilities and requirements. It is true that the AE and DE-B spacecraft operate in LEO, with pitch control at one rpo since these spacecraft are momentum biased. The accommodation of the MGCO payload and mission requirements, however, would result in a complex and tightly constrained configuration and instrument accommodation and the problematical augmentation of solar array area. As for the communications spacecraft, their design is based upon requirements in a greatly different operational and environmental regime. For example, their basic function is to carry a narrow class of payloads, via RF repeaters. Consequently, their physical design features little versatility in the accommodation of diverse payload instruments. Notably, this type of spacecraft includes a small and limited command and data handling subsystem. Furthermore, the spacecraft subsystems, e.g., thermal and power, are matched to the very different characteristics of High Earth Orbits (HEO).

Preliminary design notes on the study of science-instrument accommodation and fields of view for the TIROS based MGCO spacecraft are included herein. The attached figures illustrate the points made in the notes.

Figure D-1 is a simplified line drawing showing the basic features of the MGCO spacecraft in its fully operational configuration. The acronyms in the call outs on Figure D-1 are written out in Section D17.

Figure D-2 shows the ranges and extreme limits of the fields of view (FOVs) of the MGCO science instruments including their coolers, superimposed on the basic line drawing of Figure D-1. The compliance of the configuration design with the FOV requirements specified by JPL is shown effectively. Although the achieved compliance with the JPL specified stray radiation constraints is not depicted explicitly, it may also be seen from a glance at Figure D-2. The values of the angular limits of the FOVs shown in the figure are measured from the nadir direction, which has been arbitrarily assigned 0° . The 8° shown for the MVIRS is the full angular width of the fan-like cross-track FOV.

Figure D-3 shows a representation of the solid angles throughout which the high gain antenna (HGA) and the solar array will be required to point, during the drift and mapping phases of the mission, superimposed on the basic line drawing of Figure D-1. In Figure D-2, the origins of these pointing solid-angles are located at representative, nominal pivot points of the HGA and the solar array. Three cones emanate from each of these two origins. During the drift and mapping phases of the Sun/Earth direction sweeps out the solid angle which lies between those two of the triplet of cones whose axes of symmetry are parallel to the orbit normal. Whenever the Sun/Earth direction passes through Mars, however, there is occultation and this part of the pointing solid angle is useless for power/communications. The occultation cones are symmetrical about the nadir; their half angle is 65° measured from the nadir.

Figure D-4 shows the FOVs of the attitude determination sensors, superimposed on the basic line drawing of Figure D-1. The decision on the types and numbers of celestial sensors to be used remains to be finalized. In these figures, a feasible configuration incorporating a single DMSP type celestial sensor (Honeywell) is depicted. The inclusion of another celestial sensor has little

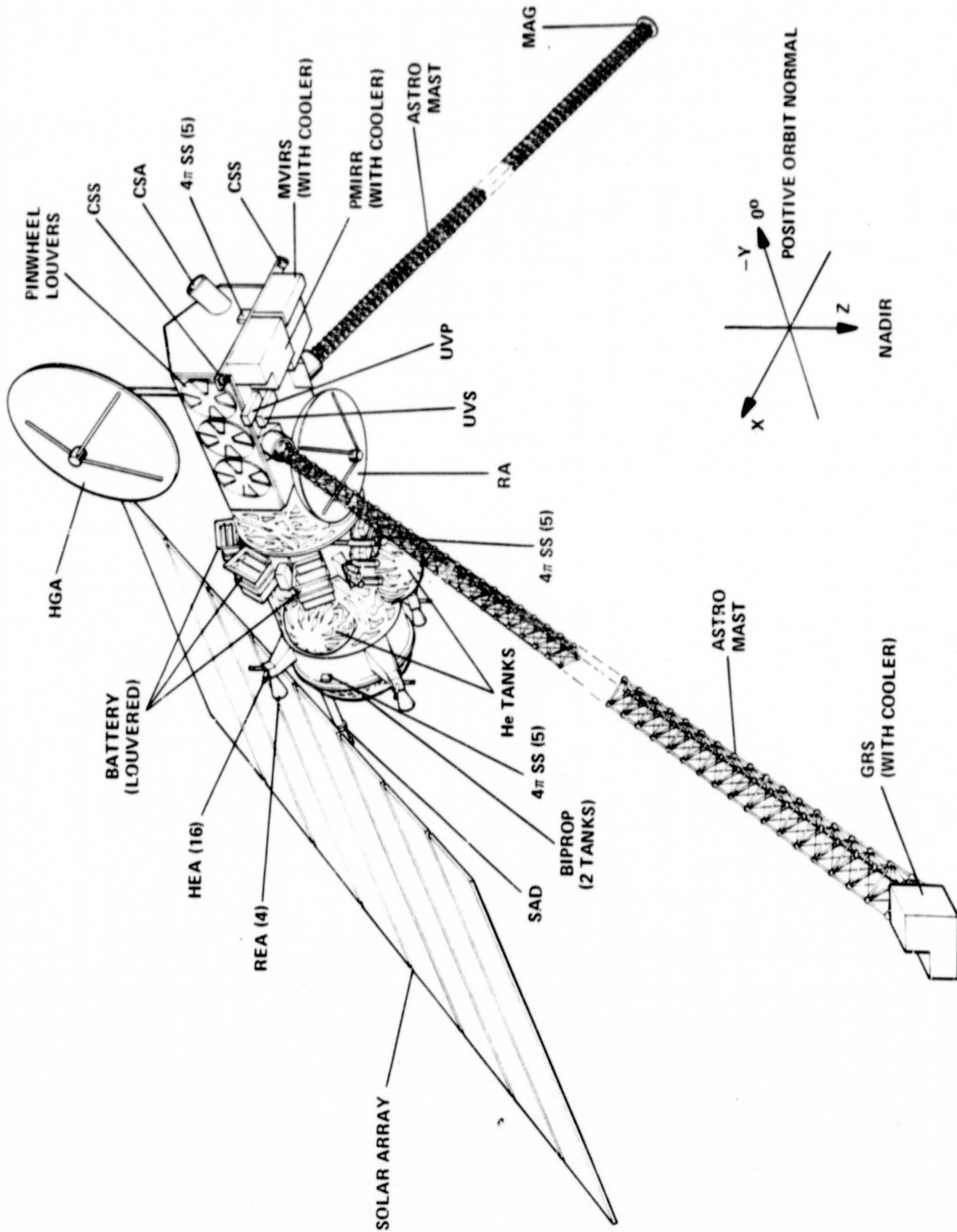


Figure D-1. MCGO Science Accommodation and Fields-of-View Study

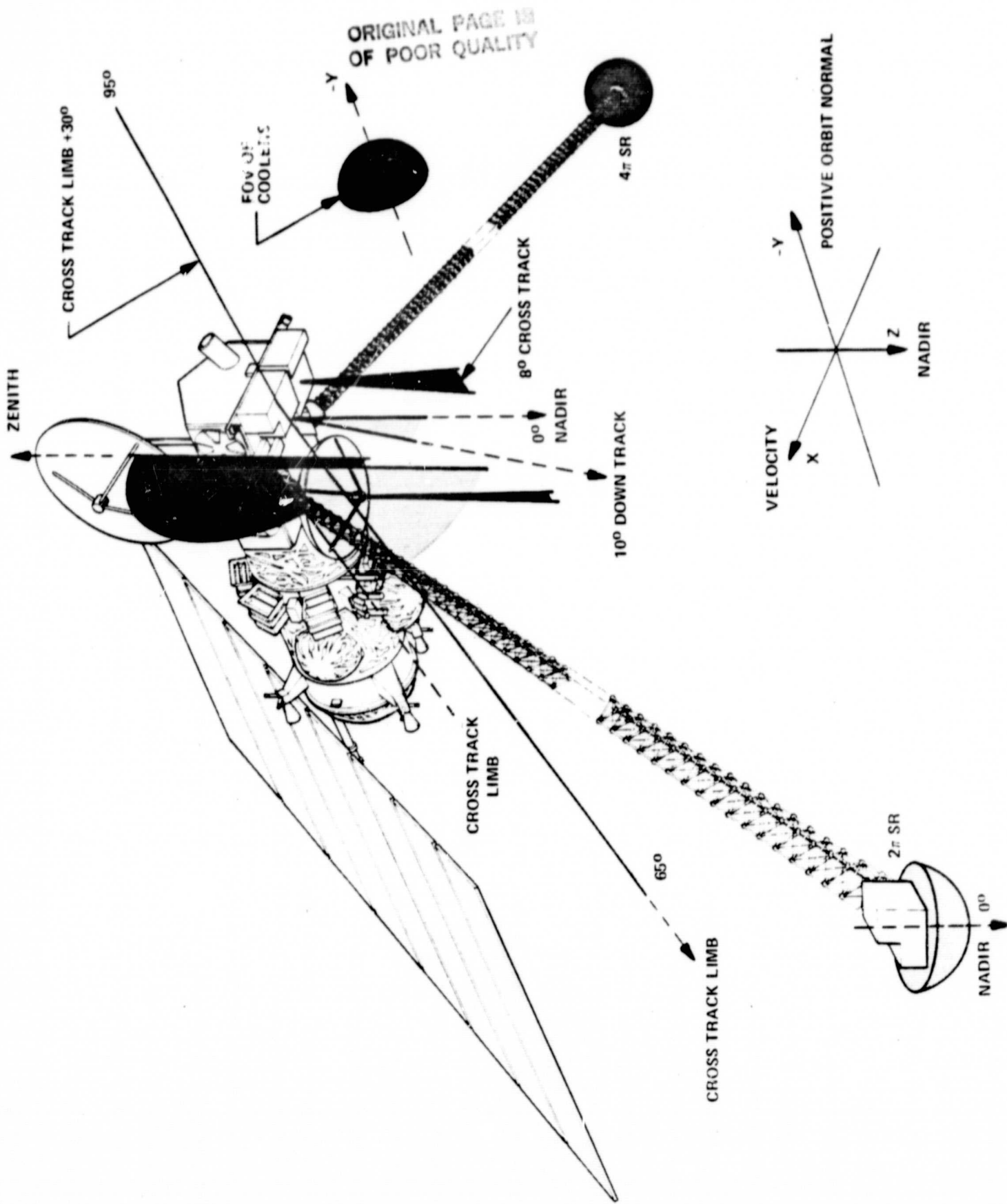


Figure D-2. MGC0 Science Accommodation and Fields-of-View Study

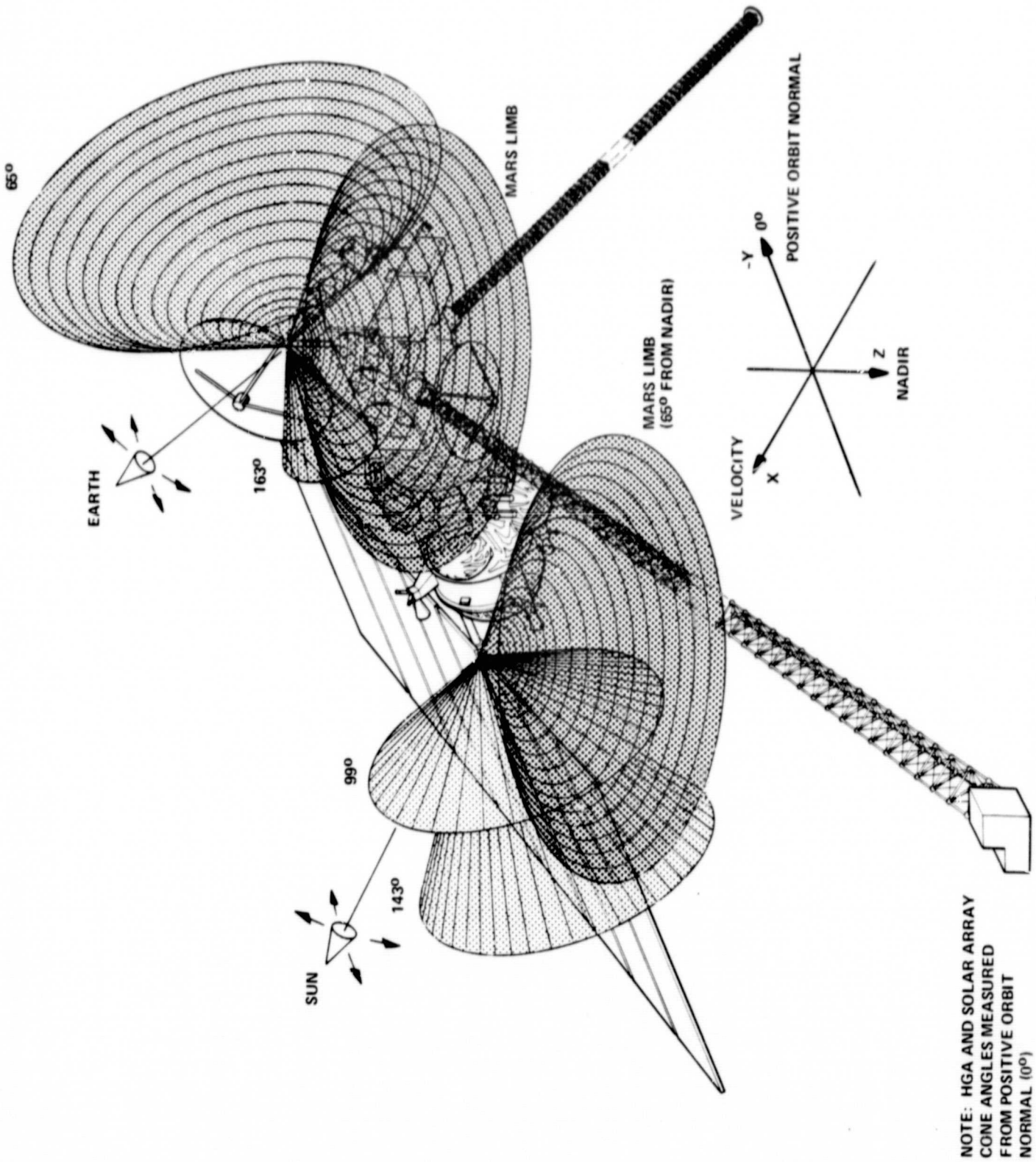


Figure D-3. MGC0 Science Accommodation and Fields-of-View Study

ORIGINAL PAGE IS
OF POOR QUALITY

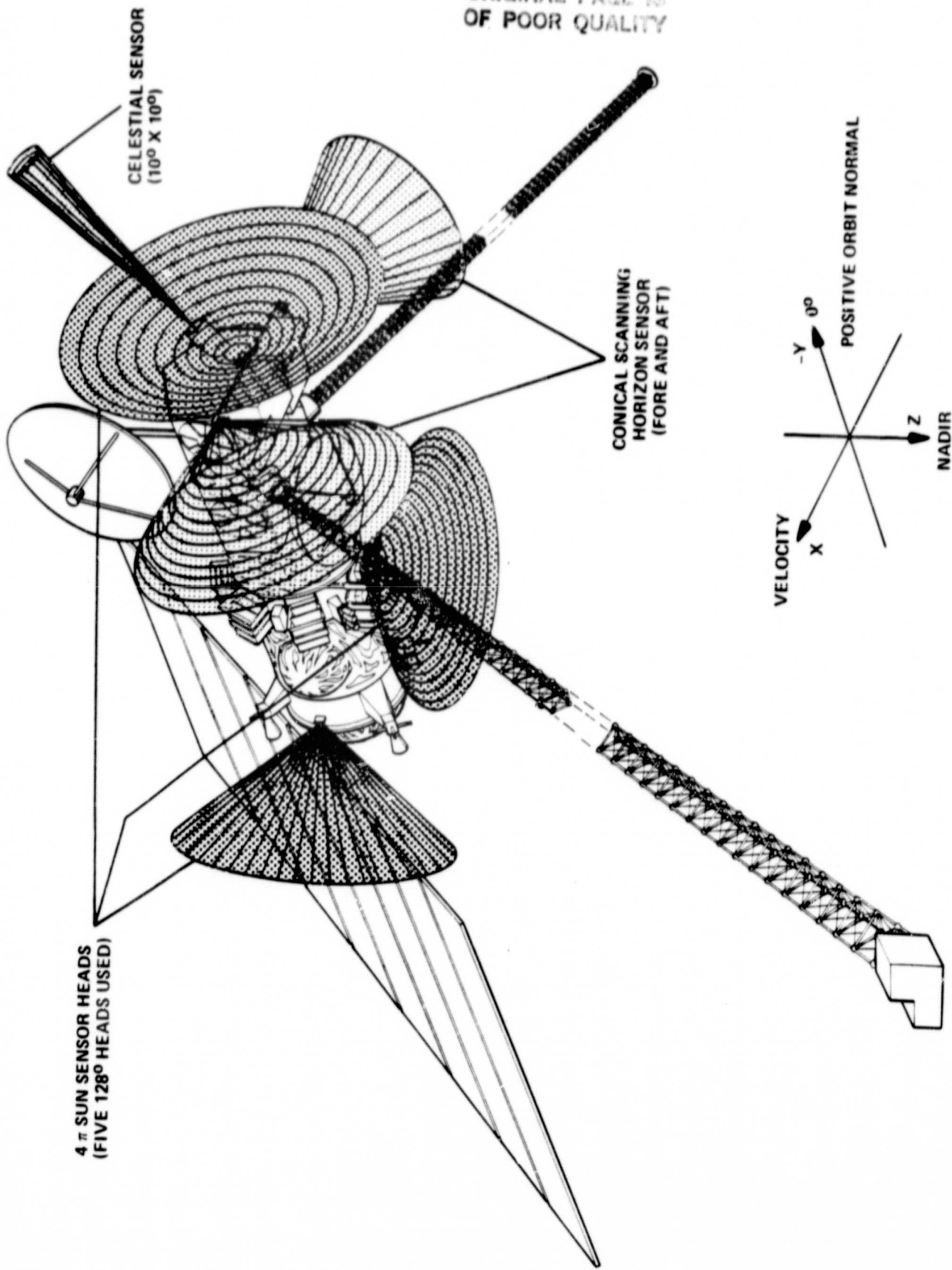


Figure D-4. MGCO Science Accommodation and Fields-of-View Study

impact on this instrument accommodation and FOVs study. The baffle tube of a second celestial sensor would project out of the cold end-face of the Equipment Support Module (ESM) in a similar way to the one shown. The cone angle of the FOV of the conical scanning horizon sensors (CSSs) remains TBD, but is shown herein as 90° (full cone) as in the CSSs proposed for SAATN and 5D-3. The final selection of this cone angle will probably slightly change the final design choice for the orientation of the MAG and GRS booms from that depicted in Figure D-4, so that these booms are outside the FOVs of the CSSs as well as the HGA and the other sensors. Only three of the five sensor heads of the 4π steradian sun sensor, and their FOVs, are shown in these figures. The head on the -Z side of the propulsion module and the head on the -X side of the propulsion module cannot be seen in this perspective view.

D2. GENERAL

- All science instruments mounted to bottom panel of ESM (pallet)
 - Allows physical integration and operational simulations to be performed at JPL from bus.
 - Attitude of pallet determined and controlled by spacecraft ADACS.
- Sign Convention
 - +X Nominal direction of flight (down track)
 - +Y Orbit anti-normal (-Y, positive orbit normal, determined from orbital velocity by right hand screw rule).
 - +Z Local vertical towards nadir.

D3. GRS

- Boom at an angle of upto $\sim 65^\circ$ from nadir
 - Boom and GRS outside FOVs of other instruments and useful FOV of HGA
 - Boom may be canted towards the orbit anti-normal (RSS end of bus) in order to avoid the FOVs of the conical scanning horizon sensors (CSSs) and the stray light constraint zones of the other instruments.
- FOV and stray radiation requirements satisfied.
- Since RA is best placed at +Y end of pallet and PMIRR and MVIRS are best placed at -Y end of pallet, the GRS and MAG booms will probably be mounted along the +X and -X edges of the pallet.
- Separate booms will be assumed for the GRS and MAG unless these instruments can be shown to be non mutually interfering when in close proximity to each other.

- Boom locks in fully extended position with 2π Steradian FOV of GRS centered on nadir and FOV of GRS cooler (approximately 2π Steradians) centered on positive orbit normal (towards cold space).
- Boom may be partially deployed and may be retracted.
- Boom selection TBD
 - Astromast Shown in Figure D-1
 - Astromast Clock angle and extension difficult to ascertain in partially deployed condition

D4. MVIRS

- Located at -Y end of pallet
 - Cooler has clear view of cold space (approximately 2π Steradians)
- FOV and stray radiation requirements satisfied.

D5. PMIRR

- Located at -Y end of pallet
 - Cooler has clear view of cold space (approximately 2π Steradians)
 - Location towards -Y +X corner of pallet may be preferable to accommodate view 10° down track
 - Instrument has clear view up to and beyond (the specified) 30° above one cross-track limb
- FOV and stray radiation requirements satisfied.

D6. RA

- Located with center approximately on +Y edge of pallet, so that half of the dish is under the propulsion module.
 - Location with center in +X +Y corner or -X +Y corner would minimize use of pallet mounting area.
- FOV and stray radiation requirements satisfied.

D7. UVS

- Location on +X edge of pallet may favor view of down-track limb (same limb as viewed by UVP).
- FOV and stray radiation requirements satisfied.

C-2

D8. UVP

- Mounted to hang over +X edge of pallet
 - Allows FOV between zenith, nadir and down-track limb
- FOV requirements satisfied
- By locating UVP sensor head far enough out beyond +X edge of pallet, the specified 30° (half angle) stray radiation requirement can be satisfied. Other approaches to satisfying this stray radiation requirement might be to include an entrance baffle up the side of the ESM, or to select surface finishes for the adjacent side of the ESM so that the stray radiation level is acceptable.
- The current design for the configuration and size of the HGA results in occasional interference with the FOV of the UVP to a level acceptable to JPL. This issue will be studied further. The UVP is the only instrument whose operation is compromised in the current baseline design.

D9. MAG

- See comments in Section D3.
- No special requirement on orientation of MAG at end of boom.

D10. SOLAR ARRAY

- Solar panels held folded around louvered panels of ESM through launch phase.
- Within minutes of TOS burnout and separation, solar panels deployed into planar array in X-Y plane with solar cells facing -Z direction. Boom still held along apex of ESM. Spacecraft attitude controlled so that solar array plane is perpendicular to Sun line.
- Following Mars Orbit Insertion (MOI) solar array boom deployed along +Y axis. Solar array boom rotation and solar array cant angle controlled so that solar array plane is perpendicular to Sun line.
- Current baseline mission design involves plane change maneuvers (for achievement of Sun synchronism) and orbit maintenance maneuvers to be performed with solar array and boom in fully deployed configuration and with plane of solar array parallel to Y axis. Thrust level and location of thrusters for these maneuvers TBD. Probable reconfiguration of HGA and boom from that shown herein.
- Angular range of rotation of solar array boom necessitated by mission requirements is less than 360° , due to occultation of Sun by Mars when Sun direction is closer than 65° to nadir, which occurs for part of every orbit during drift and mapping phases.
- Solar array cant angle controllable between zero (launch and cruise phases) and approximately 53° (corresponding to maximum angle between Sun line and positive orbit normal of 143° during operational phases).

- Baffle tube of celestial sensor shown external to dog house. Optics, sensor heads and electronics may be located inside ESM, possibly mounted on internal face of pallet, in order to minimize relative motions of celestial sensor and science instruments.

D13. CONICAL SCANNING HORIZON SENSORS

- Located one fore and one aft, on brackets next to coolers for PMIRR and MVIRS at cold end of ESM.
- Similar sensors proposed for DMSP Block 5D-3 and NOAA SAATN manufactured by Barnes Engineering Co. and Ithaco Inc.
- Rotation of prism or other entrance optics causes FOV ($\sim 3^\circ$) to cone at approximately 4 revs/sec. The half-cone angle for the proposed Block 5D-3 and SAATN Earth orbiters is 45° . The half-cone angle for the MGCO mission is TBD.
- Center lines of cones lie in X-Z plane, depressed by TBD° from X axis.
- GRS and MAG booms may be canted towards -Y in order to avoid FOVs of conical scan sensors (this is not shown in Figure D-1) as well as being depressed below X-Y plane towards +Z in order not to obstruct HGA pointing. Otherwise conical scan sensors electronics would gate detected signal in order to reject effect of FOV interference by GRS and MAG booms.

D14. 4π STERADIAN SUN SENSOR

- Employs five sensor heads, each with a 128° conical FOV.
- Three heads located on "Equator" of spacecraft (X-Y plane) with centers of FOVs 120° apart. One head on top of spacecraft, with FOV centered on -Z axis. One head on bottom of spacecraft, with FOV centered on +Z axis.
 - 2 equatorial heads and the -Z head mounted on reaction control equipment support structure (RSS). Third equatorial head mounted on cold end face of ESM. +Z head mounted on RSS near battery charge electronics (BTX).
- Head on -Z and -X sides of spacecraft is not visible in Figure D-4.

D15. PROPULSION MODULE

The configuration for the propulsion module has not been finalized.

The possible changes that may be made to the configuration shown in Figures D-1 through D-4, attached figures, however, will not impact the science instrument accommodation and fields of view study presented herein.

The tankage of the configuration shown consists of two 42-inch diameter bipropellant tanks along the Y axis, with four 20-inch diameter helium tanks nestled symmetrically between them. As in the SAATN and Block 5D-3 spacecraft designs there are four rocket engine assemblies (REAs) spaced at 90° intervals around the end ring of the reaction control equipment support structure (RSS). The 16 helium engine assemblies (HEAs) are nominally co-located with the REAs in eight redundant pairs with their lines of action passing through the adjacent REAs.

D16. BATTERIES

The configuration discussed includes two batteries. Each battery consists of two boxes, and therefore there are four battery boxes. Only three of these battery boxes shown are visible in the perspective view. The battery boxes are mounted externally to the RSS in the TIROS and Block 5D designs, in accordance with considerations of volume and thermal control. The panels of vane louvers on the battery boxes have a clear view of cold space (centered on the -Y direction) during the drift and mapping phases of the mission, as do all the other coolers in the MGCO spacecraft design.

D17. GLOSSARY

ADACS	Attitude Determination and Control Subsystem
BIPROP	Bi-propellant
BTX	Battery Charge Electronics
CSA	Celestial Sensor Assembly
CSS	Conical Scanning Horizon Sensor
DMSP	Defense Meteorological Satellite Program
ESM*	Equipment Support Module

*NOTE: The ESM is the main equipment Module with a pentagonal cross section, which contains most of the electronics, recorders, etc. on the TIROS series of spacecraft.

All of the science instruments are mounted on the MARS facing panel of this module, except for those mounted on booms.

FOV	Field of View
GRS	Gamma Ray Spectrometer
He	Helium
HEA	Helium Engine Assembly
HEO	High Earth Orbit
HGA	High Gain Antenna
LEO	Low Earth Orbit
MAG	Magnetometer
MGCO	Mars Geoscience and Climatology Orbiter
MVIRS	Mapping Visible and Infrared Spectrometer
NOAA	National Oceanic and Atmospheric Administration
PMIRR	Pressure Modulated Infrared Radiometer
RA	Radar Altimeter
REA	Rocket Engine Assembly
RF	Radio Frequency
RSS	Reaction Control Equipment Support Structure
SAATN	STS/Atlas Advanced TIROS-N
SAD	Solar Array Drive
TBD	To Be Determined
TOS	Transfer Orbit Stage
UVP	Ultraviolet Photometer
UVS	Ultraviolet Spectrometer